Ph.D. DISSERTATION

Performance Analysis of Wireless Relay Networks in the Presence of Cochannel Interference

동일채널간섭이 존재하는 페이딩채널에서 무선 중계 네트워크의 성능 분석

BY

Dongwook Choi

AUGUST 2014

DEPARTMENT OF ELECTRICAL AND
COMPUTER ENGINEERING
COLLEGE OF ENGINEERING
SEOUL NATIONAL UNIVERSITY

Performance Analysis of Wireless Relay Networks in the Presence of Cochannel Interference

동일채널간섭이 존재하는 페이딩채널에서
무선 중계 네트워크의 성능 분석

지도교수 이 재 홍

이 논문을 공학박사 학위논문으로 제출함

2014 년 6 월

서울대학교 대학원

전기정보공학부

최 동 욱

최동욱의 공학박사 학위논문을 인준함

2014 년 6 월

위 원 장 박 세 웅

부위원장 이 재 홍

위 원 서 승 우

위 원 이 정 우

위 원 문 희 찬

Performance Analysis of Wireless Relay Networks in the Presence of Cochannel Interference

Doctoral Dissertation
Submitted in June of 2014 to the Graduate School
of Seoul National University
in Partial Fulfillment of the Requirements
for the Degree of Doctor of Philosophy

in

Electrical and Computer Engineering

by

Dongwook Choi

Department of Electrical and Computer Engineering
College of Engineering
Seoul National University

Abstract

Wireless relay technology is one of the most promising technologies for the future communication systems which provide higher data rate and better quality of service (QoS). Thanks to its advantages, it has been adopted in wireless standards such as IEEE 802.16j and 3GPP LTE-Advanced. However, there are still many challenges to be addressed for developing protocols of wireless relay networks. Especially, in multi-tier cellular networks (e.g. small cell underlaid macro cell), cochannel interference from multiple interferers in other macro cells and neighboring small cells is one of the major limiting factors due to frequency reuse for high spectrum utilization. In the full-duplex relay networks, cochannel loop interference from a transmit antenna to a receive antenna of a terminal is an important limiting factor to determine the performance of full-duplex relay networks.

The dissertation consists of three main results. First, we analyze the performance of a two-way relay network experiencing cochannel interference from multiple interferers due to frequency reuse in cellular networks. In the two-way relay network, two users exchange their information with the help of an amplify-and-forward (AF) relay. We discuss two different scenarios: Outages are declared individually for each user

(individual outage) and an outage is declared simultaneously for all users (common outage). We derive the closed-form expression for the individual outage probability and the exact integral expression for the common outage probability of the two-way relay network with multiple interferers. The validity of our analytical results is verified by a comparison with simulation results. It is shown that the analytical results perfectly match the simulation results of the individual and common outage probabilities. Also, it is shown that the individual and common outage probabilities increase as the number of interferers increases.

Second, we investigate two-way full-duplex relaying with cochannel loop interference. In the two-way full-duplex relaying, two full-duplex users exchange data with each other via a full-duplex relay and each node attempts to subtract the estimate of the cochannel loop interference from its received signal. We derive the exact integral and approximate closed-form expressions for the outage probability of the two-way full-duplex relaying in case of perfect and imperfect channel state information. Monte Carlo simulation verifies the validity of analytical results.

Third, we investigate a cognitive small cell network which is overlaid with a cellular network. We analyze the performance of the cognitive small cell network in the presence of cochannel interference from the cellular network. Analytical results are verified by Monte Carlo simulations. It is shown that the analytical results are in complete agreement with simulation results. It is shown that the outage probability increases as the number of cells increases.

Keywords: Wireless relay technology, cochannel interference, two-way relaying, multi-hop relaying, full-duplex relaying, cognitive radio, spectrum-sharing, outage probability.

Student ID: 2007-23057

Contents

Abstract i

1 Introduction **1**

1.1 Background and Related Works 2

1.1.1 Relay Technology 2

1.1.2 Cognitive Radio 5

1.2 Outline of Dissertation 7

1.3 Notations 8

2 Two-Way Relay Network with Cochannel Interference **12**

2.1 System Model 14

2.2 Outage Probability Derivation 18

2.2.1 Moment Generating Functions 18

2.2.2 Individual Outage Probability 20

2.2.3 Common Outage Probability 23

2.3 Numerical Results 25

2.4 Summary 44

3 Two-Way Full-Duplex Relaying with Cochannel Loop Interference 49

3.1 System Model 50

3.2 Outage Probability Derivation 56

3.2.1 Signal-to-Interference-plus-Noise Ratio 56

3.2.2 Cumulative Density Function 57

3.2.3 Outage Probability 60

3.3 Numerical Results 61

3.4 Summary 69

4 Multi-hop Cognitive Radio Network with Cochannel Interference 79

4.1 System Model 80

4.2 Outage Probability Derivation 83

4.2.1 Signal-to-Interference-plus-Noise Ratio 83

4.2.2 Cumulative Density Function 83

4.2.3 Outage Probability 87

4.3 Numerical Results 88

4.4 Summary 99

5 Conclusions 110

5.1 Summary 110

5.2 Future Works 111

Bibliography 113

Korean Abstract 128

Acknowledgments **130**

List of Tables

1.1 Table of abbreviations 11

List of Figures

2.1 Two-way relay network with multiple interferers, where the users a and b exchange information with each other by the help of a relay r. . . . 15

2.2 Individual outage probability versus ζ for various number of interferers. $\mu_{l,i} = 1$. 29

2.3 Individual outage probability versus ζ for various number of interferers. $\mu_{l,i} = 0.1$. 32

2.4 Individual outage probability versus γ_{th} for various number of interferers. $\mu_{l,i} = 0.1$. 37

2.5 Common outage probability versus ζ for various number of interferers. $\mu_{l,i} = 1$. 40

2.6 Common outage probability versus ζ for various number of interferers. $\mu_{l,i} = 0.1$. 43

2.7 Common outage probability versus γ_{th} for various number of interferers. $\mu_{l,i} = 0.1$. 48

3.1 System model for two-way full-duplex relaying with cochannel loop interference. 51

3.2 Outage probability of the user a versus SNR for two-way full-duplex relaying. Variances of the channel estimation errors are set to 0 or 1. . 64
3.3 Outage probability of the user a versus SNR for two-way full-duplex relaying. Variances of the channel estimation errors are set to 0 or 0.1. 65
3.4 Outage probability of the user a versus SNR for two-way full-duplex relaying. Variances of the channel estimation errors are set to 0 or 0.01. 66
3.5 Outage probability of the user a versus SNR for two-way full-duplex relaying. Variances of the channel estimation errors are set to 0 or 0.001. 67
3.6 Outage probability of the user a versus ξ for two-way full-duplex relaying. SNR = 30 dB. 72
3.7 Outage probability of the user a versus ξ for two-way full-duplex relaying. SNR = 25 dB. 75
3.8 Outage probability of the user a versus ξ for two-way full-duplex relaying. SNR = 20 dB. 78

4.1 Underlay cognitive radio network which is overlaid with a cellular network. 81
4.2 Outage probability versus $P_{\max}/N_0$ for various number of cells. $R = 0.1$, $I = 0$ dB. 92
4.3 Outage probability versus $P_{\max}/N_0$ for various interference threshold. $R = 0.1$, $\alpha = 4$, $L = 3$. 93
4.4 Outage probability versus $P_{\max}/N_0$ for various number of cells. $R = 0.2$, $I = 0$ dB. 97

4.5 Outage probability versus $P_{\max}/N_0$ for various interference threshold. $R = 0.2$, $\alpha = 4$, $L = 3$. 98

4.6 Outage probability versus the number of hops for $P_{\max}/N_0 = 20, 24, 28, 32$. $L = 1$, $I = 20$ dB, $R = 0.5$. 102

4.7 Outage probability versus the number of hops for $P_{\max}/N_0 = 20, 24, 28, 32$. $L = 2$, $I = 20$ dB, $R = 0.5$. 105

4.8 Outage probability versus the number of hops for $P_{\max}/N_0 = 20, 24, 28, 32$. $L = 3$, $I = 20$ dB, $R = 0.5$. 108

Chapter 1

Introduction

The next-generation wireless systems are required to support higher data rate and better quality of service (QoS). In order to meet these requirements for the next-generation wireless systems, the conventional approach is to increase the number of base stations over a given area. However, it requires excessive cost for implementing these base stations. As one of the attractive approaches, the relay technology has been widely studied. It supports communication between the source and the destination reliably and cheaply. Thanks to its advantage, there has been drawing interest from both academia and industry. Also, its applications to wireless networks have been studied widely.

In this chapter, Section 1.1 provides the background of the relay technology and its application to the cognitive radio. Section 1.2 shows the outline of this dissertation. In Section 1.3, we provide the notations, functions, and the list of abbreviations used throughout the dissertation.

1.1 Background and Related Works

1.1.1 Relay Technology

Relay technology is one of most promising technologies for the next-generation wireless systems which provide higher data rate and better quality of service (QoS) [1]-[9]. In the relay communications, the source transmits its signal to the destination with the help of one or multiple intermediate relays. As the distance between two adjacent terminals decreases, the effect of channel impairments such as path-loss is reduced. It enables to provide coverage extension and enhanced capacity.

The basic concept of the relay technology was firstly introduced by Van der Meulen in 1971 by analyzing the upper and lower bounds on the capacity for the three terminal network which consists of a source, a relay, and a destination [10]. In 1979, Cover and El Gamal analyzed the capacity for degraded, reversely degraded, and feedback relay channels [11].

After these early works, the relay technology did not have much attention for a long time since it was hard to implement practically. However, it has been changed since the concepts of the information theory were implemented successfully [12], [13]. In 1998, Sendonaris *et. al.* introduced the concepts of two-user cooperation in the framework of a code-division multiple-access system, where each of the two users is responsible for transmitting not only their own signal but also the signal of other user [2]-[3], [14]. In 2000, Schein *et. al.* investigated a real, discrete-time Gaussian parallel network which consists of a source, two relays, and a destination [15]. In 2002, Gastpar *et. al.* analyzed

the asymptotically capacity of the wireless network as the number of relays increases [16]. In 2003, Laneman *et. al.* developed and analyzed space–time coded cooperative diversity protocols where the relays that can fully decode the received signal from the source in the first time slot utilize a space-time code to cooperatively relay to the destination [17]. Also, in 2004, they introduced various cooperative diversity protocols such as amplify-and-forward (AF), decode-and-forward (DF), selection relaying, and incremental relaying [5]. All these works have assumed a unidirectional transmission through relays, which is referred to as the one-way relaying.

Two-way relaying has been drawn much interest recently due to its capability to further enhance the spectral efficiency by using either superposition coding or physical-layer network coding at the relays, compared to one-way relaying [18]-[23]. In 2005, Rankov *et. al.* introduced and analyzed various bidirectional cooperative relaying protocols where multiple terminals communicate with multiple partners via multiple AF or DF relays [18]-[20]. In 2007, Popovski *et. al.* investigated the conditions for sum-rate maximization of the two-way relaying [21]. In 2009, Koike-Akino *et. al.* developed various modulation schemes to optimize two-way relaying systems, for which network coding is employed at the physical layer [22]. All these works have assumed a dual-hop transmission.

Multi-hop transmission has been extensively investigated in both academia and industry in order to combat the performance degradation caused by propagation loss, [6], [24]-[29]. In multi-hop transmission, when the direct path between a source and a destination is deeply faded, the source communicates with the destination via multiple

intermediate relays. In 2003, Hasna *et. al.* analyzed the end-to-end outage probability of multi-hop relay networks with AF relays over Nakagami-m fading channels [24]. In 2004, Boyer *et. al.* developed four different multi-hop protocols: Amplified relaying multi-hop protocol, decoded relaying multi-hop protocol, decoded relaying multihop diversity protocol, and amplified relaying multihop diversity protocol [25]. In 2006 and 2008, Hossain *et. al.* investigated the multi-hop relay networks based on the automatic repeat request [26], [27]. In 2012, Jang *et. al.* developed a DF-based multi-hop transmission system where the relays forward the source data simultaneously and derive a closed-form expression of the outage probability [30]. All these works have assumed that a relay does not transmit and receive simultaneously, which is referred to as the half-duplex relaying.

Full-duplex relaying, where the transmission and the reception occur at the same time on the same channel, achieves up to double the capacity of a half-duplex scheme [31]-[37]. Although the full-duplex scheme suffers from cochannel loop interference, it has drawn attention due to recent advances on interference cancellation and transmit/receive antenna isolation to mitigate the loop interference [38]-[40]. In 2006, Liu provided a communication protocol for full-duplex relay and analyzed its performance theoretically [31]. In 2009, Riihonen *et. al.* investigated a dual-hop full-duplex relay network which consists of a source, a full-duplex relay, and a destination [33]. They analyzed an outage probability by taking into account cochannel loop interference, which covers both AF and DF protocols both in downlink and in uplink. Ju *et. al.* analyzed the bit error rate and achievable rate of a dual-hop full-duplex relay network

where there is no direct path [32]. In 2012, Ng *et. al.* investigated a joint optimization problem for resource allocation and scheduling in full-duplex multiple input multiple output orthogonal frequency division multiple access (MIMO-OFDMA) relaying systems with AF and DF [34]. Krikidis *et. al.* developed an optimal relay selection scheme that maximizes the instantaneous full-duplex channel capacity and requires global channel state information (CSI) as well as several sub-optimal relay selection schemes that utilize partial CSI such as a) source-relay and relay-destination links, b) loop interference, c) source-relay links and loop interference [35]. Tabataba *et. al.* derived achievable rates for AF-based full-duplex analog network coding with channel estimation errors as well as information rate cut-set bounds in traditional routing with channel estimation errors [36].

1.1.2 Cognitive Radio

According to surveys of spectrum utilization, it is found that some frequency bands in the spectrum are largely unoccupied most of the time, some other frequency bands are only partially occupied, and the remaining frequency bands are heavily used [41]-[44]. In the conventional policy, those rarely utilized frequency bands are allocated to specific services which cannot be accessed by unlicensed users, even if the transmission of them does not cause any harmful interference to the licensed users. In order to improve the spectrum utilization, cognitive radio (CR) has been recently proposed as a key technology for the next-generation wireless systems, which allows unlicensed users to utilize licensed frequency bands opportunistically [44]-[46].

There are two approaches in the CR network: Spectrum sensing and spectrum sharing. In the spectrum sensing CR network, the unlicensed users are allowed to utilize the licensed frequency bands if the licensed users do not utilize this frequency bands [47]-[56]. In [47], Ghasemi *et. al.* provided an overview of the regulatory requirements and major challenges associated with the practical implementation of spectrum sensing in cognitive radio networks. In [48] and [49], Ganesan *et. al.* analyzed the benefits of cooperation in spectrum sensing in a multi-user network. In order to improve the performance of the spectrum sensing CR network such as the missed-detection probability and the false alarm probability, the relay technology has been applied to the spectrum sensing CR network recently [48]-[53]. In [50], Letaief *et. al.* investigated two cooperative spectrum sensing techniques: Decision fusion and data fusion. In the decision fusion, each cooperative relay makes a binary decision based on the local observation and then forwards 1 bit of the decision to the fusion center. At the fusion center, all 1-bit decisions are fused together according to an OR logic. In the data fusion, instead of transmitting the 1-bit decision to the fusion center, each cooperative relay send its observation value directly to the fusion center, and then it makes a final decision.

In the spectrum sharing CR network, the unlicensed users are allowed to utilize the licensed frequency bands if the QoS of the licensed users is guaranteed [57]-[61]. The unlicensed users in the spectrum sharing CR network use the licensed frequency bands more often compared to that in the spectrum sensing CR network. However, since the licensed users and unlicensed users use the same frequency bands, the licensed users

are affected by the interference from the unlicensed users, and vice versa. Recently, the relay technology and the spectrum sharing are combined together to improve the performance of the spectrum sharing CR network such as the data rate and the outage probability. In [58] and [60], Zou *et. al.* and Li analyzed the outage probability of a unlicensed user for the CR network with multiple relays. However, they did not consider the interference from the licensed users. In [61], Xu *et. al.* investigated a dual-hop DF CR network in the presence of the licensed user's interference.

1.2 Outline of Dissertation

In this dissertation, we consider the wireless relay networks in the presence of cochannel interference. In Chapters 2 and 4, each terminal is affected by the cochannel interference which is caused by transmissions from adjacent cells. However, in Chapter 3, each terminal is affected by the cochannel loop interference which is caused by transmission from its own transmit antenna.

In Chapter 2, we analyze the performance of a two-way relay network experiencing cochannel interference from multiple interferers due to aggressive frequency reuse in cellular networks. We discuss two different scenarios: Outages are declared individually for each user (individual outage) and an outage is declared simultaneously for all users (common outage). We derive the closed-form expression for the individual outage probability and the exact integral expression for the common outage probability of the two-way relay network with multiple interferers. The validity of our analytical

results is verified by a comparison with simulation results. It is shown that the analytical results perfectly match the simulation results of the individual and common outage probabilities. Also, it is shown that the individual and common outage probabilities increase as the number of interferers increases. In Chapter 3, we investigate two-way full-duplex relaying with residual cochannel loop interference. In the two-way full-duplex relaying, two full-duplex users exchange data with each other via a full-duplex relay and each node attempts to subtract the estimate of the cochannel loop interference from its received signal. We derive the exact integral and approximate closed-form expressions for the outage probability of the two-way full-duplex relaying in case of perfect and imperfect channel state information. Monte Carlo simulation verifies the validity of analytical results. In Chapter 4, we investigate a cognitive small cell network which is overlaid with a cellular network. We analyze the performance of the cognitive small cell network in the presence of cochannel interference from the cellular network. Analytical results are verified by Monte Carlo simulations. It is shown that the analytical results are in complete agreement with simulation results. It is shown that the outage probability increases as the number of cells increases. Finally, in Chapter 5, the conclusions and future works are drawn.

1.3 Notations

We use the following notation: $\mathcal{L}^{-1}[\cdot]$ denotes the inverse Laplace transform. $\mathbb{E}_X[\cdot]$ denotes the expectation with respect to the random variable X. $\mathrm{Re}[x]$ denotes the real part of x. $\mathrm{Im}[x]$ denotes the imaginary part of x. Also, we explain mathematical

functions and definitions used throughout the dissertation.

Definition 1 (Gamma Function [62]). *The Gamma function is defined as*

$$\Gamma(x) = \int_0^\infty e^{-t} t^{x-1} dt \tag{1.1}$$

for $\mathrm{Re}[x] > 0$.

As a special case of the Gamma function, the incomplete Gamma function is defined as

$$\Gamma(\alpha, x) = \int_x^\infty e^{-t} t^{\alpha-1} dt. \tag{1.2}$$

Definition 2 (Hypergeometric Function [62]). *The generalized hypergeometric function is defined as*

$${}_pF_q(\alpha_1, \alpha_2, \cdots, \alpha_p; \beta_1, \beta_2, \cdots, \beta_q; z) = \sum_{k=0}^{\infty} \frac{(\alpha_1)_k (\alpha_2)_k \cdots (\alpha_p)_k}{(\beta_1)_k (\beta_2)_k \cdots (\beta_q)_k} \frac{z^k}{k!} \tag{1.3}$$

where p, q, $\alpha_1, \alpha_2, \cdots, \alpha_p$, $\beta_1, \beta_2, \cdots, \beta_q$ *are nonnegative integers,* z *is a complex variable, and* $(a)_k$ *is Pochhammer symbol defined as* $(a)_k = a(a+1)\cdots(a+k-1)$.

As a special case of the hypergeometric function, the confluent hypergeometric function is given by

$${}_1F_1(\alpha; \gamma; z) = 1 + \frac{\alpha}{\gamma}\frac{z}{1!} + \frac{\alpha(\alpha+1)}{\gamma(\gamma+1)}\frac{z^2}{2!} + \frac{\alpha(\alpha+1)(\alpha+2)}{\gamma(\gamma+1)(\gamma+2)}\frac{z^3}{3!} + \cdots. \tag{1.4}$$

A second notation is given by

$$\Phi(\alpha, \gamma; z) = {}_1F_1(\alpha; \gamma; z). \tag{1.5}$$

Using (1.4) and (1.5), the confluent hypergeometric function of the second kind is defined as

$$\Psi(\alpha, \gamma; z) = \frac{\Gamma(1-\gamma)}{\Gamma(\alpha-\gamma+1)}\Phi(\alpha, \gamma; z) + \frac{\Gamma(\gamma-1)}{\Gamma(\alpha)} z^{1-\gamma} \Phi(\alpha-\gamma+1, 2-\gamma; z). \tag{1.6}$$

Definition 3 (Exponential Integral [62]). *The exponential integral is defined as*

$$\mathrm{Ei}\,(x) = -\int_{-x}^{\infty} \frac{e^{-t}}{t} dt \tag{1.7}$$

for $x > 0$.

Definition 4 (Meijer's G-Function [62]). *The Meijer's G-function is defined as*

$$G_{p,q}^{m,n}\left(x \left| \begin{matrix} a_1,\cdots,a_p \\ b_1,\cdots,b_q \end{matrix} \right.\right) = \frac{1}{2\pi i} \int \frac{\sum_{j=1}^{m} \Gamma\left(b_j - s\right) \sum_{j=1}^{n} \Gamma\left(1 - a_j + s\right)}{\sum_{j=m+1}^{q} \Gamma\left(1 - b_j + s\right) \sum_{j=n+1}^{p} \Gamma\left(a_j - s\right)} x^s ds \tag{1.8}$$

for $0 \leq m \leq q$ *and* $0 \leq n \leq p$. *And the poles of* $\Gamma\left(b_j - s\right)$ *must not coincide with the poles of* $\Gamma\left(1 - a_k + s\right)$ *for any* j *and* k *where* $j = 1, \cdots, m$ *and* $k = 1, \cdots, n$.

Table 1.1 lists the abbreviations used throughout the dissertation.

Table 1.1. Table of abbreviations

AF	amplify-and-forward
AWGN	additive white Gaussian noise
BC	broadcast
CDF	cumulative distribution function
CR	cognitive radio
CSCG	circularly symmetric complex Gaussian
CSI	channel state information
DF	decode-and-forward
MA	multiple-access
MGF	moment generating function
MIMO	multiple input multiple output
OFDM	orthogonal frequency division multiple access
PDF	probability density function
QoS	quality of service
SER	symbol error rate
SI	self-interference
SINR	signal-to-interference-plus-noise ratio
SIR	signal-to-interference ratio
SNR	signal-to-noise ratio

Chapter 2

Two-Way Relay Network with Cochannel Interference

In a two-way relay network, two users exchange information with each other via a single or multiple relays [20]-[22], [63]. Compared to conventional one-way relay networks [2], [5], the two-way relay network provides improved spectral efficiency by using either superposition coding or physical-layer network coding at the relays [20].

The performance of the two-way relay network over fading channels has been extensively analyzed [64]-[66]. In [64], the authors derive the individual outage probability, sum-rate, and bit error rate of a two-way relay network with multiple relays over Rayleigh fading channels. In [65], the authors investigate the common outage probability and symbol error rate (SER) of a two-way relay network with multiple relays over Rayleigh fading channels. In [66], the authors derive the individual outage probability, SER, and sum-rate of a two-way relay network with a single relay

over Nakagami-m fading channels. Most previous works on two-way relay networks are focused on wireless networks with no interference. However, in practical cellular networks, cochannel interference from multiple interferers is one of the major limiting factors due to aggressive frequency reuse for high spectrum utilization [67]-[70]. Especially in multi-tier cellular networks (e.g. femtocell underlaid macro cell), cochannel interference from multiple interferers in other macro cells and neighboring femtocells causes unacceptable outage probability [71]-[72]. Hence, it is important to study the relation between signal-to-interference ratio (SIR) and outage probability.

Although the cochannel interference from multiple interferers affects the performance of two-way relay networks, there have been few works on the two-way relay network with multiple interferers. In [73], the authors derive the common outage probability of a two-way relay network with multiple interferers. However, the analytical result for the common outage probability of the two-way relay network has no closed-expression but does have a complicated integral expression, and the authors assume no interference at the relay. In [74], the authors derive the individual outage probability of a two-way relay network with multiple interferes. However, in order to simplify the performance analysis, they obtain the individual outage probability based on the upper bound of the signal-to-interference-plus-noise ratio.

In this chapter, we investigate the two-way relay network with multiple interferers over Rayleigh fading channels. We consider the interference model where both the users and the relay receive the interfering signals from multiple cochannel interferers. We derive the closed-form expression for the individual outage probability and the

exact integral expression for the common outage probability of the two-way relay network with multiple interferers. Analytical formulas are also verified by simulations.

2.1 System Model

Consider a two-way relay network with multiple interferers as shown in Fig. 2.1, where the solid and dotted lines stand for the desired signal and the interference, respectively. The users a and b exchange information each other by the help of a relay r. Assume that there is no direct path between the users a and b, and the users a, b, and the relay r receive the interfering signals from L_a, L_b, and L_r interferers, respectively.

Assume that the channel from the node i to the node j, $i, j \in \{a, b, r\}$, has the channel coefficient $h_{i,j}$ which is an independent zero-mean circularly symmetric complex Gaussian random variable with the variance $\lambda_{i,j}$. Assume that the variance $\lambda_{i,j}$ is given by $\lambda_{i,j} = \delta d_{i,j}^{-\nu}$ where δ is the attenuation parameter, $d_{i,j}$ is the distance from the node i to the node j, and ν is the path loss exponent [75]. Similarly, the channel from the lth interferer affecting the node i to the node i is characterized by the channel coefficient $g_{l,i}$ which is an independent zero-mean circularly symmetric complex Gaussian random variable with the variance $\mu_{l,i}$. Assume that the variance $\mu_{l,i}$ is given by $\mu_{l,i} = \delta d_{l,i}^{-\nu}$ where $d_{l,i}$ is the distance from the lth interferer affecting the node i to the node i. Assume that the channels are reciprocal, i.e., $h_{i,j} = h_{j,i}$ and $g_{l,i} = g_{i,l}$.

Assume that the users a and b communicate with each other in two phases:

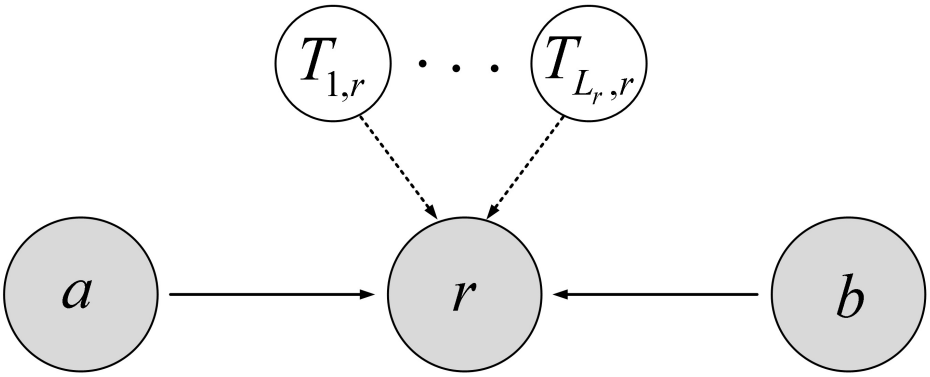

(a) Multiple access phase

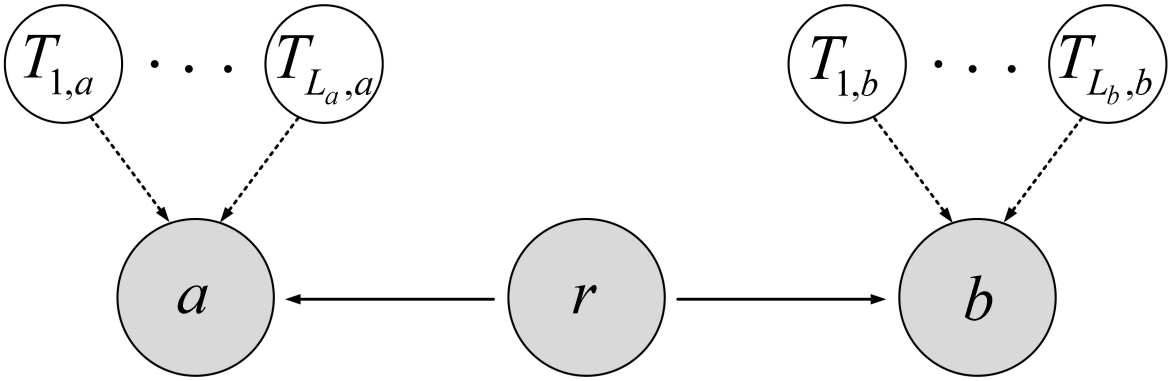

(b) Broadcast phase

Figure 2.1. Two-way relay network with multiple interferers, where the users a and b exchange information with each other by the help of a relay r.

Multiple-access (MA) and broadcast (BC) phases. In the MA phase, to equalize the channels $h_{a,r}$ and $h_{b,r}$, the users a and b multiply their symbols with the equalization coefficients $c_{a,r}$ and $c_{b,r}$, respectively, which are chosen as $c_{a,r} = \frac{h^*_{r,a}}{|h_{r,a}|^2}$ and $c_{b,r} = \frac{h^*_{r,b}}{\left|h_{r,b}\right|^2}$ [76]. And then, they transmit their symbols to the relay r simultaneously. The relay r receives the transmitted symbols from the two users along with the interfering symbols from L_r interferers.

The received signal at the relay r is given by

$$\begin{aligned} y_r &= h_{a,r}c_{a,r}x_a + h_{b,r}c_{b,r}x_b + \sum_{l=1}^{L_r} g_{l,r}x_{l,r} + v_r \\ &= x_a + x_b + \sum_{l=1}^{L_r} g_{l,r}x_{l,r} + v_r \end{aligned} \tag{2.1}$$

where x_i, $i \in \{a, b, r\}$, is the transmitted symbol from the node i, $x_{l,i}$ is the interfering symbol from the lth interferer affecting the node i, and v_i is the additive white Gaussian noise (AWGN) at the node i.

In the BC phase, the relay r amplifies and forwards its received signal to the users a and b. The received signals at the users a and b are given by

$$\begin{aligned} y_a = h_{r,a}\alpha_r x_a + h_{r,a}\alpha_r x_b + h_{r,a}\alpha_r \sum_{l=1}^{L_r} g_{l,r}x_{l,r} \\ + h_{r,a}\alpha_r v_r + \sum_{l=1}^{L_a} g_{l,a}x_{l,a} + v_a \end{aligned} \tag{2.2}$$

and

$$\begin{aligned} y_b = h_{r,b}\alpha_r x_a + h_{r,b}\alpha_r x_b + h_{r,b}\alpha_r \sum_{l=1}^{L_r} g_{l,r}x_{l,r} \\ + h_{r,b}\alpha_r v_r + \sum_{l=1}^{L_b} g_{l,b}x_{l,b} + v_b, \end{aligned} \tag{2.3}$$

respectively, where α_r is the amplification factor of the fixed-gain relay r [77]. Assuming perfect self-interference cancelation at the users a and b, the users a and b extract the symbols x_b and x_a from y_a and y_b, respectively [20].

The users and the relays are corrupted by cochannel interference and thermal noise. However, the level of cochannel interference is high enough compared to the level of thermal noise and so that the thermal noise is neglected as in all interference-limited environments [78]-[81]. Thus, the SIR is used for the performance analysis. After perfect self-interference cancelation, SIRs at the users a and b are given by

$$\begin{aligned}\Gamma_{b,r,a} &= \frac{|h_{r,a}|^2\alpha_r^2 P_b}{|h_{r,a}|^2\alpha_r^2\sum_{l=1}^{L_r}|g_{l,r}|^2P_{l,r}+\sum_{l=1}^{L_a}|g_{l,a}|^2P_{l,a}} \\ &= \left(\frac{\sum_{l=1}^{L_r}|g_{l,r}|^2P_{l,r}}{P_b}+\frac{\sum_{l=1}^{L_a}|g_{l,a}|^2P_{l,a}}{|h_{r,a}|^2\alpha_r^2P_b}\right)^{-1} \\ &= (X_{b,r}+Y_{b,r,a})^{-1} \end{aligned} \tag{2.4}$$

and

$$\begin{aligned}\Gamma_{a,r,b} &= \frac{|h_{r,b}|^2\alpha_r^2 P_a}{|h_{r,b}|^2\alpha_r^2\sum_{l=1}^{L_r}|g_{l,r}|^2P_{l,r}+\sum_{l=1}^{L_b}|g_{l,b}|^2P_{l,b}} \\ &= \left(\frac{\sum_{l=1}^{L_r}|g_{l,r}|^2P_{l,r}}{P_a}+\frac{\sum_{l=1}^{L_b}|g_{l,b}|^2P_{l,b}}{|h_{r,b}|^2\alpha_r^2P_a}\right)^{-1} \\ &= (X_{a,r}+Y_{a,r,b})^{-1}, \end{aligned} \tag{2.5}$$

respectively, where P_i and $P_{l,i}$ are the transmit power of the node i and its lth interferer, respectively, $X_{i,j} = \sum_{l=1}^{L_j} \frac{\left|g_{l,j}\right|^2 P_{l,j}}{P_i}$, and $Y_{i,j,k} = \frac{X_{i,k}}{\left|h_{j,k}\right|^2 \alpha_j^2}$ for $i, j, k \in \{a, b, r\}$.

2.2 Outage Probability Derivation

2.2.1 Moment Generating Functions

From the probability density functions (PDFs) of the random variables $X_{i,j}$ and $Y_{i,j,k}$, we derive their moment generating functions (MGFs).

The PDF of $X_{i,j}$ is given by

$$f_{X_{i,j}}(x) = \sum_{l=1}^{\rho(\mathbf{\Omega}_{i,j})} \sum_{m=1}^{\tau_l(\mathbf{\Omega}_{i,j})} \chi_{l,m}\left(\mathbf{\Omega}_{i,j}\right) \frac{\Omega_{i,j,[l]}^{-m}}{\Gamma\left(m\right)} x^{m-1} \exp\left(-\frac{x}{\Omega_{i,j,[l]}}\right) \tag{2.6}$$

where $\mathbf{\Omega}_{i,j} = \operatorname{diag}\left(\frac{\mu_{1,j}P_{1,j}}{P_i}, \frac{\mu_{2,j}P_{2,j}}{P_i}, \cdots, \frac{\mu_{L_j,j}P_{L_j,j}}{P_i}\right)$, $\rho(\mathbf{\Omega}_{i,j})$ is the number of distinct diagonal elements of $\mathbf{\Omega}_{i,j}$, $\Omega_{i,j,[l]}$, $l = 1, 2, \cdots, \rho(\mathbf{\Omega}_{i,j})$, are the distinct diagonal elements of $\mathbf{\Omega}_{i,j}$ in decreasing order, i.e., $\Omega_{i,j,[1]} > \Omega_{i,j,[2]} > \cdots > \Omega_{i,j,[\rho(\mathbf{\Omega}_{i,j})]}$, $\tau_l(\mathbf{\Omega}_{i,j})$ is the multiplicity of $\Omega_{i,j,[l]}$, $\Gamma\left(m\right)$ is the Gamma function defined as $\Gamma\left(m\right) = (m-1)!$ for a positive integer m, and the characteristic coefficient $\chi_{l,m}\left(\mathbf{\Omega}_{i,j}\right)$ is given by [82], [83]

$$\begin{aligned}\chi_{l,m}\left(\mathbf{\Omega}_{i,j}\right) = &\frac{1}{\left(\tau_l\left(\mathbf{\Omega}_{i,j}\right) - m\right)! \Omega_{i,j,[l]}^{\tau_l(\mathbf{\Omega}_{i,j})-m}} \\ &\times \left\{ \frac{d^{\tau_l(\mathbf{\Omega}_{i,j})-m}}{dx^{\tau_l(\mathbf{\Omega}_{i,j})-m}} \left(1 + x\Omega_{i,j,[l]}\right)^{\tau_l(\mathbf{\Omega}_{i,j})} \det\left(\mathbf{I}_{L_j} + x\mathbf{\Omega}_{i,j}\right)^{-1} \right\} \Bigg|_{x=-\frac{1}{\Omega_{i,j,[l]}}}.\end{aligned} \tag{2.7}$$

The Laplace transform of $f_{X_{i,j}}(x)$ is given by

$$\begin{aligned}\Phi_{X_{i,j}}(s) &= \int_0^\infty e^{-sx} f_{X_{i,j}}(x)dx \\ &= \sum_{l=1}^{\rho(\mathbf{\Omega}_{i,j})} \sum_{m=1}^{\tau_l(\mathbf{\Omega}_{i,j})} \chi_{l,m}(\mathbf{\Omega}_{i,j}) \frac{\Omega_{i,j,[l]}^{-m}}{\Gamma(m)} \int_0^\infty e^{-sx} x^{m-1} e^{-\frac{x}{\Omega_{i,j,[l]}}} dx \\ &= \sum_{l=1}^{\rho(\mathbf{\Omega}_{i,j})} \sum_{m=1}^{\tau_l(\mathbf{\Omega}_{i,j})} \chi_{l,m}(\mathbf{\Omega}_{i,j}) \Omega_{i,j,[l]}^{-m} \left(s + \frac{1}{\Omega_{i,j,[l]}}\right)^{-m} \end{aligned} \tag{2.8}$$

where the last equality follows from the fact that $\int_0^\infty e^{-vt} t^{u-1} e^{-\rho t} dt = \Gamma(u)(v+\rho)^{-u}$ in [84, eq. (4.5.3)]. The MGF of $X_{i,j}$ is given by $\mathcal{M}_{X_{i,j}}(s) = \Phi_{X_{i,j}}(-s)$.

Define $Z_{i,j,k} \triangleq 1/Y_{i,j,k} = |h_{j,k}|^2 \alpha_j^2 / X_{i,k}$. The cumulative distribution function (CDF) of $Z_{i,j,k}$ is given by

$$\begin{aligned}F_{Z_{i,j,k}}(z) &= \Pr\left(\frac{|h_{j,k}|^2 \alpha_j^2}{X_{i,k}} \leq z\right) \\ &= \mathbb{E}_{X_{i,k}}\left[F_{Z_{i,j,k}|X_{i,k}}(z)\right] \\ &= \mathbb{E}_{X_{i,k}}\left[1 - \exp\left(-\frac{zX_{i,k}}{\lambda_{j,k}\alpha_j^2}\right)\right] \\ &= 1 - \sum_{l=1}^{\rho(\mathbf{\Omega}_{i,k})} \sum_{m=1}^{\tau_l(\mathbf{\Omega}_{i,k})} \chi_{l,m}(\mathbf{\Omega}_{i,k}) \frac{\Omega_{i,k,[l]}^{-m}}{\Gamma(m)} \\ &\qquad \times \int_0^\infty x^{m-1} \exp\left\{-\left(\frac{z}{\lambda_{j,k}\alpha_j^2} + \frac{1}{\Omega_{i,k,[l]}}\right)x\right\} dx \\ &= 1 - \sum_{l=1}^{\rho(\mathbf{\Omega}_{i,k})} \sum_{m=1}^{\tau_l(\mathbf{\Omega}_{i,k})} \chi_{l,m}(\mathbf{\Omega}_{i,k}) \left(1 + \frac{\Omega_{i,k,[l]}}{\lambda_{j,k}\alpha_j^2} z\right)^{-m} \end{aligned} \tag{2.9}$$

where the last equality follows from the fact that $\int_0^\infty t^{u-1} e^{-vt} dt = \frac{1}{v^u}\Gamma(u)$ in [62, eq. (3.381.4)].

The PDF of $Z_{i,j,k}$ is given by

$$f_{Z_{i,j,k}}(z) = \frac{\partial F_{Z_{i,j,k}}(z)}{\partial z} = \sum_{l=1}^{\rho(\mathbf{\Omega}_{i,k})} \sum_{m=1}^{\tau_l(\mathbf{\Omega}_{i,k})} \chi_{l,m}(\mathbf{\Omega}_{i,k}) \frac{m\Omega_{i,k,[l]}}{\lambda_{j,k}\alpha_j^2} \left(1 + \frac{\Omega_{i,k,[l]}}{\lambda_{j,k}\alpha_j^2} z\right)^{-m-1}. \quad (2.10)$$

By using [85, Ch. 5.2], the PDF of $Y_{i,j,k}$ is given by

$$f_{Y_{i,j,k}}(y) = \frac{1}{y^2} f_{Z_{i,j,k}}\left(\frac{1}{y}\right) = \frac{1}{y^2} \sum_{l=1}^{\rho(\mathbf{\Omega}_{i,k})} \sum_{m=1}^{\tau_l(\mathbf{\Omega}_{i,k})} \chi_{l,m}(\mathbf{\Omega}_{i,k}) m \left(\frac{\lambda_{j,k}\alpha_j^2}{\Omega_{i,k,[l]}}\right)^m \left(\frac{1}{y} + \frac{\lambda_{j,k}\alpha_j^2}{\Omega_{i,k,[l]}}\right)^{-m-1}. \quad (2.11)$$

The Laplace transform of $f_{Y_{i,j,k}}(y)$ is given by

$$\begin{aligned}\Phi_{Y_{i,j,k}}(s) &= \int_0^\infty e^{-sy} f_{Y_{i,j,k}}(y) dy \\ &= \sum_{l=1}^{\rho(\mathbf{\Omega}_{i,k})} \sum_{m=1}^{\tau_l(\mathbf{\Omega}_{i,k})} \chi_{l,m}(\mathbf{\Omega}_{i,k}) m \left(\frac{\Omega_{i,k,[l]}}{\lambda_{j,k}\alpha_j^2}\right) \int_0^\infty e^{-sy} y^{m-1} \left(y + \frac{\Omega_{i,k,[l]}}{\lambda_{j,k}\alpha_j^2}\right)^{-m-1} dy \\ &= \sum_{l=1}^{\rho(\mathbf{\Omega}_{i,k})} \sum_{m=1}^{\tau_l(\mathbf{\Omega}_{i,k})} \chi_{l,m}(\mathbf{\Omega}_{i,k}) m\Gamma(m) \Psi\left(m, 0; \frac{s\Omega_{i,k,[l]}}{\lambda_{j,k}\alpha_j^2}\right) \quad (2.12)\end{aligned}$$

where the last equality follows from the fact that $\int_0^\infty e^{-ut} t^v (t+\xi)^\rho dt = \Gamma(v+1)\xi^{v+\rho+1} \times \Psi(v+1, v+\rho+2; u\xi)$ in [86, vol. 4, eq. (2.1.3.1)]. The MGF of $Y_{i,j,k}$ is given by $\mathcal{M}_{Y_{i,j,k}}(s) = \Phi_{Y_{i,j,k}}(-s)$.

2.2.2 Individual Outage Probability

We derive the outage probabilities of the users a and b using the MGF-based approach [87].

Define $W_{b,r,a} \triangleq 1/\Gamma_{b,r,a} = X_{b,r} + Y_{b,r,a}$. Since $X_{b,r}$ and $Y_{b,r,a}$ are independent, the MGF of $W_{b,r,a}$ is given by

$$\mathcal{M}_{W_{b,r,a}}(s) = \mathcal{M}_{X_{b,r}}(s)\,\mathcal{M}_{Y_{b,r,a}}(s). \tag{2.13}$$

By the integration property of Laplace transform [62], the CDF of $W_{b,r,a}$ is given by

$$\begin{aligned} F_{W_{b,r,a}}(w) &= \mathcal{L}^{-1}\left[\frac{\mathcal{M}_{W_{b,r,a}}(-s)}{s}\right] \\ &= \sum_{l=1}^{\rho(\mathbf{\Omega}_{b,r})}\sum_{m=1}^{\tau_l(\mathbf{\Omega}_{b,r})}\sum_{p=1}^{\rho(\mathbf{\Omega}_{b,a})}\sum_{q=1}^{\tau_p(\mathbf{\Omega}_{b,a})}\chi_{l,m}(\mathbf{\Omega}_{b,r})\,\chi_{p,q}(\mathbf{\Omega}_{b,a})q\Gamma(q)\,\Omega_{b,r,[l]}^{-m} \\ &\quad\times\mathcal{L}^{-1}\left[s^{-1}\left(s+\frac{1}{\Omega_{b,r,[l]}}\right)^{-m}\Psi\left(q,0;\frac{s\Omega_{b,a,[p]}}{\lambda_{r,a}\alpha_r^2}\right)\right]. \end{aligned} \tag{2.14}$$

By combining [86, vol. 5, eq. (3.34.1.1)] and [86, vol. 5, eq. (1.1.1.12)], we obtain

$$\begin{aligned} &\mathcal{L}^{-1}\left[s^u(s-v)^\rho\Psi(\eta,\xi;\varpi s)\right] \\ &\quad= \int_0^{\varphi}(\varphi-t)^{-u-\rho-1}\frac{t^{\eta-1}(\varpi+t)^{\xi-\eta-1}}{\varpi^{\xi-1}\Gamma(-u-\rho)\,\Gamma(\eta)}{}_1F_1(-\rho;-u-\rho;v(\varphi-t))dt. \end{aligned} \tag{2.15}$$

where ${}_1F_1(\cdot)$ is the hypergeometric function defined in [86, vol. 3, eq. (7.2.2.1)]. From (2.14) and (2.15), it becomes

$$\begin{aligned} F_{W_{b,r,a}}(w) &= \sum_{l=1}^{\rho(\mathbf{\Omega}_{b,r})}\sum_{m=1}^{\tau_l(\mathbf{\Omega}_{b,r})}\sum_{p=1}^{\rho(\mathbf{\Omega}_{b,a})}\sum_{q=1}^{\tau_p(\mathbf{\Omega}_{b,a})}\chi_{l,m}(\mathbf{\Omega}_{b,r})\,\chi_{p,q}(\mathbf{\Omega}_{b,a})\frac{q\Omega_{b,r,[l]}^{-m}\Omega_{b,a,[p]}}{\lambda_{r,a}\alpha_r^2\Gamma(m+1)} \\ &\quad\times\int_0^{w}t^{q-1}\left(t+\frac{\Omega_{b,a,[p]}}{\lambda_{r,a}\alpha_r^2}\right)^{-q-1}(w-t)^m{}_1F_1\left(m;m+1;-\frac{1}{\Omega_{b,r,[l]}}(w-t)\right)dt. \end{aligned} \tag{2.16}$$

Using ${}_1F_1(u;u+1;v) = \frac{(-1)^u u!}{v^u}\left\{1-e^v\sum_{\rho=0}^{u-1}\frac{(-1)^\rho v^\rho}{\rho!}\right\}$ in [86, vol. 3, eq. (7.11.1.13)] and the binomial expansion, i.e., $(u+v)^\eta = \sum_{\rho=0}^{\eta}\binom{\eta}{\rho}v^\rho u^{\eta-\rho}$, in [62, eq. (1.111)],

(2.16) is rewritten as

$$F_{W_{b,r,a}}(w) = \sum_{l=1}^{\rho(\mathbf{\Omega}_{b,r})} \sum_{m=1}^{\tau_l(\mathbf{\Omega}_{b,r})} \sum_{p=1}^{\rho(\mathbf{\Omega}_{b,a})} \sum_{q=1}^{\tau_p(\mathbf{\Omega}_{b,a})} \chi_{l,m}(\mathbf{\Omega}_{b,r}) \chi_{p,q}(\mathbf{\Omega}_{b,a}) q \frac{\Omega_{b,a,[p]}}{\lambda_{r,a}\alpha_r^2}$$
$$\times \int_0^w t^{q-1} \left(t + \frac{\Omega_{b,a,[p]}}{\lambda_{r,a}\alpha_r^2}\right)^{-q-1} \left\{1 - \sum_{\sigma=1}^{m-1} \sum_{\kappa=0}^{\sigma} \frac{(-1)^\kappa w^{\sigma-\kappa} e^{-\frac{1}{\Omega_{b,r,[l]}}(w-t)}}{\Omega_{b,r,[l]}^\sigma \kappa!\,(\sigma-\kappa)! t^{-\kappa}}\right\} dt. \quad (2.17)$$

Using $\int \frac{t^u e^{vt}}{(t+\xi)^\rho} dt = (-1)^u \xi^u e^{-v\xi} \sum_{\varpi=0}^{u} \frac{(-1)^\varpi}{\xi^\varpi} \binom{u}{\varpi} \int x^{\varpi-\rho} e^{vx} dx$ for $x = t + \xi$ in [86, vol. 1, eq. (1.3.2.23)], $\int \frac{e^{vt}}{t^u} dt = -e^{vt} \sum_{\varpi=1}^{u-1} \frac{v^{\varpi-1}}{(u-1)(u-2)\cdots(u-\varpi)t^{u-\varpi}} + \frac{v^{u-1}}{(u-1)!} \mathrm{Ei}(vt)$ in [86, vol. 1, eq. (1.3.2.11)], and $\int t^u e^{vt} dt = e^{vt} \left\{\frac{t^u}{v} + \sum_{\varpi=1}^{u} (-1)^\varpi \frac{u(u-1)\cdots(u-\varpi+1)}{v^{\varpi+1}} t^{u-\varpi}\right\}$ in [86, vol. 1, eq. (1.3.2.6)], (2.17) becomes

$$F_{W_{b,r,a}}(w) = \sum_{l=1}^{\rho(\mathbf{\Omega}_{b,r})} \sum_{m=1}^{\tau_l(\mathbf{\Omega}_{b,r})} \sum_{p=1}^{\rho(\mathbf{\Omega}_{b,a})} \sum_{q=1}^{\tau_p(\mathbf{\Omega}_{b,a})} \chi_{l,m}(\mathbf{\Omega}_{b,r}) \chi_{p,q}(\mathbf{\Omega}_{b,a}) \left\{\Xi_{p,q}\left(w + \frac{\Omega_{b,a,[p]}}{\lambda_{r,a}\alpha_r^2}\right)\right.$$
$$\left. - \Xi_{p,q}\left(\frac{\Omega_{b,a,[p]}}{\lambda_{r,a}\alpha_r^2}\right) - \Upsilon_{l,m,p,q}\left(w + \frac{\Omega_{b,a,[p]}}{\lambda_{r,a}\alpha_r^2}\right) + \Upsilon_{l,m,p,q}\left(\frac{\Omega_{b,a,[p]}}{\lambda_{r,a}\alpha_r^2}\right)\right\} \quad (2.18)$$

where

$$\Xi_{p,q}(x) = \sum_{\sigma=0}^{q-1} \frac{(-1)^{\sigma+q-1} q!}{\sigma!\,(q-1-\sigma)!\,(\sigma-q)} \left(\frac{\Omega_{b,a,[p]}}{\lambda_{r,a}\alpha_r^2}\right)^{q-\sigma} x^{\sigma-q}, \quad (2.19)$$

$$\Upsilon_{l,m,p,q}(x) = \sum_{\sigma=1}^{m-1} \sum_{\kappa=0}^{\sigma} \sum_{f=0}^{\kappa+q-1} \frac{(-1)^{f+q-1} q\,(\kappa+q-1)!(w)^{\sigma-\kappa}}{\kappa! f!\,(\sigma-\kappa)!\,(\kappa+q-1-f)!} \left(\frac{1}{\Omega_{b,r,[l]}}\right)^\sigma$$
$$\times \left(\frac{\Omega_{b,a,[p]}}{\lambda_{r,a}\alpha_r^2}\right)^{\kappa+q-f} \exp\left\{-\frac{1}{\Omega_{b,r,[l]}}\left(\frac{\Omega_{b,a,[p]}}{\lambda_{r,a}\alpha_r^2} + w\right)\right\} \Lambda_{l,q,f}(x), \quad (2.20)$$

$$\Lambda_{l,q,f}(x)=\begin{cases} e^{\frac{1}{\Omega_{b,r,[l]}}x}\left\{\frac{x^{f-q-1}}{\left(\Omega_{b,r,[l]}\right)^{-1}}+\sum\limits_{\varepsilon=1}^{f-q-1}(-1)^{\varepsilon}\frac{\prod_{\psi=1}^{\varepsilon}(f-q-\psi)}{\left(\Omega_{b,r,[l]}\right)^{-\varepsilon-1}x^{\varepsilon-f+q+1}}\right\}, & f>q+1 \\ \Omega_{b,r,[l]}e^{\frac{1}{\Omega_{b,r,[l]}}x}, & f=q+1 \\ \mathrm{Ei}\left(\frac{1}{\Omega_{b,r,[l]}}x\right), & f=q \\ -e^{\frac{1}{\Omega_{b,r,[l]}}x}\sum\limits_{\varepsilon=1}^{q-f}\frac{\left(\Omega_{b,r,[l]}\right)^{1-\varepsilon}x^{\varepsilon+f-q-1}}{\prod_{\psi=1}^{\varepsilon}(q-f+1-\psi)}+\frac{\left(\Omega_{b,r,[l]}\right)^{f-q}}{(q-f)!}\mathrm{Ei}\left(\frac{1}{\Omega_{b,r,[l]}}x\right), & f<q. \end{cases} \tag{2.21}$$

By using the definition of the individual outage [88], the outage probability of the user a is obtained as

$$\begin{aligned} P_{out,a}(\gamma_{th}) =& \Pr\left(\Gamma_{b,r,a}<\gamma_{th}\right) \\ =& \Pr\left(W_{b,r,a}>\frac{1}{\gamma_{th}}\right) \\ =& 1-F_{W_{b,r,a}}\left(\frac{1}{\gamma_{th}}\right) \end{aligned} \tag{2.22}$$

where γ_{th} is a SIR threshold. In (2.22), the outage occurs when the SIR at the user a falls below a given γ_{th}. The outage probability of the user b can be obtained to be the same as that of the user a.

2.2.3 Common Outage Probability

Let $V_i \triangleq \sum_{l=1}^{L_i}|g_{l,i}|^2 P_{l,i}$. Then, the PDF of V_i is given by

$$f_{V_i}(v)=\sum_{l=1}^{\rho(\mathbf{\Sigma}_i)}\sum_{m=1}^{\tau_l(\mathbf{\Sigma}_i)}\chi_{l,m}\left(\mathbf{\Sigma}_i\right)\frac{\Sigma_{i,[l]}^{-m}}{\Gamma\left(m\right)}v^{m-1}\exp\left(-\frac{v}{\Sigma_{i,[l]}}\right) \tag{2.23}$$

where $\mathbf{\Sigma}_i=\mathrm{diag}\left(\mu_{1,i}P_{1,i},\mu_{2,i}P_{2,i},\cdots,\mu_{L_i,i}P_{L_i,i}\right)$, $\rho(\mathbf{\Sigma}_i)$ is the number of distinct diagonal elements of $\mathbf{\Sigma}_i$, $\Sigma_{i,[l]}$, $l=1,2,\cdots,\rho(\mathbf{\Sigma}_i)$, are the distinct diagonal elements of

$\mathbf{\Sigma}_i$ in decreasing order, i.e., $\Sigma_{i,[1]} > \Sigma_{i,[2]} > \cdots > \Sigma_{i,[\rho(\mathbf{\Sigma}_i)]}$, $\tau_l(\mathbf{\Sigma}_i)$ is the multiplicity of $\Sigma_{i,[l]}$, and the characteristic coefficient $\chi_{l,m}\left(\mathbf{\Sigma}_i\right)$ is given by [82], [83].

$$\chi_{l,m}\left(\mathbf{\Sigma}_i\right) = \frac{1}{\left(\tau_l\left(\mathbf{\Sigma}_i\right) - m\right)! \Sigma_{i,[l]}^{\tau_l(\mathbf{\Sigma}_i)-m}} \times \left\{ \frac{d^{\tau_l(\mathbf{\Sigma}_i)-m}}{dv^{\tau_l(\mathbf{\Sigma}_i)-m}} \left(1 + v\Sigma_{i,[l]}\right)^{\tau_l(\mathbf{\Sigma}_i)} \det\left(\mathbf{I}_{L_i} + v\mathbf{\Sigma}_i\right)^{-1} \right\} \Bigg|_{v=-\frac{1}{\Sigma_{i,[l]}}}. \tag{2.24}$$

By integrating (2.11) over the interval $[0, y]$, the CDF of $Y_{i,j,k}$ is given by

$$\begin{aligned} F_{Y_{i,j,k}}(y) &= \int_0^y f_{Y_{i,j,k}}(t)\, dt \\ &= \sum_{l=1}^{\rho\left(\mathbf{\Omega}_{i,k}\right)} \sum_{m=1}^{\tau_l\left(\mathbf{\Omega}_{i,k}\right)} \chi_{l,m}\left(\mathbf{\Omega}_{i,k}\right) \left(\frac{y}{y + \frac{\Omega_{i,k,[l]}}{\lambda_{j,k}\alpha_j^2}} \right)^m \end{aligned} \tag{2.25}$$

where the last equality follows from the fact that $\int \frac{(t+u)^\rho}{(t+v)^{\rho+2}} dt = \frac{1}{(\rho+1)(v-u)} \left(\frac{t+u}{t+v}\right)^{\rho+1}$ in [86, vol. 1, eq. (1.2.6.5)].

The common outage probability is given by [88]

$$
\begin{aligned}
&P_{out}\left(\gamma_{th}\right) \\
&= \Pr\left(\min\left(\gamma_{a,r,b}, \gamma_{b,r,a}\right) < \gamma_{th}\right) \\
&= \Pr\left(\min\left(\gamma_{a,r,b}, \gamma_{b,r,a}\right) < \gamma_{th}\right) \\
&= 1 - \Pr\left(\gamma_{a,r,b} > \gamma_{th}, \gamma_{b,r,a} > \gamma_{th}\right) \\
&= 1 - \Pr\left(Y_{a,r,b} < \frac{1}{\gamma_{th}} - \frac{V_r}{P_a}, Y_{b,r,a} < \frac{1}{\gamma_{th}} - \frac{V_r}{P_b}\right) \\
&= 1 - \mathbb{E}_{V_r}\left[F_{Y_{a,r,b}|V_r}\left(\frac{1}{\gamma_{th}} - \frac{V_r}{P_a}\right) F_{Y_{b,r,a}|V_r}\left(\frac{1}{\gamma_{th}} - \frac{V_r}{P_b}\right)\right] \\
&= 1 - \mathbb{E}_{V_r}\left[F_{Y_{a,r,b}}\left(\frac{1}{\gamma_{th}} - \frac{V_r}{P_a}\right) F_{Y_{b,r,a}}\left(\frac{1}{\gamma_{th}} - \frac{V_r}{P_b}\right)\right] \\
&= 1 - \sum_{l_1=1}^{\rho\left(\boldsymbol{\Omega}_{a,b}\right)\tau_{l_1}\left(\boldsymbol{\Omega}_{a,b}\right)} \sum_{m_1=1}^{\rho\left(\boldsymbol{\Omega}_{b,a}\right)\tau_{l_2}\left(\boldsymbol{\Omega}_{b,a}\right)} \sum_{l_2=1}^{\rho(\boldsymbol{\Sigma}_r)\tau_p(\boldsymbol{\Sigma}_r)} \sum_{m_2=1}^{} \sum_{p=1}^{} \sum_{q=1}^{} \frac{\chi_{l_1,m_1}\left(\boldsymbol{\Omega}_{a,b}\right)\chi_{l_2,m_2}\left(\boldsymbol{\Omega}_{b,a}\right)\chi_{p,q}\left(\boldsymbol{\Sigma}_r\right)}{\Omega_{r,[p]}^{q}\Gamma\left(q\right)} \\
&\quad \times \int_0^{\min\left(\frac{P_a}{\gamma_{th}}, \frac{P_b}{\gamma_{th}}\right)} \left(\frac{v - \frac{P_a}{\gamma_{th}}}{v - \beta_{1,l_1}}\right)^{m_1} \left(\frac{v - \frac{P_b}{\gamma_{th}}}{v - \beta_{2,l_2}}\right)^{m_2} v^{q-1} e^{-\frac{v}{\Omega_{r,[p]}}} dv
\end{aligned} \tag{2.26}
$$

where $\beta_{1,l_1} = \frac{P_a}{\gamma_{th}} + \frac{P_a \Omega_{a,b,[l_1]}}{\lambda_{r,b}\alpha_r^2}$ and $\beta_{2,l_2} = \frac{P_b}{\gamma_{th}} + \frac{P_b \Omega_{b,a,[l_2]}}{\lambda_{r,a}\alpha_r^2}$.

2.3 Numerical Results

Consider a two-way relay network with multiple interferers where the users a, b, and the relay r receive the interfering signals from L_a, L_b, and L_r interferers, respectively. Suppose that $\lambda_{i,j} = 1$, $\mu_{l,i} = 0.1, 1$, $\alpha_i = 1$, $P_i = P_T$, $P_{l,i} = P_I$, and $\zeta = P_T/P_I$ for $i, j \in \{a, b, r\}$ and $l = 1, 2, \cdots, L_i$.

The main contribution of this chapter is the derivation of the closed-form expression for the individual outage probability and the exact integral expression for the

common outage probability of the two-way relay network with multiple interferers. To provide insights into the impact of ζ on these outage probabilities, we assume that parameters except ζ have simple values such as $\lambda_{i,j} = 1$, $\mu_{l,i} = 0.1, 1$, and $\alpha_i = 1$ similar to [20], [64], [67], [69], [73], and [89]. Note that although these assumptions seem not realistic, they do not affect the accuracy of the analytical results. And since the analytical results are the function of the $\lambda_{i,j}$, $\mu_{l,i}$, and α_i, we can obtain more realistic results by changing the parameter values of $\lambda_{i,j}$, $\mu_{l,i}$, and α_i in (2.22) and (2.26).

Fig. 2.2 shows the individual outage probability versus ζ for the two-way relay network in the presence of cochannel interference with $L_a = L_b = L_r = 1, 2, \cdots, 4$ and $\mu_{l,i} = 1$. It is shown that the analytical results perfectly match the simulation results. It is shown that as ζ increases the individual outage probability decreases. It is shown that as γ_{th} increases the individual outage probability increases. Fig. 2.3 shows the individual outage probability versus ζ for the two-way relay network in the presence of cochannel interference with $L_a = L_b = L_r = 1, 2, \cdots, 4$ and $\mu_{l,i} = 0.1$. It is shown that the analytical results agree exactly with the simulation results of the individual outage probability. It is shown that as ζ increases the individual outage probability decreases. It is shown that as γ_{th} increases the individual outage probability increases. It is shown that the individual outage probability of Fig. 2.3 is lower than that of Fig. 2.2. The reason is that the variance of the channel between the terminals and the interferers become lower and the effect of the cochannel interference on the individual outage probability is reduced.

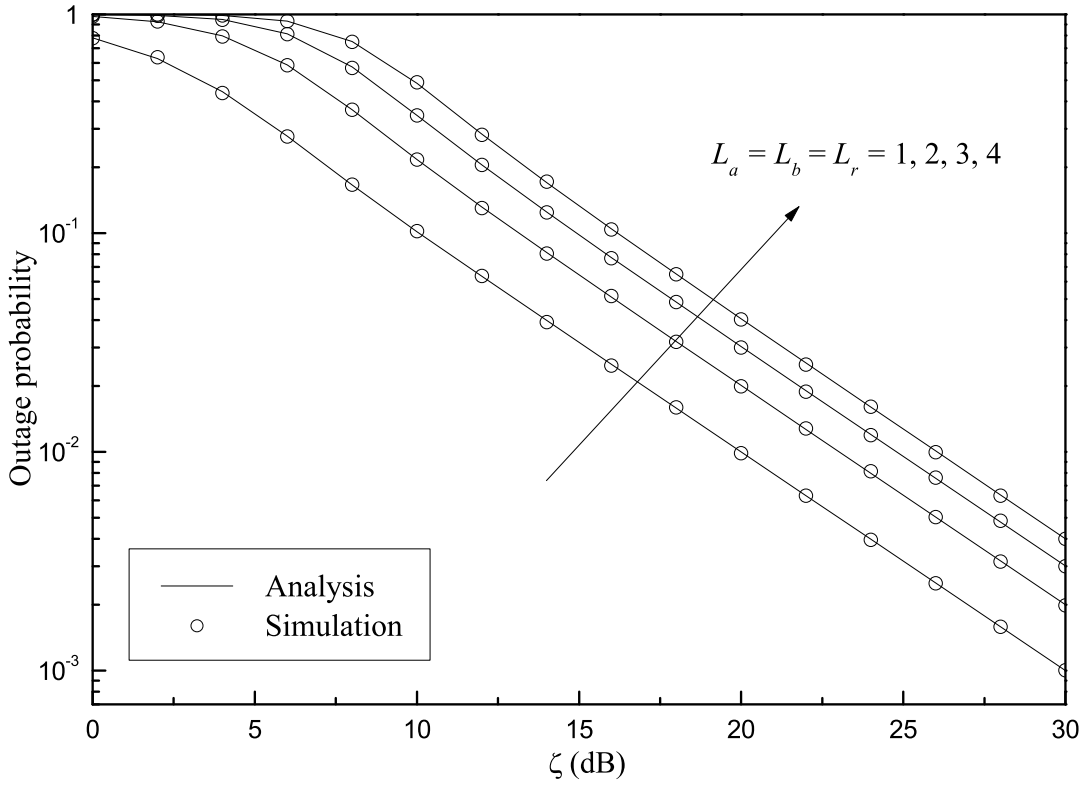

(a) $\gamma_{th} = 0$ dB

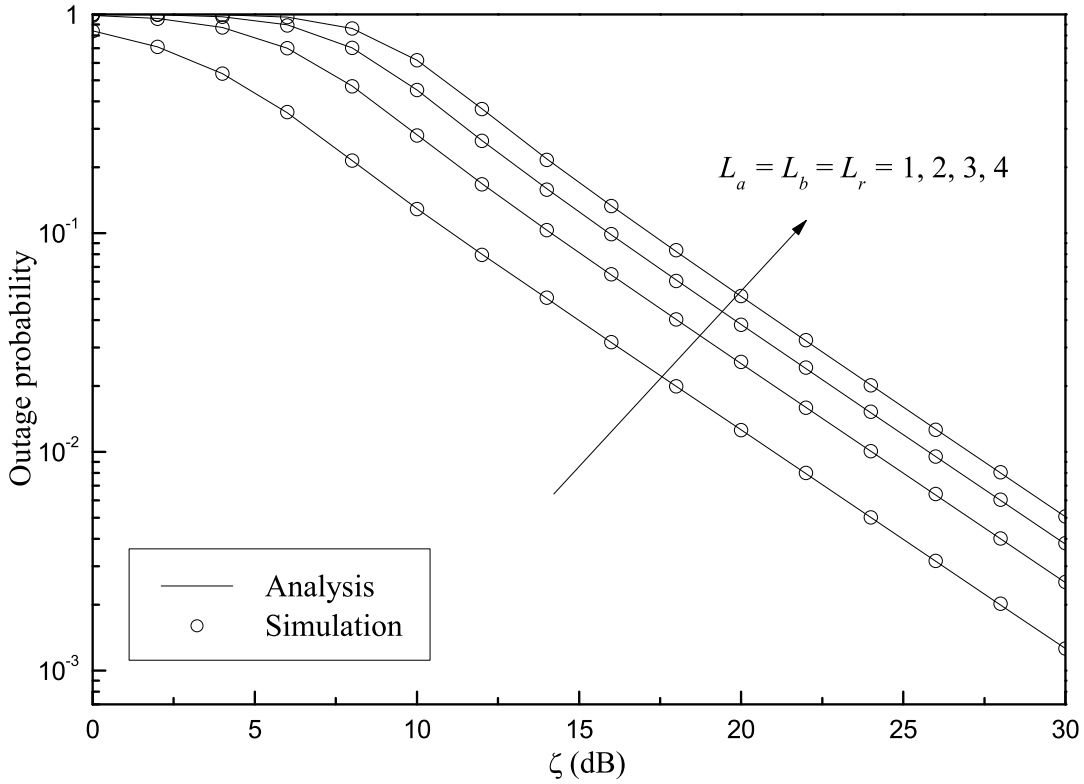

(b) $\gamma_{th} = 1$ dB

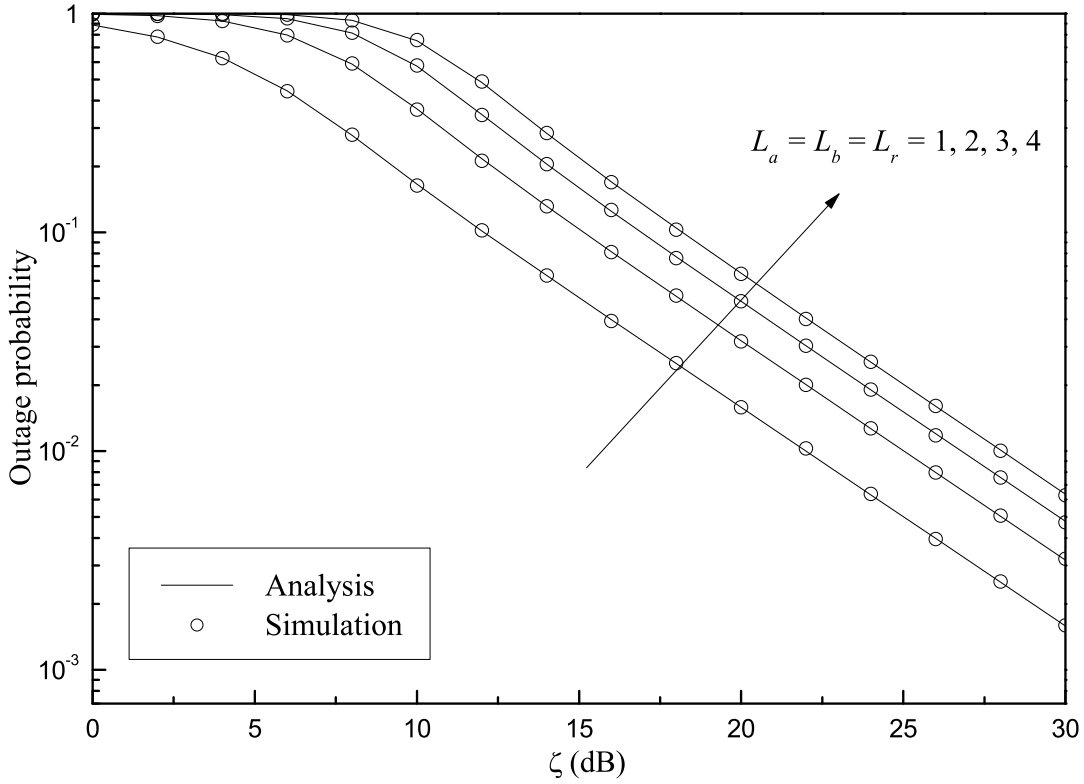

(c) $\gamma_{th} = 2$ dB

Figure 2.2. Individual outage probability versus ζ for various number of interferers. $\mu_{l,i} = 1$.

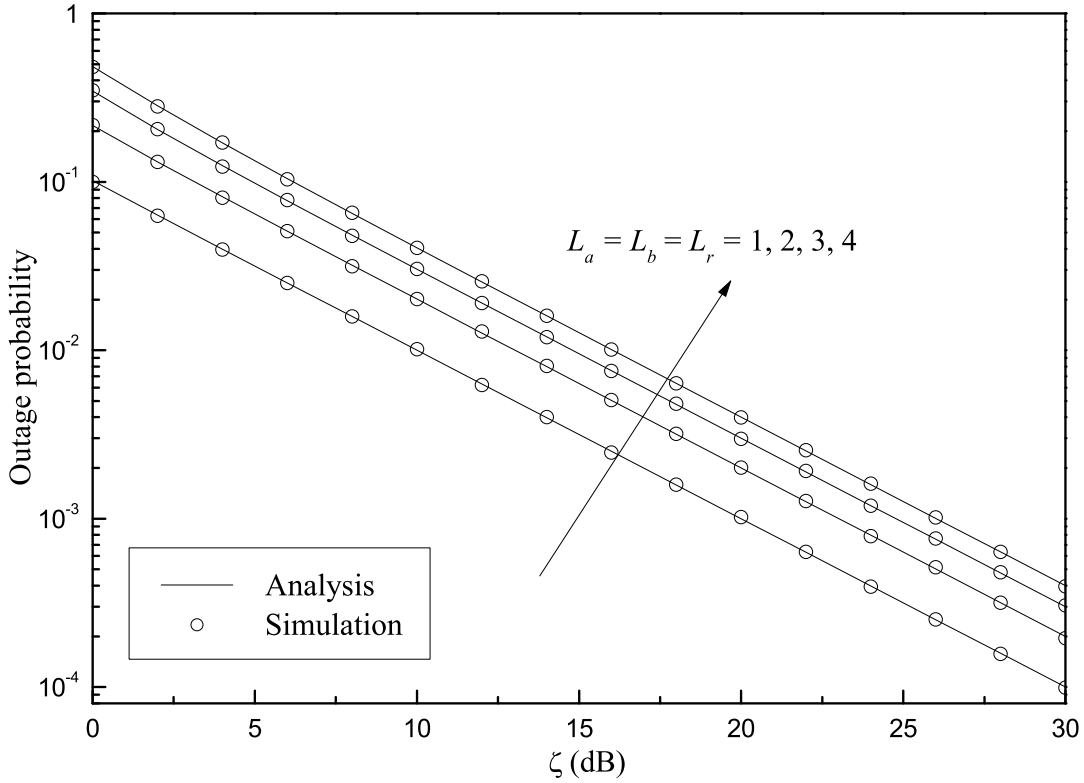

(a) $\gamma_{th} = 0$ dB

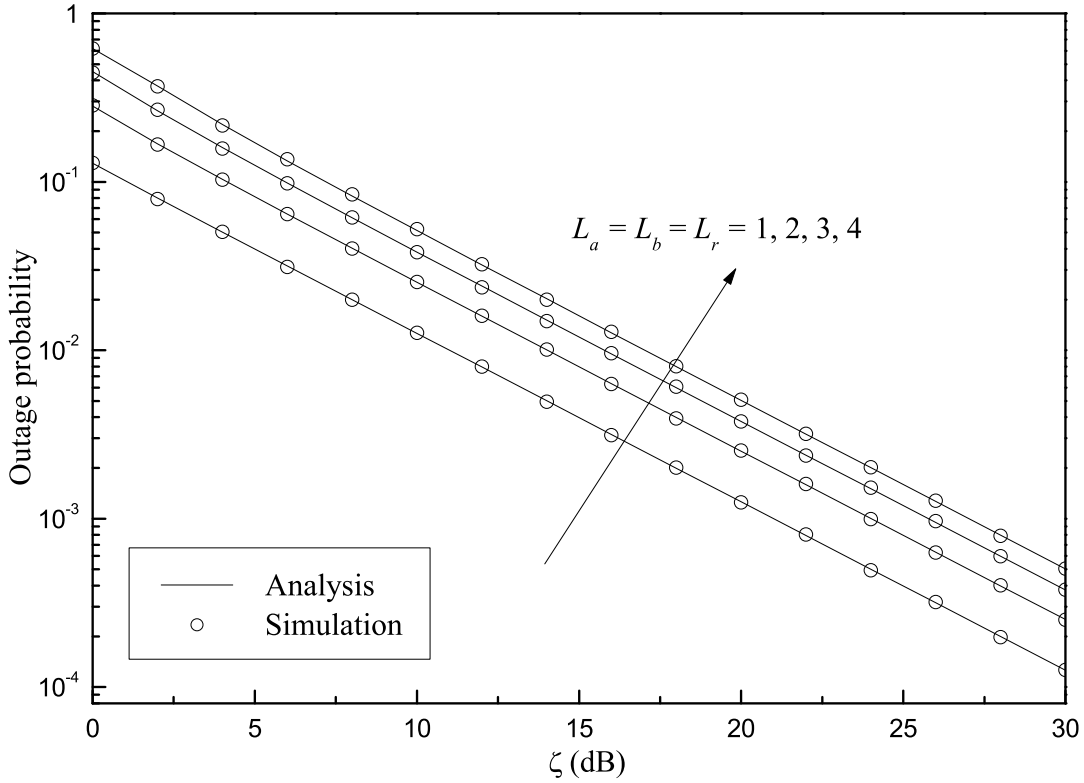

(b) $\gamma_{th} = 1$ dB

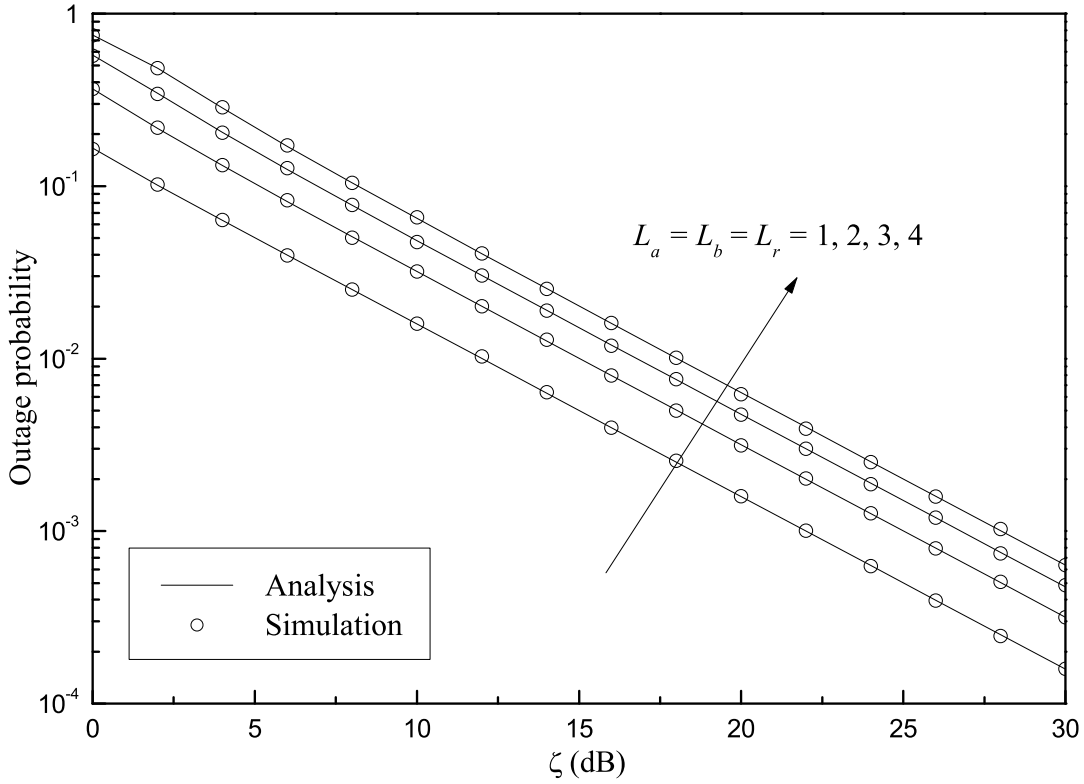

(c) $\gamma_{th} = 2$ dB

Figure 2.3. Individual outage probability versus ζ for various number of interferers. $\mu_{l,i} = 0.1$.

Fig. 2.4 shows the individual outage probability versus γ_{th} for the two-way relay network in the presence of cochannel interference with $L_a = L_b = L_r = 1, 2, \cdots, 4$ and $\mu_{l,i} = 0.1$. As expected, it is shown that as γ_{th} increases the individual outage probability increases. It is shown that as ζ increases the individual outage probability decreases. It is shown that the analytical results and the simulation results are in perfect agreement.

Fig. 2.5 shows the common outage probability versus ζ for the two-way relay network in the presence of cochannel interference with $L_a = L_b = L_r = 1, 2, \cdots, 4$ and $\mu_{l,i} = 1$. It is shown that as ζ increases the common outage probability decreases. It is shown that as γ_{th} increases the common outage probability increases. It is shown that the analytical results and the simulation results are in complete agreement. Fig. 2.6 shows the common outage probability versus ζ for the two-way relay network in the presence of cochannel interference with $L_a = L_b = L_r = 1, 2, \cdots, 4$ and $\mu_{l,i} = 1$. As expected, it is shown that the common outage probability decreases as ζ increases. It is shown that the common outage probability decreases as γ_{th} decreases. It is shown that the analytical results perfectly match the simulation results. It is shown that the common outage probability of Fig. 2.6 is lower than that of Fig. 2.5. Since the variance of the channel between the terminals and the interferers become lower, the effect of the cochannel interference on the common outage probability is reduced.

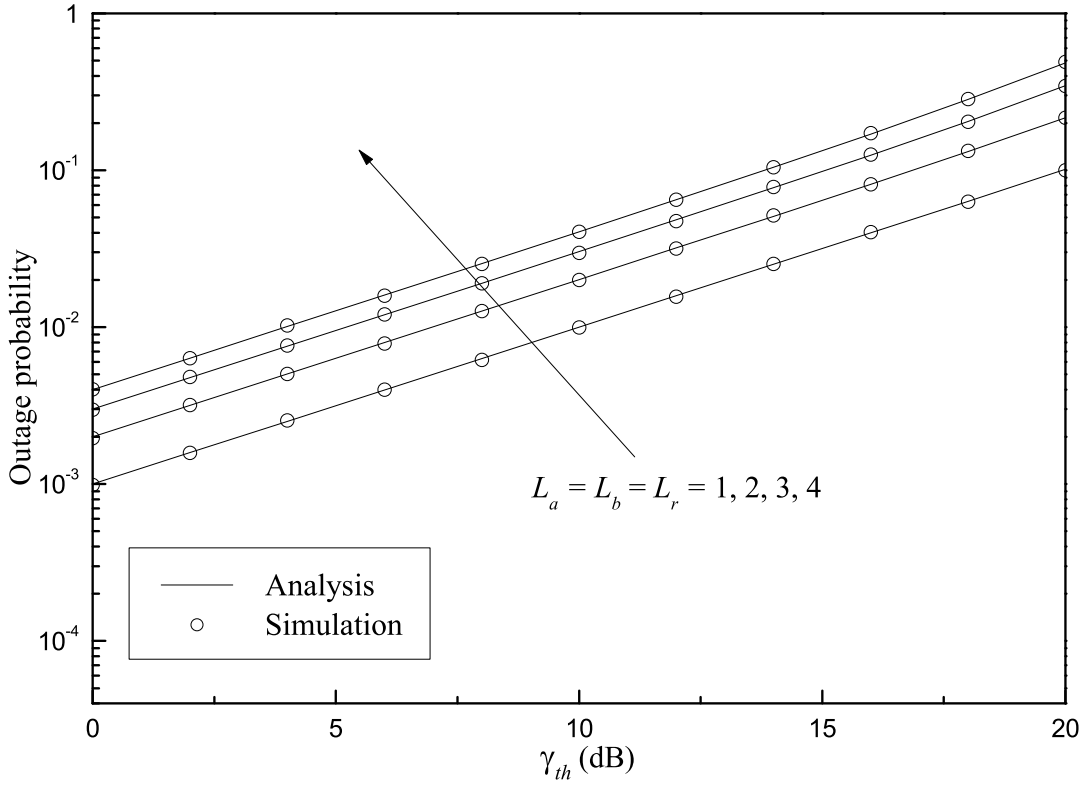
1
10^{-1}
10^{-2}
10^{-3}
10^{-4}
Outage probability
0
5
10
15
20
γ_{th} (dB)
$L_a = L_b = L_r$ = 1, 2, 3, 4
Analysis
Simulation

(a) $\zeta = 20$ dB

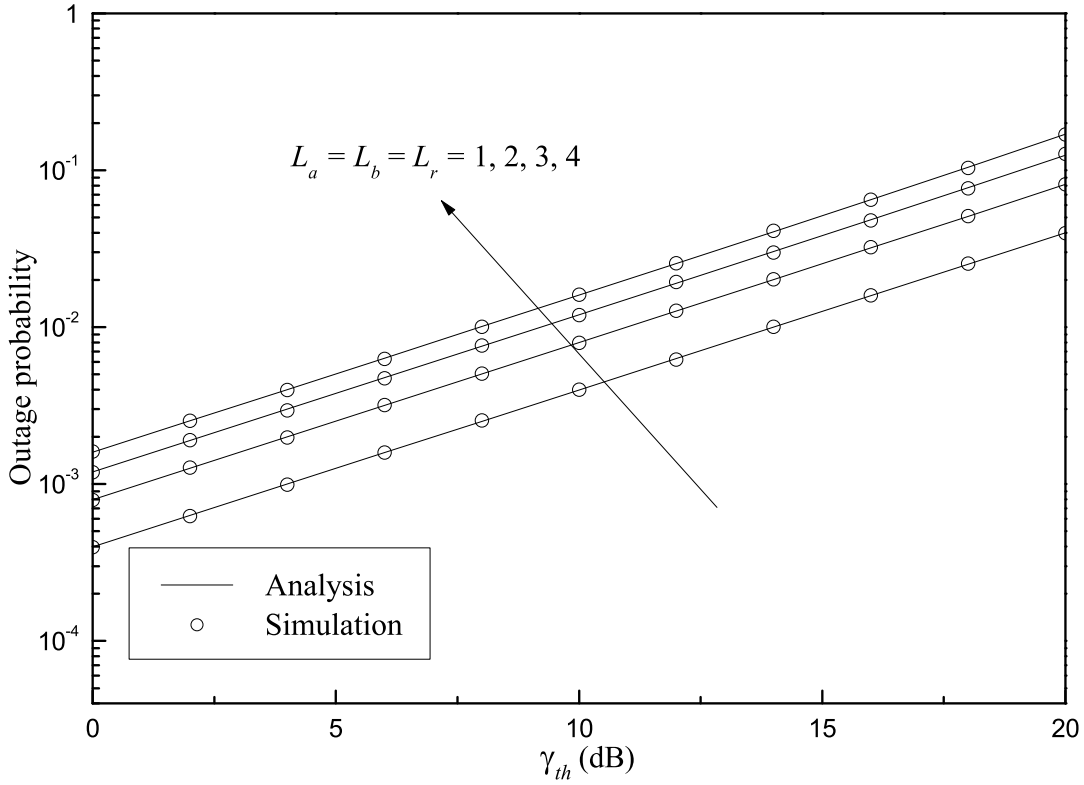
1
10^{-1}
10^{-2}
10^{-3}
10^{-4}
Outage probability
$L_a = L_b = L_r$ = 1, 2, 3, 4
Analysis
Simulation
0
5
10
15
20
γ_{th} (dB)

(b) $\zeta = 24$ dB

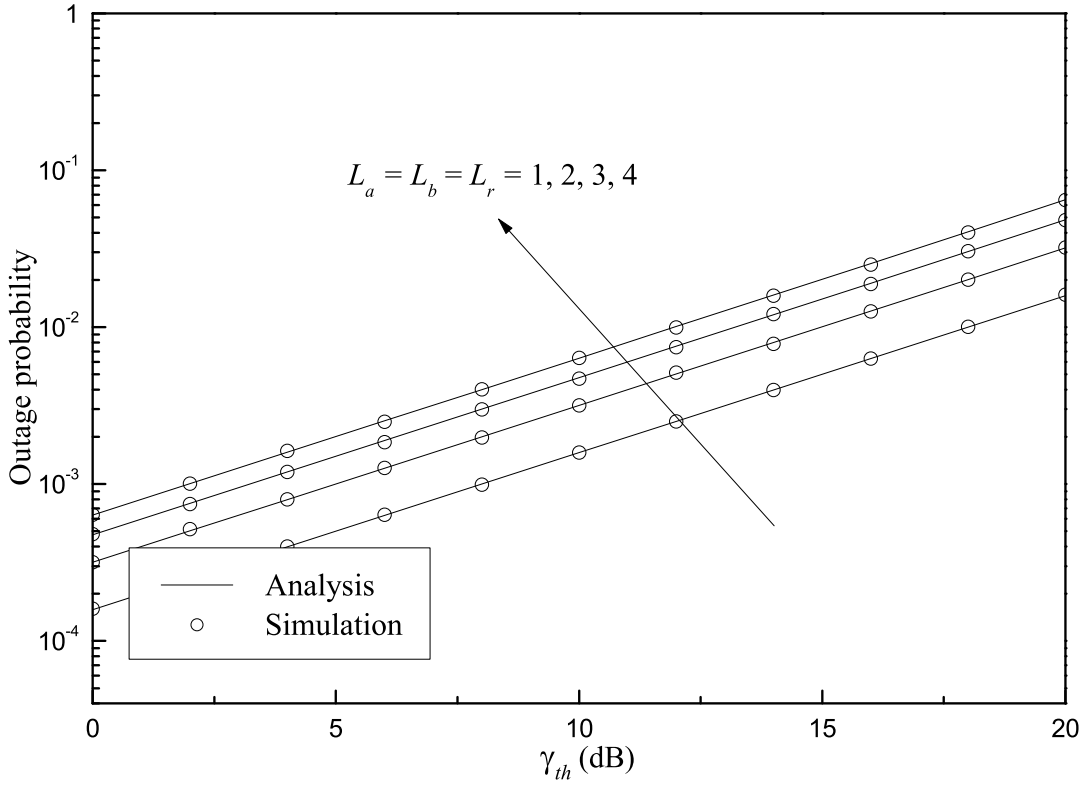
1
10^{-1}
10^{-2}
10^{-3}
10^{-4}
Outage probability
$L_a = L_b = L_r$ = 1, 2, 3, 4
Analysis
Simulation
0
5
10
15
20
γ_{th} (dB)

(c) $\zeta = 28$ dB

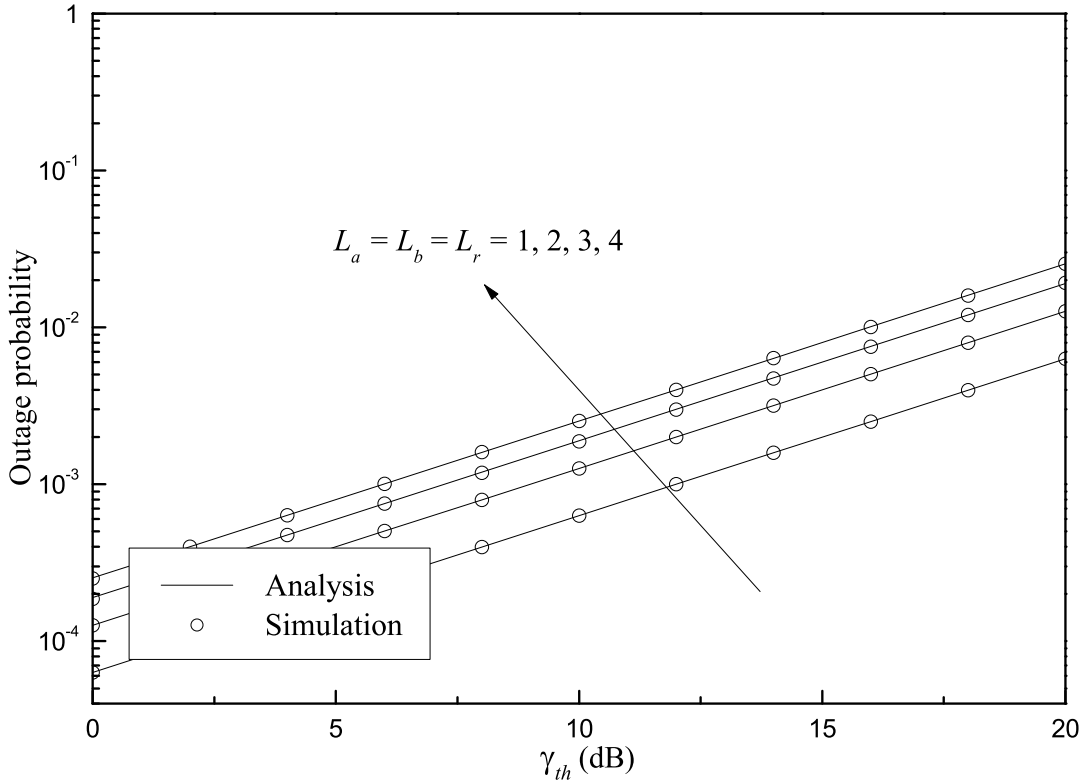

(d) $\zeta = 32$ dB

Figure 2.4. Individual outage probability versus γ_{th} for various number of interferers. $\mu_{l,i} = 0.1$.

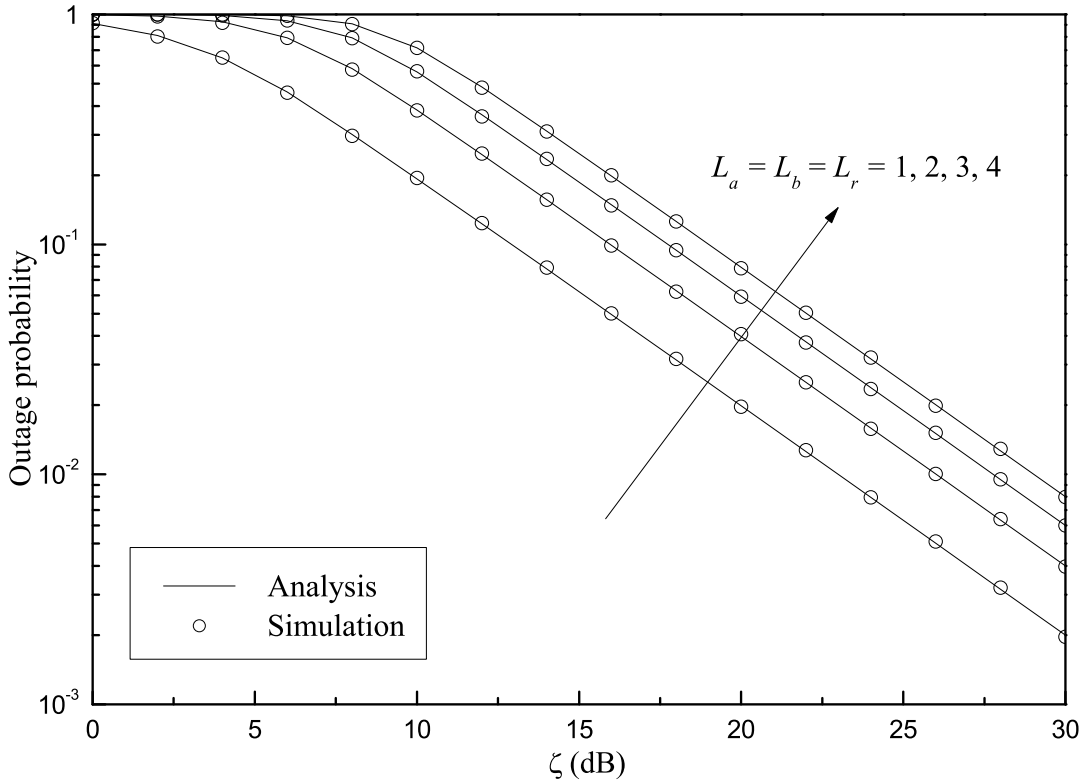

(a) $\gamma_{th} = 0$ dB

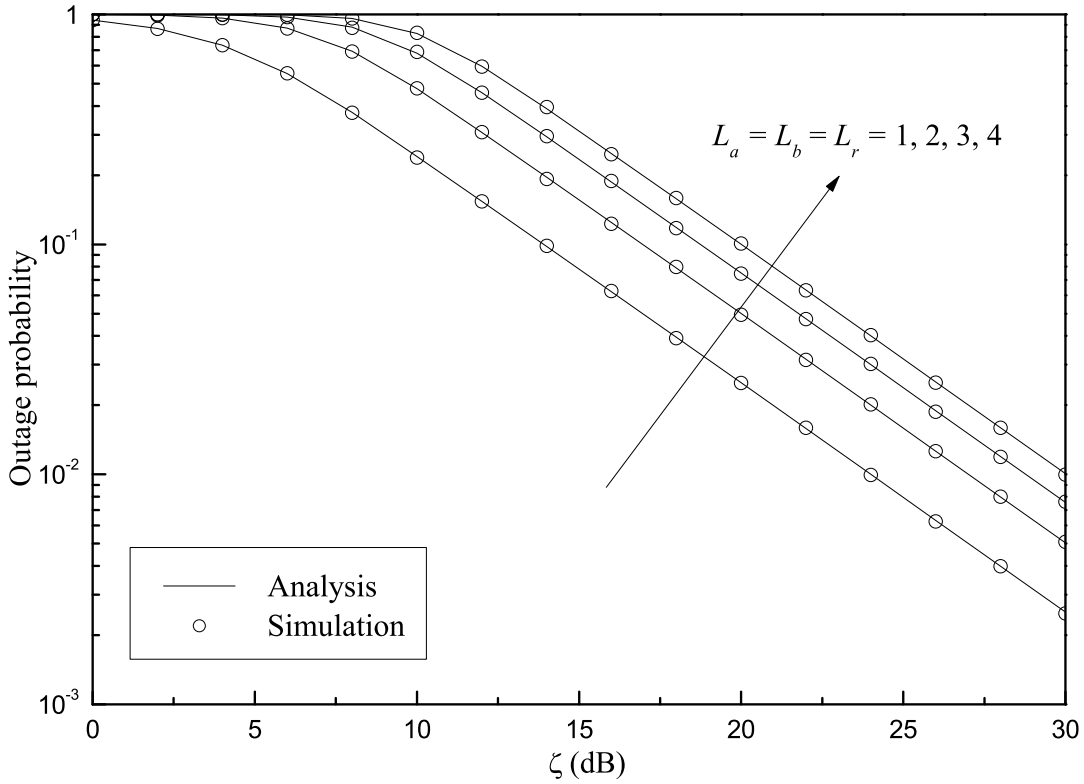

(b) $\gamma_{th} = 1$ dB

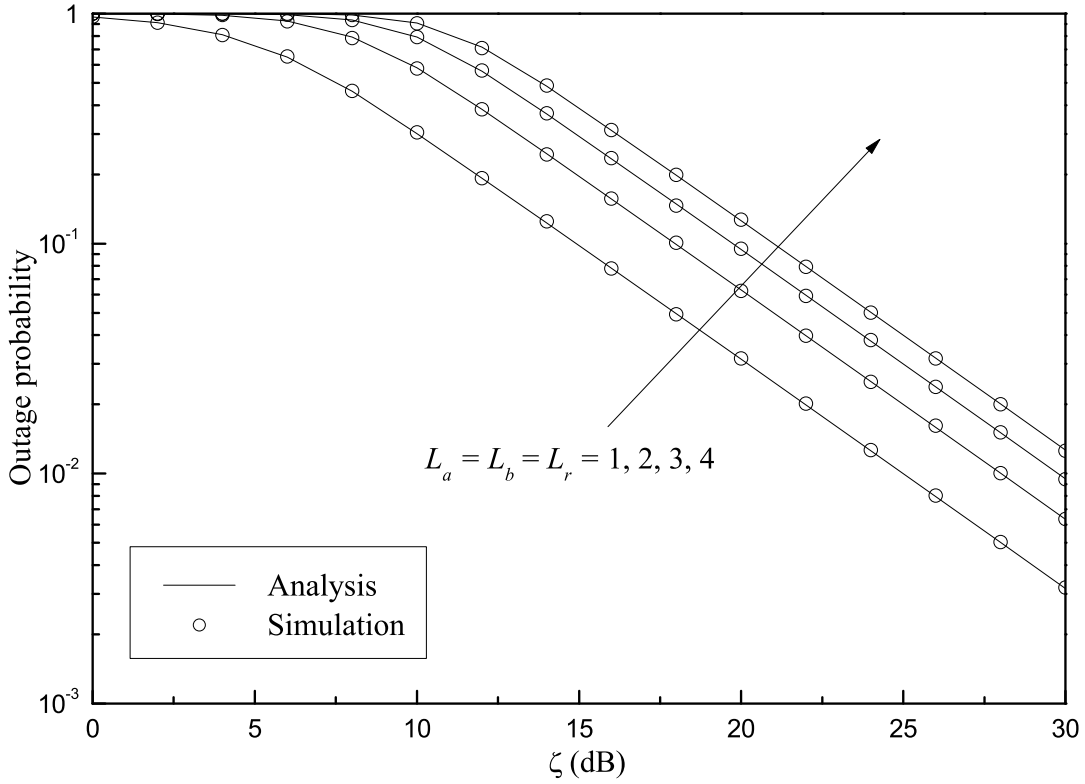

(c) $\gamma_{th} = 2$ dB

Figure 2.5. Common outage probability versus ζ for various number of interferers. $\mu_{l,i} = 1$.

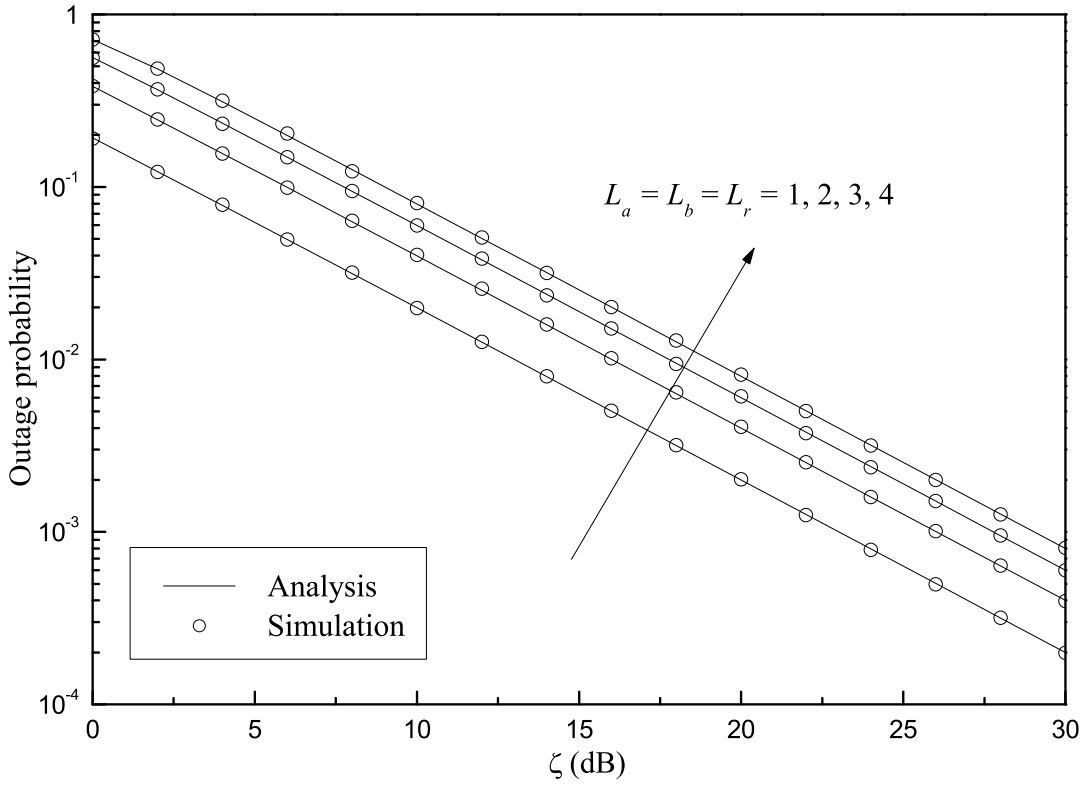

(a) $\gamma_{th} = 0$ dB

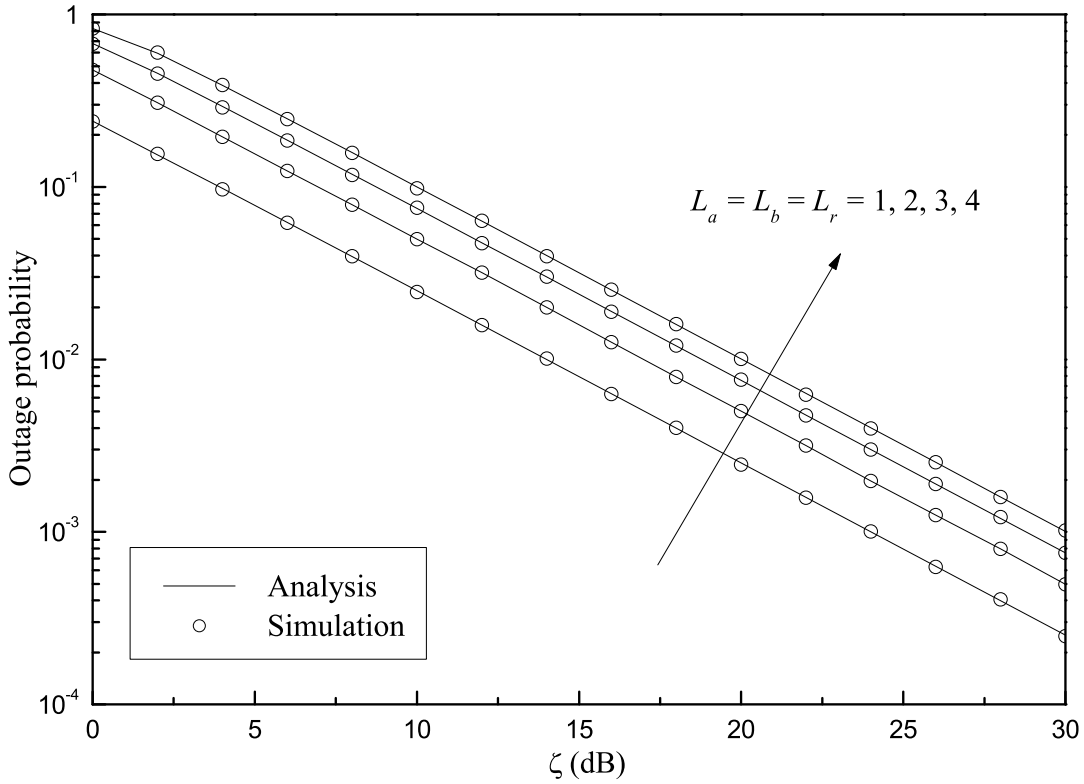

(b) $\gamma_{th} = 1$ dB

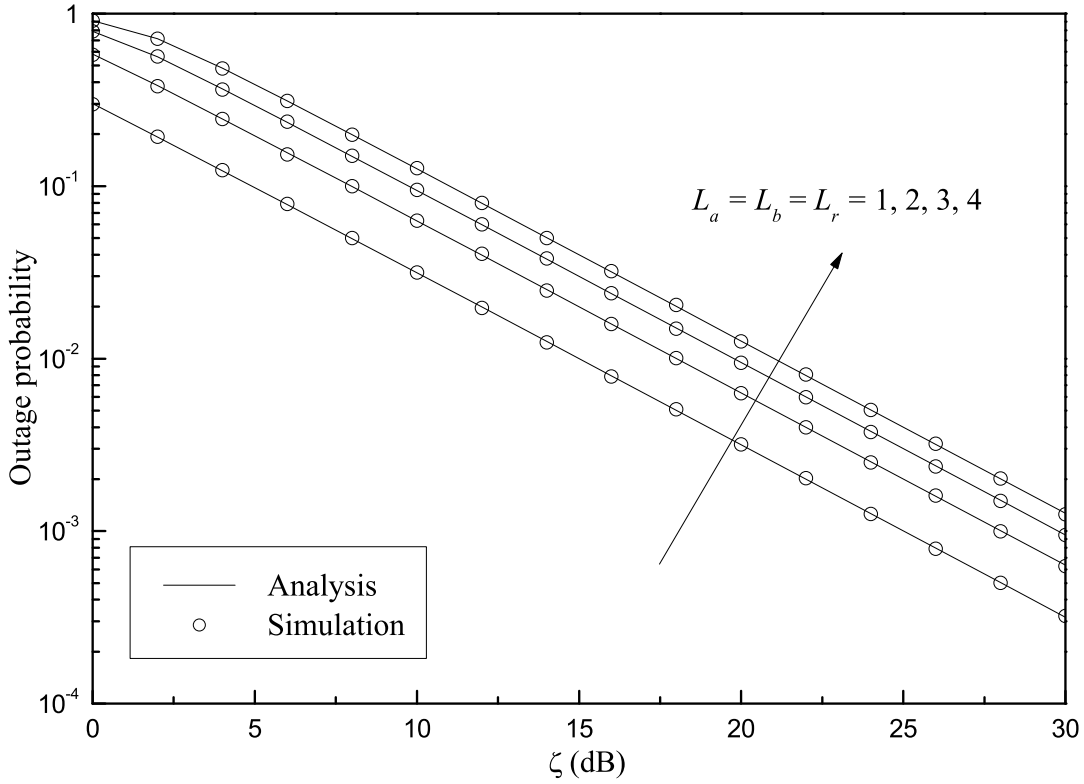

(c) $\gamma_{th} = 2$ dB

Figure 2.6. Common outage probability versus ζ for various number of interferers. $\mu_{l,i} = 0.1$.

Fig. 2.7 shows the common outage probability versus γ_{th} for the two-way relay network in the presence of cochannel interference with $L_a = L_b = L_r = 1, 2, \cdots, 4$ and $\mu_{l,i} = 0.1$. As expected, it is shown that as γ_{th} increases the common outage probability increases. It is shown that as ζ increases the common outage probability decreases. It is shown that the analytical results are in complete agreement with simulation results.

2.4 Summary

In this chapter, we consider a two-way relay network with multiple interferersWe discuss two different scenarios: Outages are declared individually for each user (individual outage) and an outage is declared simultaneously for all users (common outage). We derive the closed-form expression for the individual outage probability and the exact integral expression for the common outage probability of the two-way relay network with multiple interferers. The validity of our analytical results is verified by comparison with simulation results. It is shown that the analytical results agree exactly with the simulation results of the individual and common outage probabilities. In addition, it is shown that as the number of interferers increases the individual and common outage probabilities increase.

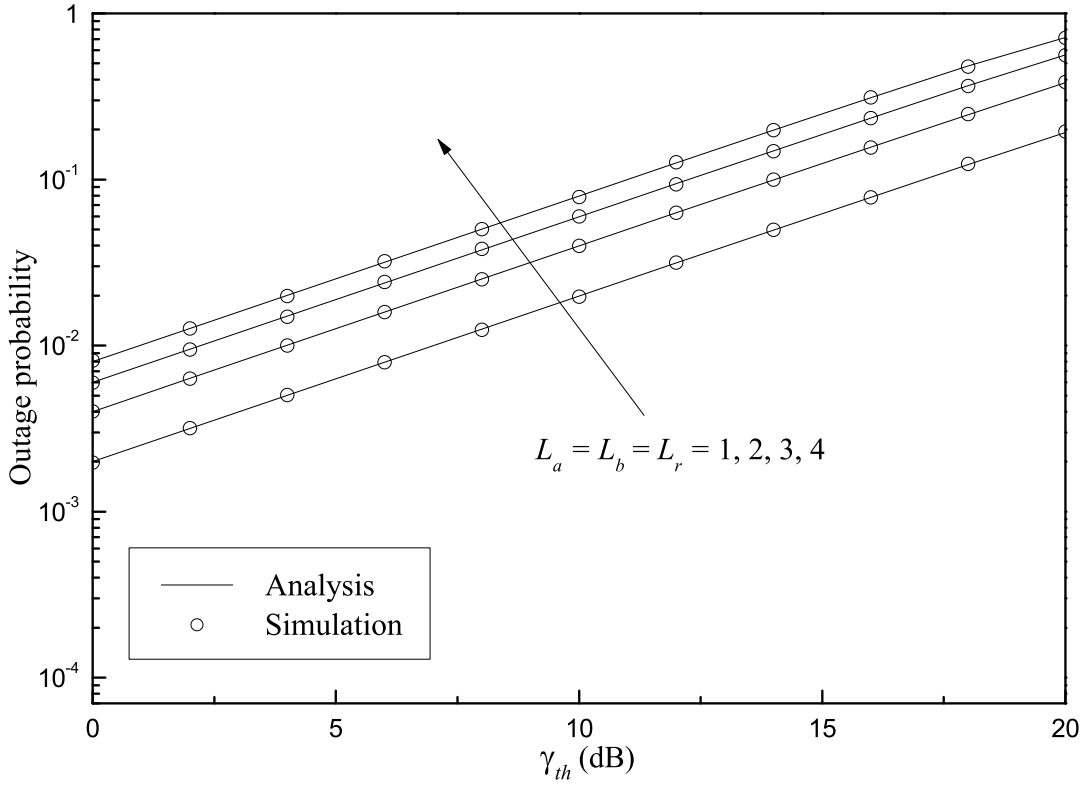
Outage probability
1
10^{-1}
10^{-2}
10^{-3}
10^{-4}
0
5
10
15
20
γ_{th} (dB)
$L_a = L_b = L_r = 1, 2, 3, 4$
Analysis
Simulation

(a) $\zeta = 20$ dB

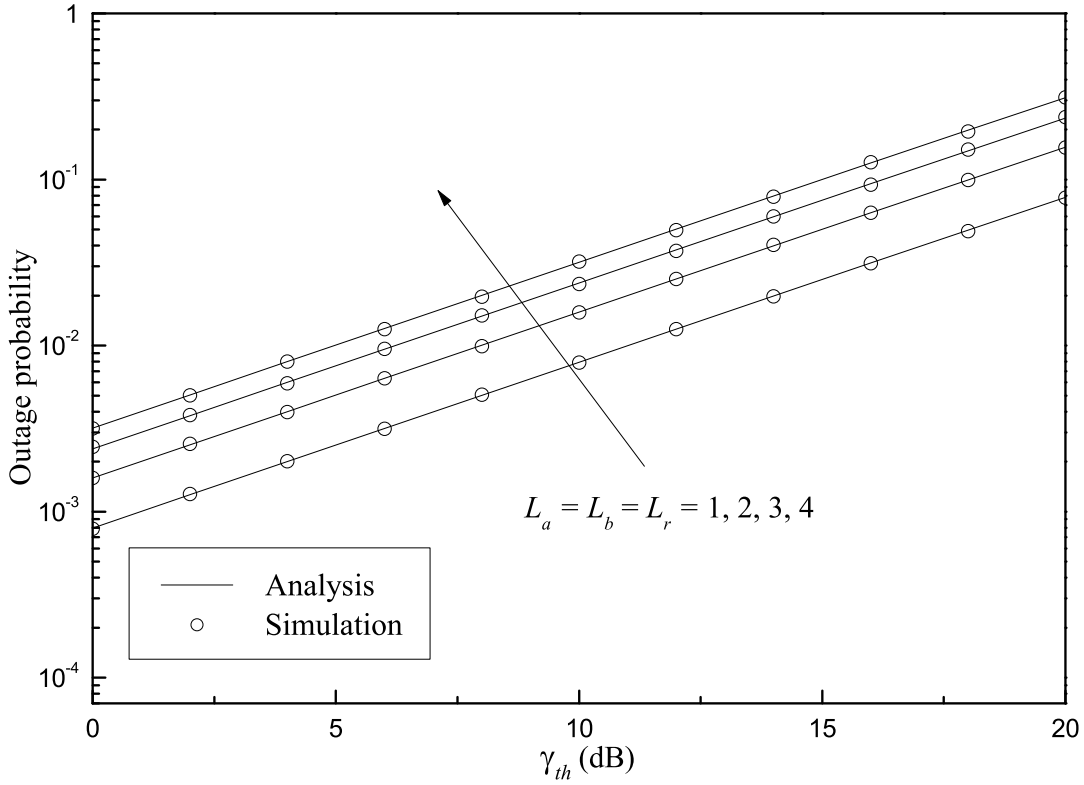
Outage probability
1
10^{-1}
10^{-2}
10^{-3}
10^{-4}
0
5
10
15
20
γ_{th} (dB)
$L_a = L_b = L_r = 1, 2, 3, 4$
Analysis
Simulation

(b) $\zeta = 24$ dB

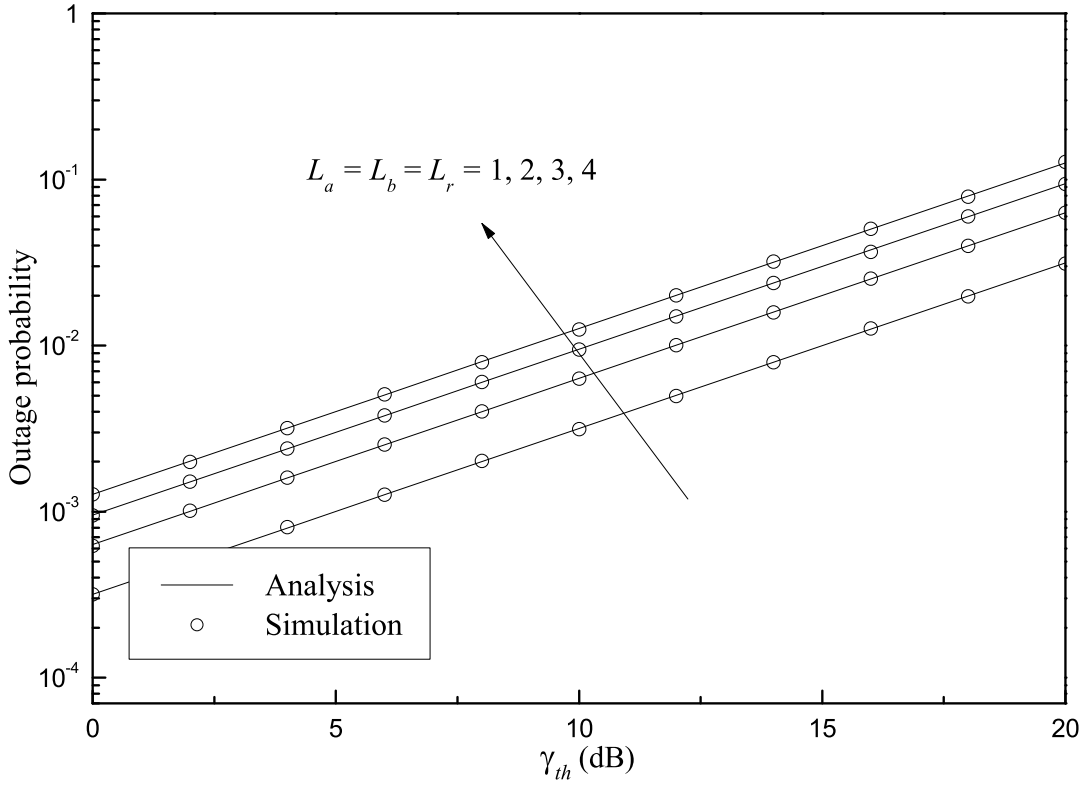
1
10^{-1}
10^{-2}
10^{-3}
10^{-4}
Outage probability
$L_a = L_b = L_r$ = 1, 2, 3, 4
Analysis
Simulation
0
5
10
15
20
γ_{th} (dB)

(c) $\zeta = 28$ dB

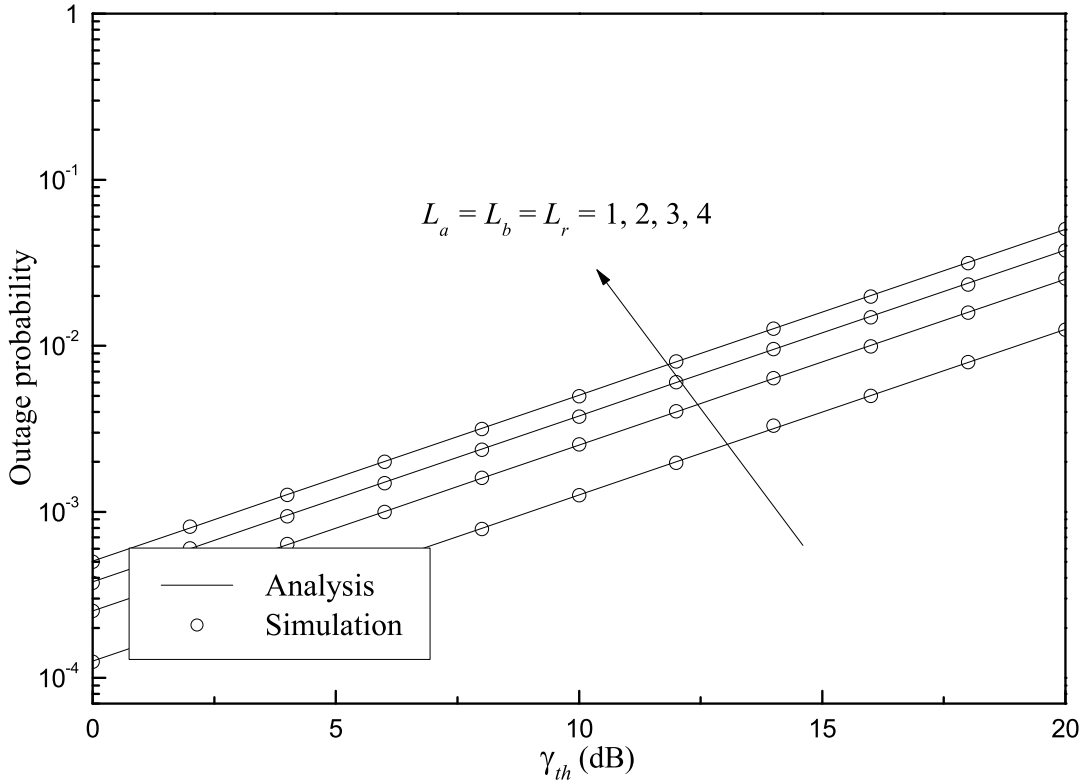

(d) $\zeta = 32$ dB

Figure 2.7. Common outage probability versus γ_{th} for various number of interferers. $\mu_{l,i} = 0.1$.

Chapter 3

Two-Way Full-Duplex Relaying with Cochannel Loop Interference

Relaying is an effective way to combat the performance degradation caused by fading, shadowing, and path loss [2], [5]. Two-way relaying, where two users exchange information with each other via a single or multiple relays, provides improved spectral efficiency compared to conventional one-way relaying by using either superposition coding or physical layer network coding at relays [20], [22].

A full-duplex scheme, where the transmission and the reception occur at the same time on the same channel, achieves up to double the capacity of a half-duplex scheme [32], [90]-[92]. Although the full-duplex scheme suffers from cochannel loop interference, it has drawn attention due to recent advances on interference cancellation and transmit/receive antenna isolation to mitigate the loop interference [38]-[40].

Relaying and full-duplex schemes are combined together to achieve higher data

rates [32], [33]-[36]. In [32], the authors investigate one-way full-duplex relaying and two-way half-duplex relaying in order to minimize/recover the spectral efficiency loss associated with owe-way half-duplex relaying which requires additional resources (e.g. time slots or frequencies) to transmit data. In [33] and [34], the authors present one-way full-duplex relaying with multiple antennas in order to provide a solution to overcome the spectral efficiency loss in one-way half-duplex relaying. In [35], the authors investigate one-way full-duplex relaying with opportunistic relay selection in order to enhance the performance of one-way half-duplex relaying. However, most previous works are focused on one-way full-duplex relaying, and there have been few works on two-way full-duplex relaying. In [36], the authors study two-way full-duplex relaying with power allocation to maximize the average rate. However, they ignore the cochannel loop interference at each node, which is one of the important factors that should be considered in the performance analysis of the full-duplex scheme. They leave it as an interesting open problem.

In this chapter, we investigate two-way full-duplex relaying in the presence of cochannel loop interference. The performance of the two-way full-duplex relaying with loop interference is analyzed in case of perfect and imperfect channel state information (CSI). Analytical results are verified by Monte Carlo simulations.

3.1 System Model

Consider two-way full-duplex relaying, where the users a and b exchange information with each other via an amplify-and-forward (AF) relay r as shown in Fig. 3.1. Assume

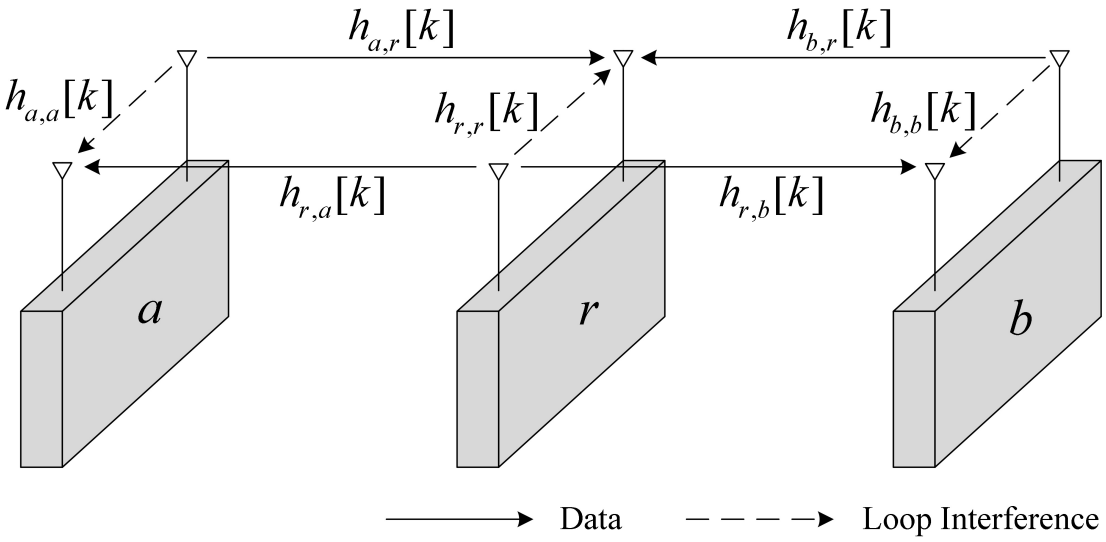

Figure 3.1. System model for two-way full-duplex relaying with cochannel loop interference.

that each of the users a, b, and the relay r has a transmit antenna and a receive antenna, and there is no direct path between the users a and b. Assume that the relay r is located at the middle between the users a and b.

All the channels are assumed to be block fading, i.e., the channel remains constant over a block but changes independently from one block to another. Assume that the channel from the node i to the node j at the block k has the channel coefficient $h_{i,j}[k]$, $i, j \in \{a, b, r\}$, which is a zero-mean circularly symmetric complex Gaussian (CSCG) random variable with the variance $\sigma^2_{h_{i,j}}$. We model the channel coefficient of loop interference as a zero-mean CSCG random variable under the assumptions that the line-of-sight component is effectively reduced by the antenna isolation/interference cancellation but the scattering multi-path components still remain due to imperfect cancellation [39], [68]. Assume that the channels are not reciprocal, i.e., $h_{i,j}[k] \neq h_{j,i}[k]$, since there are two different links, i.e., (i node's transmit antenna, j node's receive antenna) link, (j node's transmit antenna, i node's receive antenna) link. We model the channel $h_{i,j}[k]$ as the sum of the channel estimate $\hat{h}_{i,j}[k]$ and the channel estimation error $\Delta h_{i,j}[k]$, i.e., [36]

$$h_{i,j}[k] = \hat{h}_{i,j}[k] + \Delta h_{i,j}[k]. \tag{3.1}$$

Assume that the channel estimate $\hat{h}_{i,j}[k]$ and the channel estimation error $\Delta h_{i,j}[k]$ are mutually uncorrelated, which is valid for minimum mean-square error estimation. The channel estimate $\hat{h}_{i,j}[k]$ and the channel estimation error $\Delta h_{i,j}[k]$ are zero-mean CSCG random variables with the variances $\sigma^2_{\hat{h}_{i,j}}$ and $\sigma^2_{\Delta h_{i,j}} = \sigma^2_{h_{i,j}} - \sigma^2_{\hat{h}_{i,j}}$, respectively.

Assume that the users a and b communicate with each other via the AF relay r.

At the block k, the users a and b transmit their signals to the relay r simultaneously, and, at the same time, the relay r broadcasts its signal to the users a and b. Then, the relay r receives not only the transmitted signals from the users a and b but also the loop interference from the relay r itself. Then, the received signal at the relay r is given by

$$y_r[k] = \sqrt{E_a}h_{a,r}[k]x_a[k] + \sqrt{E_b}h_{b,r}[k]x_b[k] + \sqrt{E_r}h_{r,r}[k]x_r[k] + n_r[k] \tag{3.2}$$

where $x_i[k]$ is the transmit signal from the node i with unit power, E_i is the transmit energy from the node i, $i \in \{a, b, r\}$, $n_r[k]$ is the additive white Gaussian noise (AWGN) with zero mean and variance N_0 at the relay r, and the third term in the right hand side is the loop interference from the relay r itself. The relay r subtracts an estimate of the loop interference from its received signal which yields

$$\tilde{y}_r[k] = y_r[k] - \sqrt{E_r}\hat{h}_{r,r}[k]x_r[k]. \tag{3.3}$$

From (3.1), (3.2), and (3.3), we have

$$\begin{aligned}\tilde{y}_r[k] = &\sqrt{E_a}\hat{h}_{a,r}[k]x_a[k] + \sqrt{E_b}\hat{h}_{b,r}[k]x_b[k] + \sqrt{E_a}\Delta h_{a,r}[k]x_a[k] \\ &+ \sqrt{E_b}\Delta h_{b,r}[k]x_b[k] + \sqrt{E_r}\Delta h_{r,r}[k]x_r[k] + n_r[k].\end{aligned} \tag{3.4}$$

The transmit signal from the relay r is given by $x_r[k] = \alpha[k-1]\tilde{y}_r[k-1]$ where the amplification factor is given by

$$\begin{aligned}&\alpha[k-1] \\ &= \frac{1}{\sqrt{E_a|\hat{h}_{a,r}[k-1]|^2 + E_b|\hat{h}_{b,r}[k-1]|^2 + E_a\sigma^2_{\Delta h_{a,r}} + E_b\sigma^2_{\Delta h_{b,r}} + E_r\sigma^2_{\Delta h_{r,r}} + N_0}}.\end{aligned} \tag{3.5}$$

The received signals at the users a and b are given by

$$y_a[k] = \sqrt{E_r} h_{r,a}[k] x_r[k] + \sqrt{E_a} h_{a,a}[k] x_a[k] + n_a[k] \tag{3.6}$$

$$y_b[k] = \sqrt{E_r} h_{r,b}[k] x_r[k] + \sqrt{E_b} h_{b,b}[k] x_b[k] + n_b[k] \tag{3.7}$$

where $n_a[k]$ and $n_b[k]$ are the AWGN with zero mean and variance N_0 at the users a and b, respectively. The user a subtracts the estimates of the self-interference (SI) and the loop interference from its received signal which yields

$$\begin{aligned}
\tilde{y}_a[k] &= y_a[k] - \alpha[k-1]\sqrt{E_r E_a}\hat{h}_{r,a}[k]\hat{h}_{a,r}[k-1]x_a[k-1] - \sqrt{E_a}\hat{h}_{a,a}[k]x_a[k] \\
&= \alpha[k-1]\sqrt{E_r E_b}\hat{h}_{r,a}[k]\hat{h}_{b,r}[k-1]x_b[k-1] \\
&\quad + \alpha[k-1]\sqrt{E_r E_b}\Delta h_{r,a}[k]\hat{h}_{b,r}[k-1]x_b[k-1] \\
&\quad + \alpha[k-1]\sqrt{E_r E_a}\Delta h_{r,a}[k]\hat{h}_{a,r}[k-1]x_a[k-1] \\
&\quad + \alpha[k-1]\sqrt{E_r E_a}\hat{h}_{r,a}[k]\Delta h_{a,r}[k-1]x_a[k-1] \\
&\quad + \alpha[k-1]\sqrt{E_r E_a}\Delta h_{r,a}[k]\Delta h_{a,r}[k-1]x_a[k-1] \\
&\quad + \alpha[k-1]\sqrt{E_r E_b}\hat{h}_{r,a}[k]\Delta h_{b,r}[k-1]x_b[k-1] \\
&\quad + \alpha[k-1]\sqrt{E_r E_b}\Delta h_{r,a}[k]\Delta h_{b,r}[k-1]x_b[k-1] \\
&\quad + \alpha[k-1]\sqrt{E_r E_r}\hat{h}_{r,a}[k]\Delta h_{r,r}[k-1]x_r[k-1] \\
&\quad + \alpha[k-1]\sqrt{E_r E_r}\Delta h_{r,a}[k]\Delta h_{r,r}[k-1]x_r[k-1] \\
&\quad + \alpha[k-1]\sqrt{E_r}\hat{h}_{r,a}[k]n_r[k-1] + \alpha[k-1]\sqrt{E_r}\Delta h_{r,a}[k]n_r[k-1] \\
&\quad + \sqrt{E_a}\Delta h_{a,a}[k]x_a[k] + n_a[k].
\end{aligned} \tag{3.8}$$

Similarly, the node b subtracts the estimates of the self-interference and the loop

interference from its received signal which yields

$$\begin{aligned}
\tilde{y}_b[k] &= y_b[k] - \alpha[k-1]\sqrt{E_r E_b}\hat{h}_{r,b}[k]\hat{h}_{b,r}[k-1]x_b[k-1] - \sqrt{E_b}\hat{h}_{b,b}[k]x_b[k] \\
&= \alpha[k-1]\sqrt{E_r E_a}\hat{h}_{r,b}[k]\hat{h}_{a,r}[k-1]x_a[k-1] \\
&\quad + \alpha[k-1]\sqrt{E_r E_a}\Delta h_{r,b}[k]\hat{h}_{a,r}[k-1]x_a[k-1] \\
&\quad + \alpha[k-1]\sqrt{E_r E_b}\Delta h_{r,b}[k]\hat{h}_{b,r}[k-1]x_b[k-1] \\
&\quad + \alpha[k-1]\sqrt{E_r E_b}\hat{h}_{r,b}[k]\Delta h_{b,r}[k-1]x_b[k-1] \\
&\quad + \alpha[k-1]\sqrt{E_r E_b}\Delta h_{r,b}[k]\Delta h_{b,r}[k-1]x_b[k-1] \\
&\quad + \alpha[k-1]\sqrt{E_r E_a}\hat{h}_{r,b}[k]\Delta h_{a,r}[k-1]x_a[k-1] \\
&\quad + \alpha[k-1]\sqrt{E_r E_a}\Delta h_{r,b}[k]\Delta h_{a,r}[k-1]x_a[k-1] \\
&\quad + \alpha[k-1]\sqrt{E_r E_r}\hat{h}_{r,b}[k]\Delta h_{r,r}[k-1]x_r[k-1] \\
&\quad + \alpha[k-1]\sqrt{E_r E_r}\Delta h_{r,b}[k]\Delta h_{r,r}[k-1]x_r[k-1] \\
&\quad + \alpha[k-1]\sqrt{E_r}\hat{h}_{r,b}[k]n_r[k-1] + \alpha[k-1]\sqrt{E_r}\Delta h_{r,b}[k]n_r[k-1] \\
&\quad + \sqrt{E_b}\Delta h_{b,b}[k]x_b[k] + n_b[k]. \qquad (3.9)
\end{aligned}$$

For the SI cancellation, each node has to obtain the necessary CSI. At the beginning of each block (e.g., k), the CSI acquisition is achieved in four steps. In the first step, the user a transmits its pilot signal to the relay r, and the relay r estimates $h_{a,r}[k]$. In the second step, the user b transmits its pilot signal to the relay r, and the relay r estimates $h_{b,r}[k]$. In the third step, the relay r broadcasts the pilot signal, and the users a and b estimate $h_{r,a}[k]$ and $h_{r,b}[k]$, respectively. In the fourth step, the relay r feeds back $\hat{h}_{a,r}[k-1]$, $\hat{h}_{b,r}[k-1]$, and $\alpha[k-1]$ to the users a and b. In order to reduce the feedback overhead, the relay r can feed back their quantized version

to the users a and b [93]. In the following, we will focus on the node a since similar approach and analysis can be applied for the node b.

3.2 Outage Probability Derivation

3.2.1 Signal-to-Interference-plus-Noise Ratio

By dividing the desired signal power by the interference and noise power, the signal-to-interference-plus-noise ratio (SINR) at the user a is given by

$$\begin{aligned}\gamma_a = {} & E_r E_b |\hat{h}_{r,a}[k]|^2 |\hat{h}_{b,r}[k-1]|^2 \Big(E_r E_b \sigma^2_{\Delta h_{r,a}} |\hat{h}_{b,r}[k-1]|^2 + E_r E_a \sigma^2_{\Delta h_{r,a}} |\hat{h}_{a,r}[k-1]|^2 \\ & + E_r E_a |\hat{h}_{r,a}[k]|^2 \sigma^2_{\Delta h_{a,r}} + E_r E_a \sigma^2_{\Delta h_{r,a}} \sigma^2_{\Delta h_{a,r}} + E_r E_b |\hat{h}_{r,a}[k]|^2 \sigma^2_{\Delta h_{b,r}} \\ & + E_r E_b \sigma^2_{\Delta h_{r,a}} \sigma^2_{\Delta h_{b,r}} + E_r^2 |\hat{h}_{r,a}[k]|^2 \sigma^2_{\Delta h_{r,r}} \\ & + E_r^2 \sigma^2_{\Delta h_{r,a}} \sigma^2_{\Delta h_{r,r}} + E_r |\hat{h}_{r,a}[k]|^2 N_0 + E_r \sigma^2_{\Delta h_{r,a}} N_0 \\ & + |\alpha[k-1]|^{-2} E_a \sigma^2_{\Delta h_{a,a}} + |\alpha[k-1]|^{-2} N_0 \Big)^{-1} \\ = {} & \frac{\chi_1 \left|\hat{h}_{r,a}[k]\right|^2 \chi_2 \left|\hat{h}_{b,r}[k-1]\right|^2}{\chi_1 \left|\hat{h}_{r,a}[k]\right|^2 + \chi_2 \left|\hat{h}_{b,r}[k-1]\right|^2 + \chi_3 \left|\hat{h}_{a,r}[k-1]\right|^2 + \chi_4} \end{aligned} \tag{3.10}$$

where

$$\chi_1 = \frac{E_r}{E_r \sigma^2_{\Delta h_{r,a}} + E_a \sigma^2_{\Delta h_{a,a}} + N_0} \tag{3.11}$$

$$\chi_2 = \frac{E_b}{E_a \sigma^2_{\Delta h_{a,r}} + E_b \sigma^2_{\Delta h_{b,r}} + E_r \sigma^2_{\Delta h_{r,r}} + N_0} \tag{3.12}$$

$$\chi_3 = \frac{E_a}{E_a \sigma^2_{\Delta h_{a,r}} + E_b \sigma^2_{\Delta h_{b,r}} + E_r \sigma^2_{\Delta h_{r,r}} + N_0} \tag{3.13}$$

$$
\begin{aligned}
\chi_4 = \Big(& E_r E_a \sigma^2_{\Delta h_{r,a}} \sigma^2_{\Delta h_{a,r}} + E_r E_b \sigma^2_{\Delta h_{r,r}} \sigma^2_{\Delta h_{b,r}} \\
& + E_r E_r \sigma^2_{\Delta h_{r,a}} \sigma^2_{\Delta h_{r,r}} + E_r \sigma^2_{\Delta h_{r,a}} N_0 \\
& + E_a E_a \sigma^2_{\Delta h_{a,a}} \sigma^2_{\Delta h_{a,r}} + E_b E_a \sigma^2_{\Delta h_{a,a}} \sigma^2_{\Delta h_{b,r}} \\
& + E_r E_a \sigma^2_{\Delta h_{a,a}} \sigma^2_{\Delta h_{r,r}} + E_a \sigma^2_{\Delta h_{a,a}} N_0 + E_a \sigma^2_{\Delta h_{a,r}} N_0 \\
& + E_b \sigma^2_{\Delta h_{b,r}} N_0 + E_r \sigma^2_{\Delta h_{r,r}} N_0 + N_0 N_0 \Big) \\
& \times \Big(E_r \sigma^2_{\Delta h_{r,a}} + E_a \sigma^2_{\Delta h_{a,a}} + N_0 \Big)^{-1} \\
& \times \Big(E_a \sigma^2_{\Delta h_{a,r}} + E_b \sigma^2_{\Delta h_{b,r}} + E_r \sigma^2_{\Delta h_{r,r}} + N_0 \Big)^{-1}.
\end{aligned} \tag{3.14}
$$

Note that for perfect channel estimation, i.e., when $\sigma^2_{\Delta h_{i,j}} = 0$ for $i, j \in \{a, b, r\}$, (3.11)-(3.14) reduce to $\chi_1 = E_r/N_0$, $\chi_2 = E_b/N_0$, $\chi_3 = E_a/N_0$, and $\chi_4 = 1$.

3.2.2 Cumulative Density Function

The cumulative distribution function (CDF) of the SINR at the user a is given by

$$
\begin{aligned}
F_{\gamma_a}(\gamma) &= \Pr\left(\frac{\chi_1 |\hat{h}_{r,a}|^2 \chi_2 |\hat{h}_{b,r}|^2}{\chi_1 |\hat{h}_{r,a}|^2 + \chi_2 |\hat{h}_{b,r}|^2 + \chi_3 |\hat{h}_{a,r}|^2 + \chi_4} < \gamma \right) \\
&= \int_0^{\infty} \int_0^{\frac{\gamma}{\chi_2}} \Pr\left(|\hat{h}_{r,a}|^2 > \frac{\gamma\chi_3 y + \gamma\chi_2 x + \gamma\chi_4}{\chi_1 (\chi_2 x - \gamma)} \right) f_{|\hat{h}_{b,r}|^2}(x) \, f_{|\hat{h}_{a,r}|^2}(y) \, dx dy \\
&\quad + \int_0^{\infty} \int_{\frac{\gamma}{\chi_2}}^{\infty} \Pr\left(|\hat{h}_{r,a}|^2 < \frac{\gamma\chi_3 y + \gamma\chi_2 x + \gamma\chi_4}{\chi_1 (\chi_2 x - \gamma)} \right) f_{|\hat{h}_{b,r}|^2}(x) \, f_{|\hat{h}_{a,r}|^2}(y) \, dx dy
\end{aligned} \tag{3.15}
$$

where, for notational simplicity, the block indices k and $k-1$ in $\hat{h}_{r,a}[k]$, $\hat{h}_{a,r}[k-1]$, and $\hat{h}_{b,r}[k-1]$ are omitted. Since $|\hat{h}_{r,a}|^2$, $|\hat{h}_{a,r}|^2$, and $|\hat{h}_{b,r}|^2$ are independent, exponentially distributed random variables with parameters $1/\sigma^2_{\hat{h}_{r,a}}$, $1/\sigma^2_{\hat{h}_{a,r}}$, and $1/\sigma^2_{\hat{h}_{b,r}}$,

respectively, the the probability density functions of $|\hat{h}_{r,a}|^2$, $|\hat{h}_{a,r}|^2$, and $|\hat{h}_{b,r}|^2$ are given by

$$f_{|\hat{h}_{r,a}|^2}(x) = \frac{1}{\sigma^2_{\hat{h}_{r,a}}} e^{-\frac{x}{\sigma^2_{\hat{h}_{r,a}}}}, \tag{3.16}$$

$$f_{|\hat{h}_{a,r}|^2}(x) = \frac{1}{\sigma^2_{\hat{h}_{a,r}}} e^{-\frac{x}{\sigma^2_{\hat{h}_{a,r}}}}, \tag{3.17}$$

$$f_{|\hat{h}_{b,r}|^2}(x) = \frac{1}{\sigma^2_{\hat{h}_{b,r}}} e^{-\frac{x}{\sigma^2_{\hat{h}_{b,r}}}}, \tag{3.18}$$

respectively.

From (3.15)-(3.18), we have

$$F_{\gamma_a}(\gamma) = 1 - \int_0^\infty \int_{\frac{\gamma}{\chi_2}}^\infty \frac{e^{-\frac{x}{\sigma^2_{\hat{h}_{b,r}}} - \frac{y}{\sigma^2_{\hat{h}_{a,r}}} - \frac{\gamma\chi_3 y + \gamma\chi_2 x + \gamma\chi_4}{\sigma^2_{\hat{h}_{r,a}}\chi_1(\chi_2 x - \gamma)}}}{\sigma^2_{\hat{h}_{a,r}}\sigma^2_{\hat{h}_{b,r}}} dx dy. \tag{3.19}$$

Putting $x = \frac{1}{\chi_1\chi_2}(z + \chi_1\gamma)$ into (3.19), we get

$$F_{\gamma_a}(\gamma) = 1 - \frac{e^{-\frac{\gamma}{\sigma^2_{\hat{h}_{r,a}}\chi_1} - \frac{\gamma}{\sigma^2_{\hat{h}_{b,r}}\chi_2}}}{\sigma^2_{\hat{h}_{a,r}}\sigma^2_{\hat{h}_{b,r}}\chi_1\chi_2} \int_0^\infty e^{-\frac{y}{\sigma^2_{\hat{h}_{a,r}}}} \int_0^\infty e^{-\frac{\gamma\chi_3 y + \gamma^2 + \gamma\chi_4}{\sigma^2_{\hat{h}_{r,a}} z}} e^{-\frac{z}{\sigma^2_{\hat{h}_{b,r}}\chi_1\chi_2}} dz dy. \tag{3.20}$$

Using $\int_0^\infty \exp\left(-\frac{p}{x} - qx\right)dx = 2\sqrt{\frac{p}{q}}K_1\left(2\sqrt{pq}\right)$ in [101, eq. (3.471.9)] where $K_1(\cdot)$ is the first order modified bessel function of the second kind in [101, eq. (8.407.1)], (3.20) is rewritten as

$$F_{\gamma_a}(\gamma) = 1 - 2e^{-\frac{\gamma}{\sigma^2_{\hat{h}_{r,a}}\chi_1} - \frac{\gamma}{\sigma^2_{\hat{h}_{b,r}}\chi_2}} \int_0^\infty e^{-\frac{y}{\sigma^2_{\hat{h}_{a,r}}}} \sqrt{\frac{\gamma\chi_3 y + \gamma^2 + \gamma\chi_4}{\sigma^4_{\hat{h}_{a,r}}\sigma^2_{\hat{h}_{b,r}}\sigma^2_{\hat{h}_{r,a}}\chi_1\chi_2}} K_1\left(2\sqrt{\frac{\gamma\chi_3 y + \gamma^2 + \gamma\chi_4}{\sigma^2_{\hat{h}_{r,a}}\sigma^2_{\hat{h}_{b,r}}\chi_1\chi_2}}\right) dy. \tag{3.21}$$

Combining [86, vol. 4, eq. (1.1.2.3)] with [86, vol. 4, eq. (3.16.2.4)], we have

$$\begin{aligned}
&\int_0^\infty \exp\left(-\lambda x\right)\sqrt{\kappa x+\eta}K_1\left(\mu\sqrt{\kappa x+\eta}\right)dx \\
&=\frac{\kappa\mu}{4\lambda^2}\exp\left(\frac{\kappa\mu^2}{4\lambda}+\frac{\eta\lambda}{\kappa}\right)\Gamma\left(-1,\frac{\kappa\mu^2}{4\lambda}\right) \\
&\quad-\frac{1}{\kappa}\exp\left(\frac{\eta\lambda}{\kappa}\right)\int_0^\eta \exp\left(-\frac{\lambda x}{\kappa}\right)\sqrt{x}K_1\left(\mu\sqrt{x}\right)dx
\end{aligned} \tag{3.22}$$

where $\Gamma\left(\cdot,\cdot\right)$ is the incomplete gamma function in [101, eq. (8.350.2)]. From (3.21) and (3.22), we obtain

$$\begin{aligned}
&F_{\gamma_a}\left(\gamma\right) \\
&=1-e^{-\frac{\gamma}{\sigma^2_{\tilde{h}_{r,a}}\chi_1}-\frac{\gamma}{\sigma^2_{\tilde{h}_{b,r}}\chi_2}+\frac{\gamma+\chi_4}{\sigma^2_{\tilde{h}_{a,r}}\chi_3}}\Bigg\{\psi_1\gamma e^{\psi_1\gamma}\Gamma\left(-1,\psi_1\gamma\right) \\
&\quad-\frac{1}{4\psi_1\gamma}\underbrace{\int_0^{\psi_2} e^{-\frac{y}{4\psi_1\gamma}}\sqrt{y}K_1\left(\sqrt{y}\right)dy}_{\triangleq\,\Xi(\gamma)}\Bigg\}
\end{aligned} \tag{3.23}$$

where $\psi_1=\frac{\sigma^2_{\tilde{h}_{a,r}}\chi_3}{\sigma^2_{\tilde{h}_{b,r}}\sigma^2_{\tilde{h}_{r,a}}\chi_1\chi_2}$ and $\psi_2=\frac{4\gamma^2+4\gamma\chi_4}{\sigma^2_{\tilde{h}_{b,r}}\sigma^2_{\tilde{h}_{r,a}}\chi_1\chi_2}$.

The evaluation of the integral in (3.23) is difficult due to the product of the first order modified bessel function of the second kind and the exponential function. We thus make an approximation. By the M-th order Taylor series approximation of the exponential function $e^{-x}\simeq\sum_{m=0}^{M}\frac{(-x)^m}{m!}$ for small $x>0$, the integral in (3.23) is given by

$$\Xi\left(\gamma\right)\simeq\sum_{m=0}^{M}\left(-\frac{1}{4\psi_1\gamma}\right)^m\int_0^{\psi_2}\frac{(y)^{m+\frac{1}{2}}}{m!}K_1\left(\sqrt{y}\right)dy. \tag{3.24}$$

Using the Meijer's G-function [101, eq. (9.34.3)], the first order modified bessel function of the second kind of (3.24) is given by

$$K_1(\sqrt{y}) = \frac{1}{2} G_{02}^{20}\left(\frac{y}{4}\middle|\frac{1}{2}, -\frac{1}{2}\right). \tag{3.25}$$

From (3.24) and (3.25), we have

$$\Xi(\gamma) = \sum_{m=0}^{M}\left(-\frac{1}{4\psi_1\gamma}\right)^m \int_0^{\psi_2} \frac{(y)^{m+\frac{1}{2}}}{2m!} G_{02}^{20}\left(\frac{y}{4}\middle|\frac{1}{2}, -\frac{1}{2}\right) dy. \tag{3.26}$$

Using $\int_0^x y^{m+\frac{1}{2}} G_{02}^{20}\left(\frac{y}{4}\middle|\frac{1}{2}, -\frac{1}{2}\right) dy = x^{m+\frac{3}{2}} G_{13}^{21}\left(\frac{x}{4}\middle|_{\frac{1}{2},-\frac{1}{2},-m-\frac{1}{2}}^{-m-\frac{3}{2}}\right)$ in [86, vol. 3, eq. (1.16.2.1)], (3.26) is rewritten as

$$\Xi(\gamma) = \sum_{m=0}^{M}\left(-\frac{1}{4\psi_1\gamma}\right)^m \frac{1}{2m!} \psi_2^{m+\frac{3}{2}} G_{13}^{21}\left(\frac{\psi_2}{4}\middle|_{\frac{1}{2},-\frac{1}{2},-m-\frac{3}{2}}^{-m-\frac{1}{2}}\right). \tag{3.27}$$

From (3.23) and (3.27), the CDF of the SINR at the user a is given by

$$\begin{aligned} &F_{\gamma_a}(\gamma) \\ &\simeq 1 - e^{-\frac{\gamma}{\sigma^2_{\hat{h}_{r,a}}\chi_1} - \frac{\gamma}{\sigma^2_{\hat{h}_{b,r}}\chi_2} + \frac{\gamma+\chi_4}{\sigma^2_{\hat{h}_{a,r}}\chi_3}} \left\{ \psi_1\gamma e^{\psi_1\gamma}\Gamma(-1, \psi_1\gamma) + \sum_{m=0}^{M} \frac{1}{2m!}\left(-\frac{1}{4\psi_1\gamma}\right)^{m+1} \right. \\ &\left. \times \left(\frac{4\gamma^2 + 4\chi_4\gamma}{\sigma^2_{\hat{h}_{b,r}}\sigma^2_{\hat{h}_{r,a}}\chi_1\chi_2}\right)^{m+\frac{3}{2}} G_{13}^{21}\left(\frac{\gamma^2+\chi_4\gamma}{\sigma^2_{\hat{h}_{b,r}}\sigma^2_{\hat{h}_{r,a}}\chi_1\chi_2}\middle|_{\frac{1}{2},-\frac{1}{2},-m-\frac{3}{2}}^{-m-\frac{1}{2}}\right)\right\}. \end{aligned} \tag{3.28}$$

3.2.3 Outage Probability

An outage occurs when the SINR at the user a falls below a SINR threshold γ_{th}. The outage probability of the user a is given by

$$\begin{aligned} P_{out,a}(\gamma_{th}) &= \Pr(\gamma_a \leq \gamma_{th}) \\ &= F_{\gamma_a}(\gamma_{th}). \end{aligned} \tag{3.29}$$

In the high signal-to-noise ratio (SNR) regime ($E_a = E_b = E_r = E \to \infty$), the diversity order determines the slope of the outage probability of the user a versus E/N_0 [2], [5]. From (3.20) and (3.29), using $e^x \simeq 1 + x$, $\Gamma(-1, x)/x^{-1} \simeq 1$, and $K_1(x) \simeq \frac{1}{x}$ as $x \to 0$, the outage probability of the user a is approximated as

$$\begin{aligned} P_{out,a}(\gamma_{th}) &\approx \frac{\gamma_{th}}{\sigma^2_{\hat{h}_{r,a}}\chi_1} + \frac{\gamma_{th}}{\sigma^2_{\hat{h}_{b,r}}\chi_2} - \psi_1\gamma_{th} \\ &\approx \frac{\gamma_{th}\left(E\sigma^2_{\Delta h_{r,a}} + E\sigma^2_{\Delta h_{a,a}} + N_0\right)}{\sigma^2_{\hat{h}_{r,a}}E} + \frac{\gamma_{th}\left(E\sigma^2_{\Delta h_{a,r}} + E\sigma^2_{\Delta h_{b,r}} + E\sigma^2_{\Delta h_{r,r}} + N_0\right)}{\sigma^2_{\hat{h}_{b,r}}E} \\ &\quad - \frac{\sigma^2_{\hat{h}_{a,r}}\left(E\sigma^2_{\Delta h_{r,a}} + E\sigma^2_{\Delta h_{a,a}} + N_0\right)}{\sigma^2_{\hat{h}_{b,r}}\sigma^2_{\hat{h}_{r,a}}E\gamma_{th}}. \end{aligned} \tag{3.30}$$

When perfect channel estimation is available ($\sigma^2_{\Delta h_{i,j}} = 0$, $i, j \in \{a, b, r\}$), (3.30) is rewritten as

$$P_{out,a}(\gamma_{th}) \approx \left(\frac{\gamma_{th}}{\sigma^2_{\hat{h}_{r,a}}} + \frac{\gamma_{th}}{\sigma^2_{\hat{h}_{b,r}}} - \frac{\sigma^2_{\hat{h}_{a,r}}}{\sigma^2_{\hat{h}_{b,r}}\sigma^2_{\hat{h}_{r,a}}}\gamma_{th}\right)\left(\frac{E}{N_0}\right)^{-1} \tag{3.31}$$

which is a function of $(E/N_0)^{-1}$. Therefore, the diversity order is one. When perfect channel estimation is not available, we can expect that the error floor appears at high E/N_0 region.

3.3 Numerical Results

Consider two-way full-duplex relaying where users a and b exchange information with the help of an AF relay r. Suppose that the transmit energy at the users a, b, and the relay r is same, i.e., $E_a = E_b = E_r = E$. And the transmit SNR is defined as SNR =

E/N_0 [5]. For simplicity, we will use the notation $\left(\sigma^2_{\Delta h_{a,r}}, \sigma^2_{\Delta h_{r,r}}, \sigma^2_{\Delta h_{b,r}}, \sigma^2_{\Delta h_{a,a}}, \sigma^2_{\Delta h_{r,a}}\right)$ in the figure to denote the variances of the channel estimation errors.

Fig. 3.2 shows the outage probability of the user a versus SNR for the two-way full-duplex relaying when $\sigma^2_{h_{a,r}} = \sigma^2_{h_{b,r}} = \sigma^2_{h_{r,a}} = \sigma^2_{h_{r,r}} = \sigma^2_{h_{a,a}} = 10$ and $\gamma_{th} = 1$. The analytical results are generated based on (3.28) and (3.29). It is shown that the analytical results perfectly match the simulation results. In case 1, all variances of the channel estimation errors are set to 0. In cases 2-6, one of the variances of the channel estimation errors is set to 1. In case 7, all variances of the channel estimation errors are set to 1. It is shown that the outage probability of cases 2-4 is lower than that of cases 5-6. The reason is that, due to power normalization (3.5) at the relay, the effects of $\sigma^2_{\Delta h_{a,r}}$, $\sigma^2_{\Delta h_{r,r}}$, and $\sigma^2_{\Delta h_{b,r}}$ on the outage probability are reduced. It is shown that, as SNR increases, the difference in the outage probability between case 1 and cases 2-7 increases. The reason is that the outage probability of case 1 decreases as SNR increases and that of cases 2-7 exhibits error floors at high SNR region. Fig. 3.3 shows the outage probability of the user a versus SNR for the two-way full-duplex relaying when $\sigma^2_{h_{a,r}} = \sigma^2_{h_{b,r}} = \sigma^2_{h_{r,a}} = \sigma^2_{h_{r,r}} = \sigma^2_{h_{a,a}} = 10$ and $\gamma_{th} = 1$. In case 1, all variances of the channel estimation errors are set to 0.1. In cases 2-6, one of the variances of the channel estimation errors is set to 0.1. In case 7, all variances of the channel estimation errors are set to 0.1. It is shown that the outage probability of cases 2-4 is lower than that of cases 5-6. Similar to Fig. 3.2, it is shown that the outage probability of cases 2-4 is lower than that of cases 5-6. It is shown that the outage probability of cases 2-4 are almost same and that of cases 5-6 are also almost same. Fig. 3.4 shows

the outage probability of the user a versus SNR for the two-way full-duplex relaying when $\sigma^2_{h_{a,r}} = \sigma^2_{h_{b,r}} = \sigma^2_{h_{r,a}} = \sigma^2_{h_{r,r}} = \sigma^2_{h_{a,a}} = 10$ and $\gamma_{th} = 1$. In case 1, all variances of the channel estimation errors are set to 0.01. In cases 2-6, one of the variances of the channel estimation errors is set to 0.01. In case 7, all variances of the channel estimation errors are set to 0.01. It is shown that the outage probability of cases 2-4 is lower than that of cases 5-6. It is shown that, as the variances of the channel estimation errors decreases, the difference in the outage probability between case 1 and cases 2-7 decreases. Fig. 3.5 shows the outage probability of the user a versus SNR for the two-way full-duplex relaying when $\sigma^2_{h_{a,r}} = \sigma^2_{h_{b,r}} = \sigma^2_{h_{r,a}} = \sigma^2_{h_{r,r}} = \sigma^2_{h_{a,a}} = 10$ and $\gamma_{th} = 1$. In case 1, all variances of the channel estimation errors are set to 0.001. In cases 2-6, one of the variances of the channel estimation errors is set to 0.001. In case 7, all variances of the channel estimation errors are set to 0.001. It is shown that the difference in the outage probability between case 1 and cases 2-7 becomes smaller. The reason is that, as the variances of the channel estimation errors decreases, its effect on the outage probability is reduced.

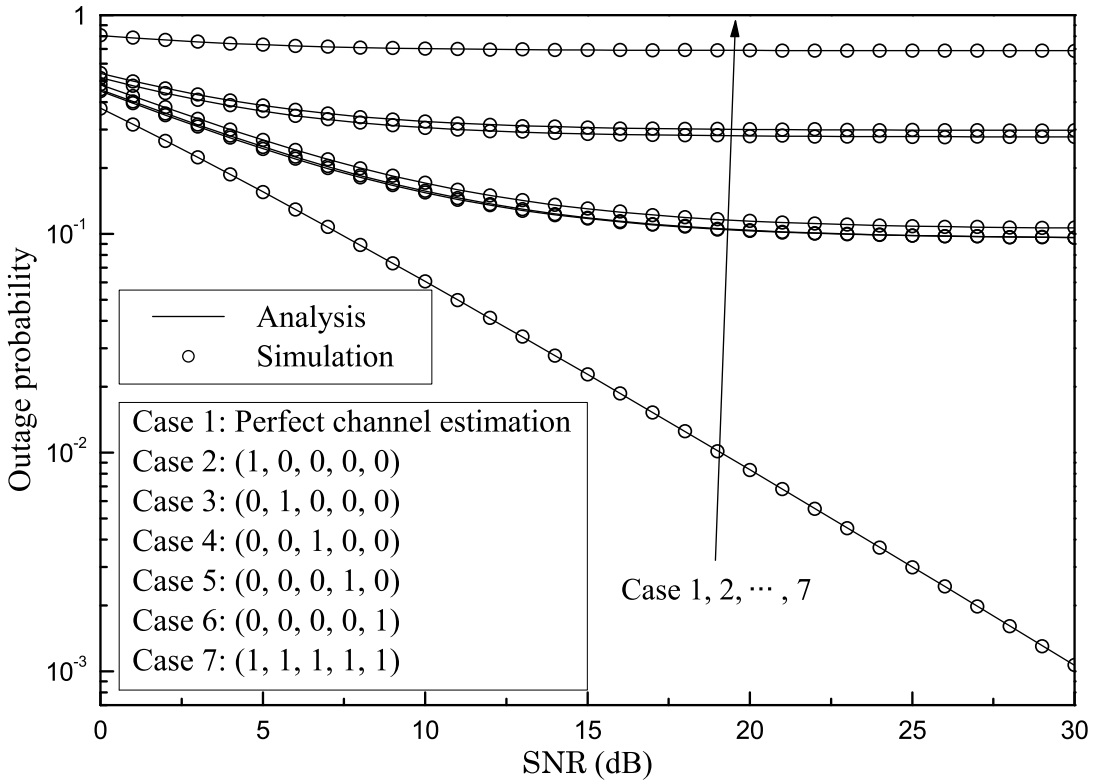

Figure 3.2. Outage probability of the user a versus SNR for two-way full-duplex relaying. Variances of the channel estimation errors are set to 0 or 1.

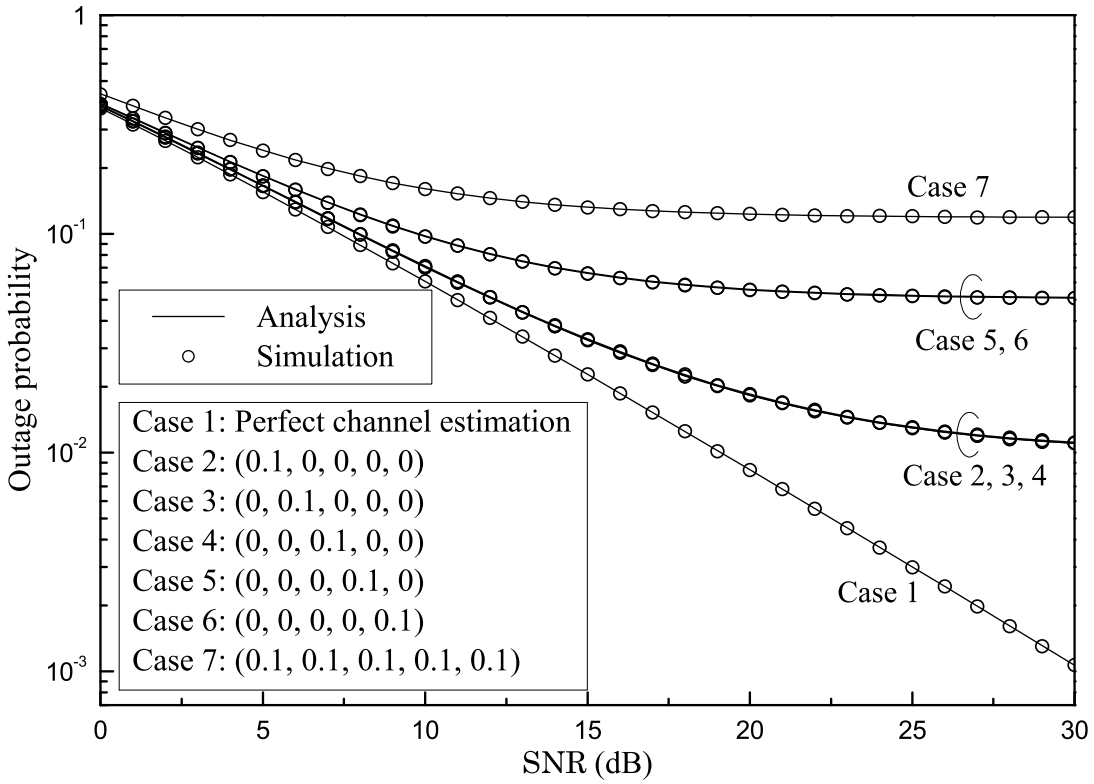

Figure 3.3. Outage probability of the user a versus SNR for two-way full-duplex relaying. Variances of the channel estimation errors are set to 0 or 0.1.

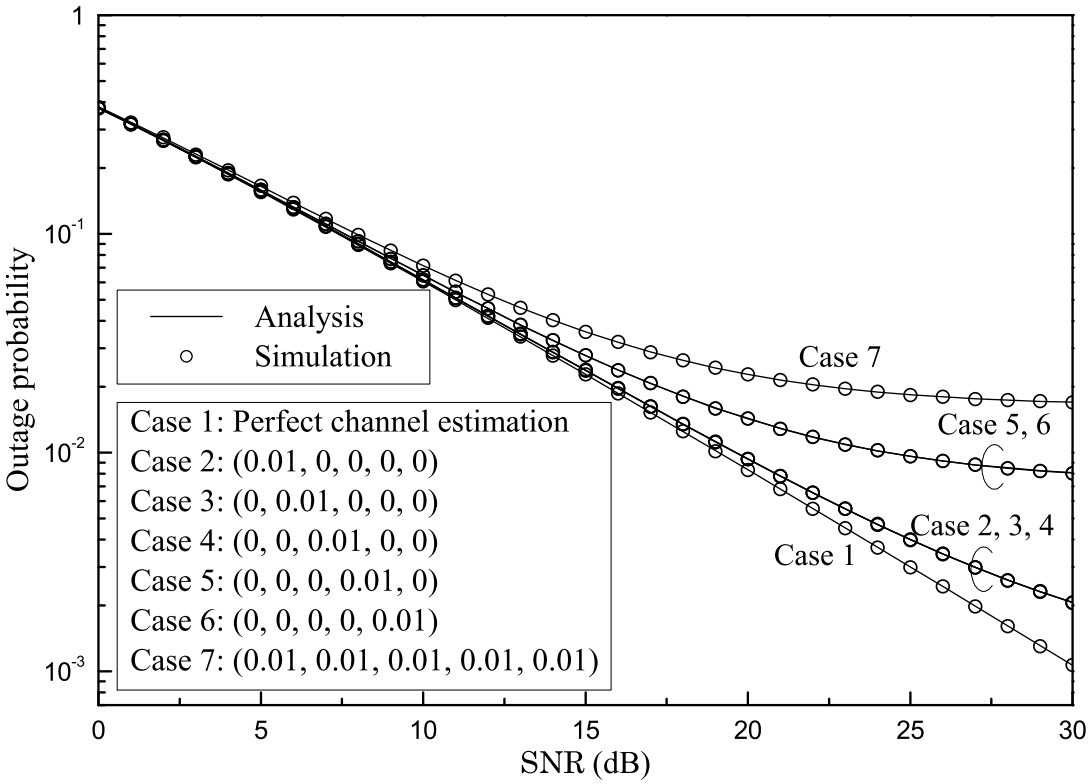

Figure 3.4. Outage probability of the user a versus SNR for two-way full-duplex relaying. Variances of the channel estimation errors are set to 0 or 0.01.

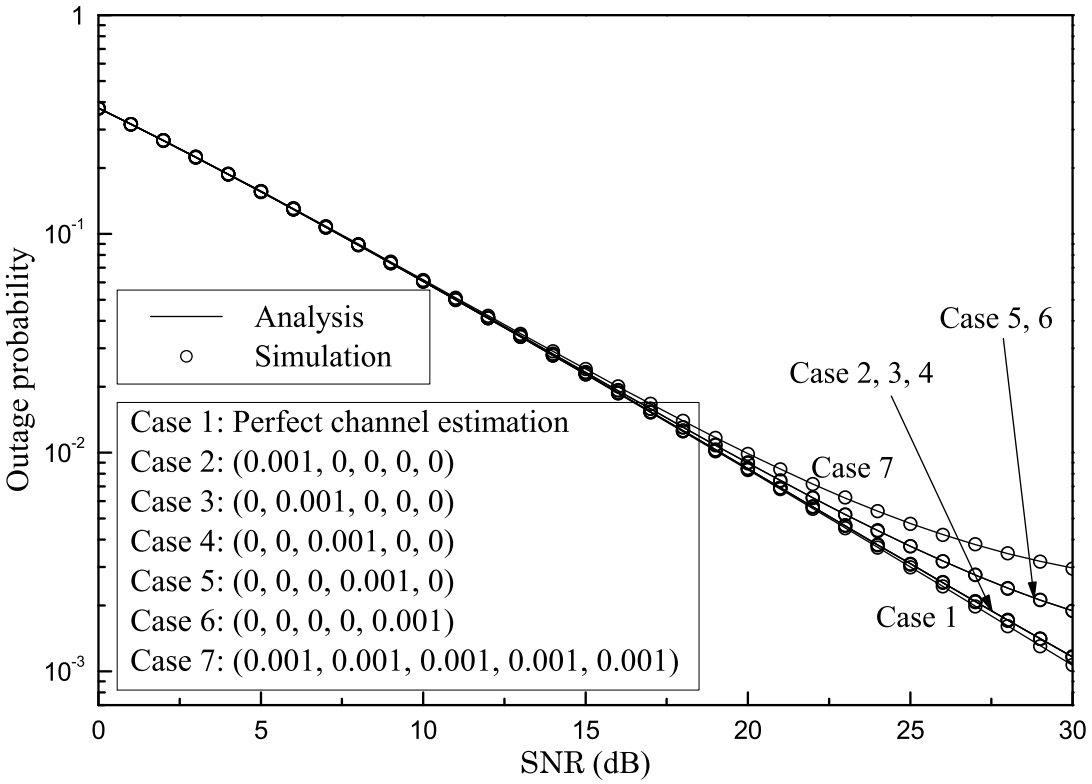

Figure 3.5. Outage probability of the user a versus SNR for two-way full-duplex relaying. Variances of the channel estimation errors are set to 0 or 0.001.

Fig. 3.6 shows the outage probability of the node a versus ξ for two-way full-duplex relaying when SNR = 30 dB and $\sigma^2_{h_{a,r}} = \sigma^2_{h_{b,r}} = \sigma^2_{h_{r,a}} = \sigma^2_{h_{r,r}} = \sigma^2_{h_{a,a}} = 10$. In case 1, all variances of the channel estimation errors are set to ω. In cases 2-6, one of the variances of the channel estimation errors is set to ξ and the others are set to ω. The analytical results are generated based on (3.28) and (3.29). Fig. 3.6(a), 3.6(b), and 3.6(c) are set to $\omega = 0.001, 0.01$, and 0.1, respectively. It is shown that the analytical results perfectly match the simulation results. It is shown that the outage probability of each case increases as ξ and ω increase. In addition, it is shown that the outage probability of cases 2-4 is lower than that of cases 5-6 when $\omega < \xi$ and that of cases 5-6 is lower than that of cases 2-4 when $\omega > \xi$. The reason is that, due to power normalization (3.5) at the relay, the effects of $\sigma^2_{\Delta h_{a,r}}$, $\sigma^2_{\Delta h_{r,r}}$, and $\sigma^2_{\Delta h_{b,r}}$ on the outage probability are reduced. Fig. 3.7 shows the outage probability of the node a versus ξ for two-way full-duplex relaying when SNR = 25 dB and $\sigma^2_{h_{a,r}} = \sigma^2_{h_{b,r}} = \sigma^2_{h_{r,a}} = \sigma^2_{h_{r,r}} = \sigma^2_{h_{a,a}} = 10$. In case 1, all variances of the channel estimation errors are set to ω. In cases 2-6, one of the variances of the channel estimation errors is set to ξ and the others are set to ω. Fig. 3.7(a), 3.7(b), and 3.7(c) are set to $\omega = 0.001, 0.01$, and 0.1, respectively. It is shown that our analytical results and the corresponding simulation results are in excellent agreement. It is shown that the outage probability of the node a decreases, as the SNR increases. Fig. 3.8 shows the outage probability of the node a versus ξ for two-way full-duplex relaying when SNR = 20 dB and $\sigma^2_{h_{a,r}} = \sigma^2_{h_{b,r}} = \sigma^2_{h_{r,a}} = \sigma^2_{h_{r,r}} = \sigma^2_{h_{a,a}} = 10$. In case 1, all variances of the channel estimation errors are set to ω. In cases 2-6, one of the variances of the

channel estimation errors is set to ξ and the others are set to ω. Fig. 3.8(a), 3.8(b), and 3.8(c) are set to $\omega = 0.001, 0.01$, and 0.1, respectively. As expected, it is shown that the outage probability of Fig. 3.8(a), 3.8(b), and 3.8(c) is larger than that of Fig. 3.6(a), 3.6(b), and 3.6(c).

3.4 Summary

In this chapter, we examine two-way full-duplex relaying in the presence of cochannel loop interference. In the two-way full-duplex relaying, two full-duplex users exchange data with each other via a full-duplex relay and each node attempts to subtract the estimate of the cochannel loop interference from its received signal. We derive the exact integral and approximate closed-form expressions for the outage probability of the two-way full-duplex relaying in case of perfect and imperfect channel state information. Monte Carlo simulation verifies the validity of analytical results. It is shown that the analysis of the outage probability well matches with simulation results. It is shown that the outage probability decreases as the variance of the channel estimation error decreases.

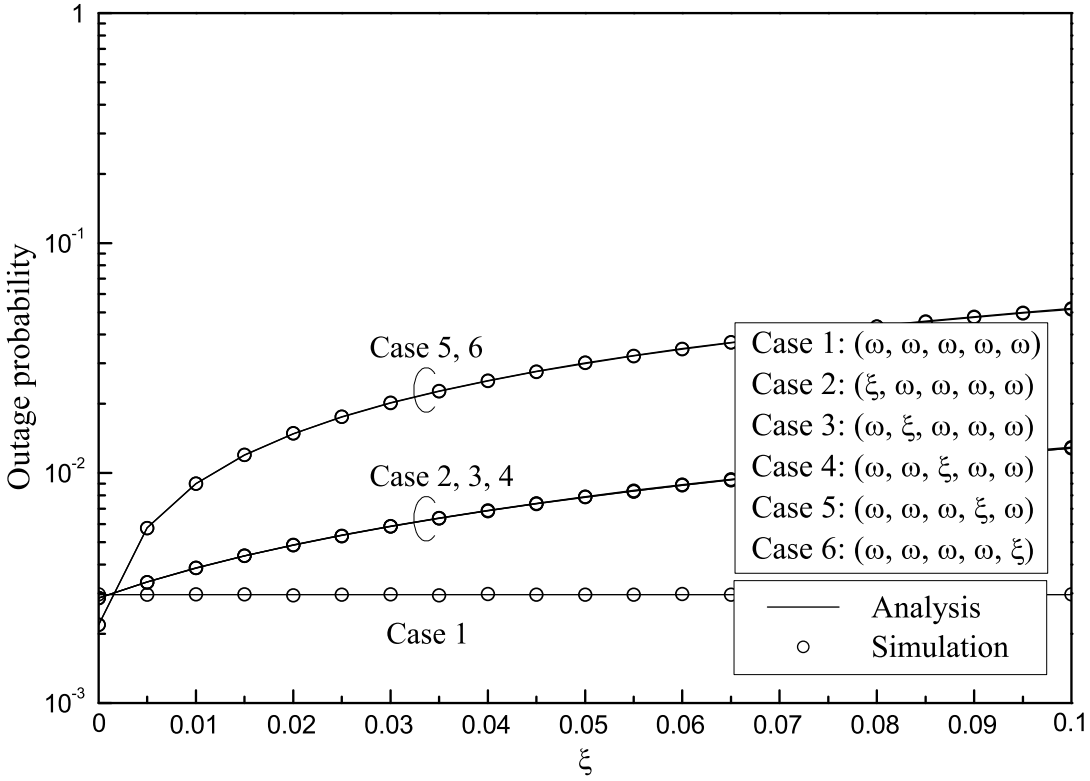
Outage probability
1
10-1
10-2
10-3
0
0.01
0.02
0.03
0.04
0.05
0.06
0.07
0.08
0.09
0.1
ξ
Case 5, 6
Case 2, 3, 4
Case 1
Case 1: (ω, ω, ω, ω, ω)
Case 2: (ξ, ω, ω, ω, ω)
Case 3: (ω, ξ, ω, ω, ω)
Case 4: (ω, ω, ξ, ω, ω)
Case 5: (ω, ω, ω, ξ, ω)
Case 6: (ω, ω, ω, ω, ξ)
Analysis
Simulation

(a) $\omega = 0.001$

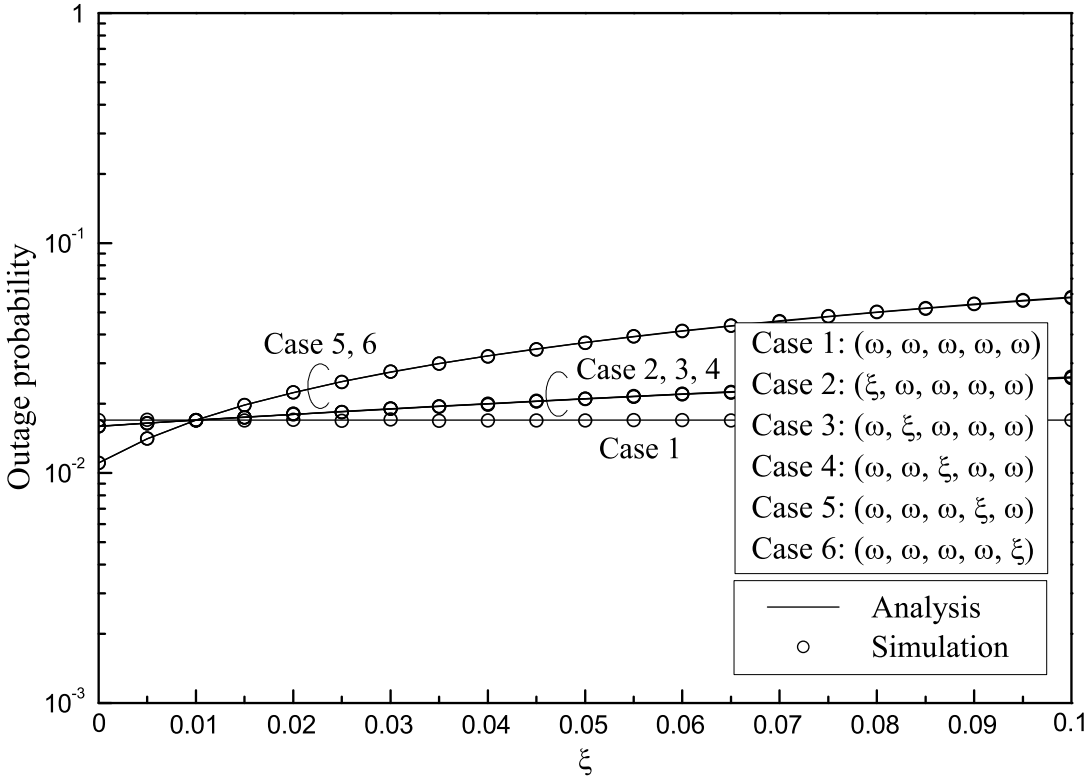
Outage probability
1
10^{-1}
10^{-2}
10^{-3}
0
0.01
0.02
0.03
0.04
0.05
0.06
0.07
0.08
0.09
0.1
ξ
Case 5, 6
Case 2, 3, 4
Case 1
Case 1: (ω, ω, ω, ω, ω)
Case 2: (ξ, ω, ω, ω, ω)
Case 3: (ω, ξ, ω, ω, ω)
Case 4: (ω, ω, ξ, ω, ω)
Case 5: (ω, ω, ω, ξ, ω)
Case 6: (ω, ω, ω, ω, ξ)
Analysis
Simulation

(b) $\omega = 0.01$

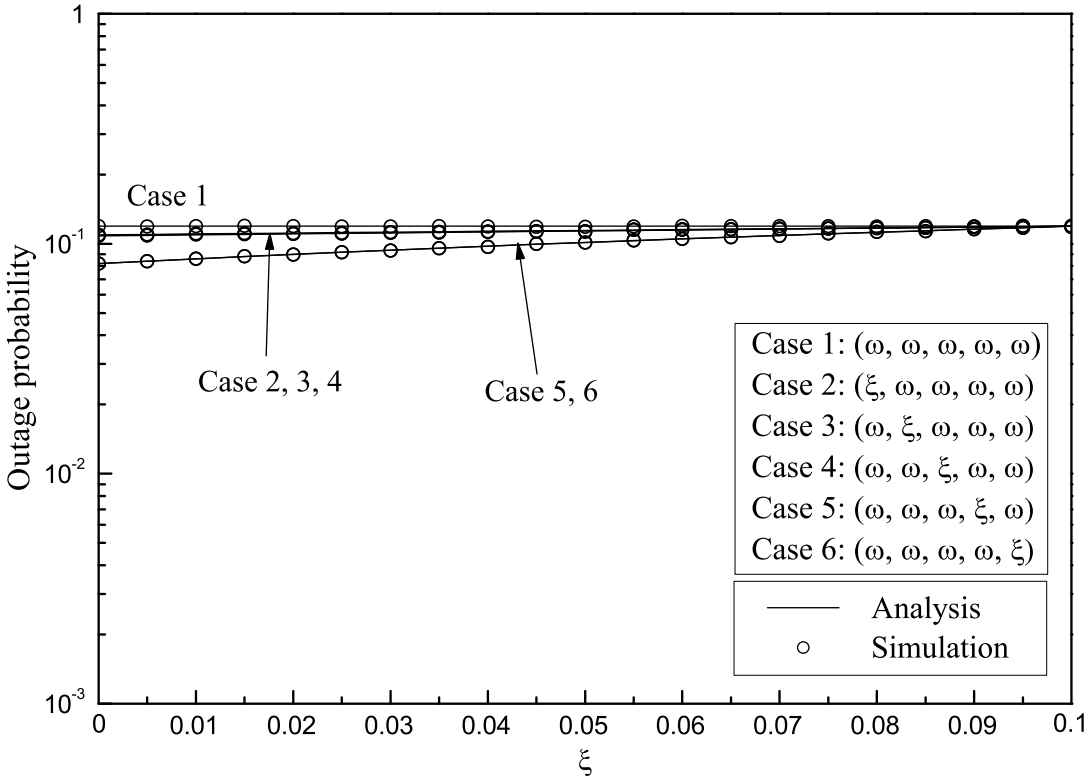

(c) $\omega = 0.1$

Figure 3.6. Outage probability of the user a versus ξ for two-way full-duplex relaying. SNR = 30 dB.

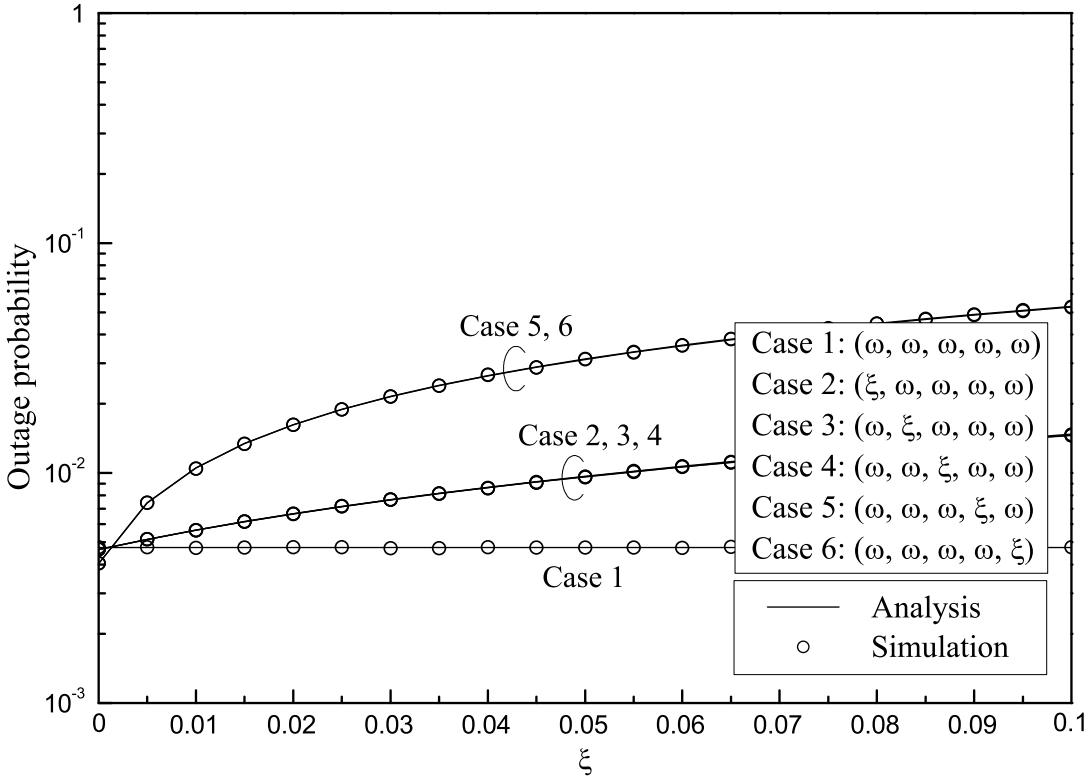
Outage probability
1
10^{-1}
10^{-2}
10^{-3}
0
0.01
0.02
0.03
0.04
0.05
0.06
0.07
0.08
0.09
0.1
ξ
Case 5, 6
Case 2, 3, 4
Case 1
Case 1: (ω, ω, ω, ω, ω)
Case 2: (ξ, ω, ω, ω, ω)
Case 3: (ω, ξ, ω, ω, ω)
Case 4: (ω, ω, ξ, ω, ω)
Case 5: (ω, ω, ω, ξ, ω)
Case 6: (ω, ω, ω, ω, ξ)
Analysis
Simulation

(a) $\omega = 0.001$

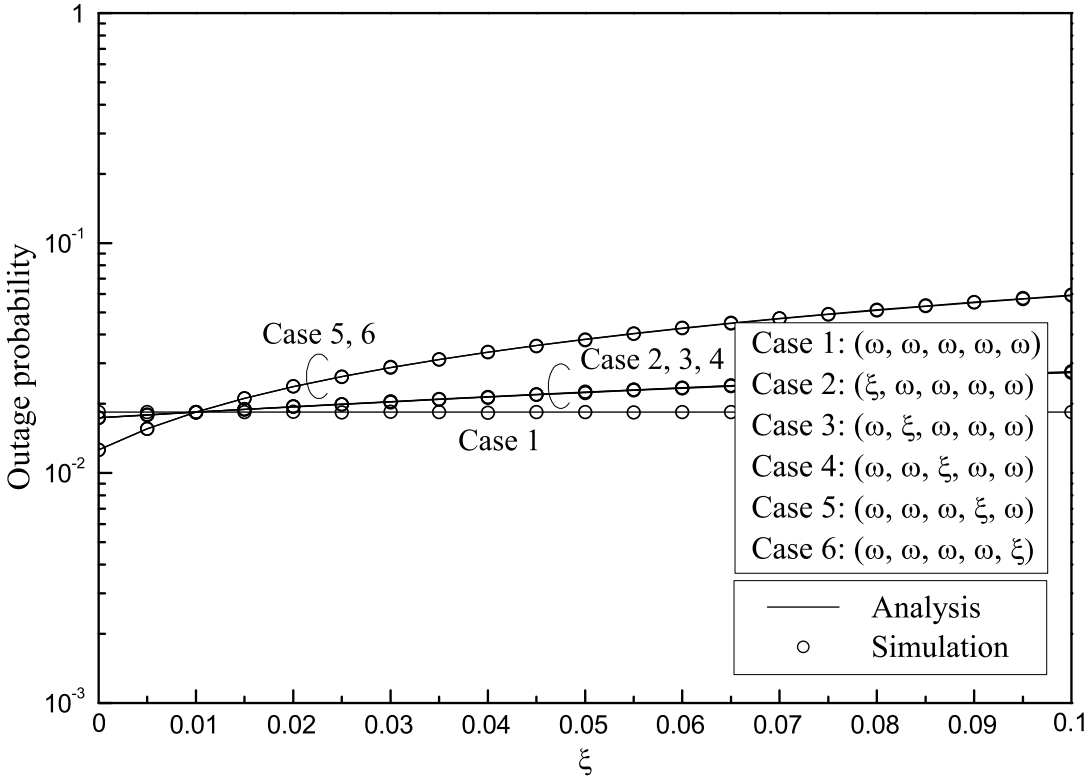
Outage probability
1
10^{-1}
10^{-2}
10^{-3}
0
0.01
0.02
0.03
0.04
0.05
0.06
0.07
0.08
0.09
0.1
ξ
Case 5, 6
Case 2, 3, 4
Case 1
Case 1: (ω, ω, ω, ω, ω)
Case 2: (ξ, ω, ω, ω, ω)
Case 3: (ω, ξ, ω, ω, ω)
Case 4: (ω, ω, ξ, ω, ω)
Case 5: (ω, ω, ω, ξ, ω)
Case 6: (ω, ω, ω, ω, ξ)
Analysis
Simulation

(b) $\omega = 0.01$

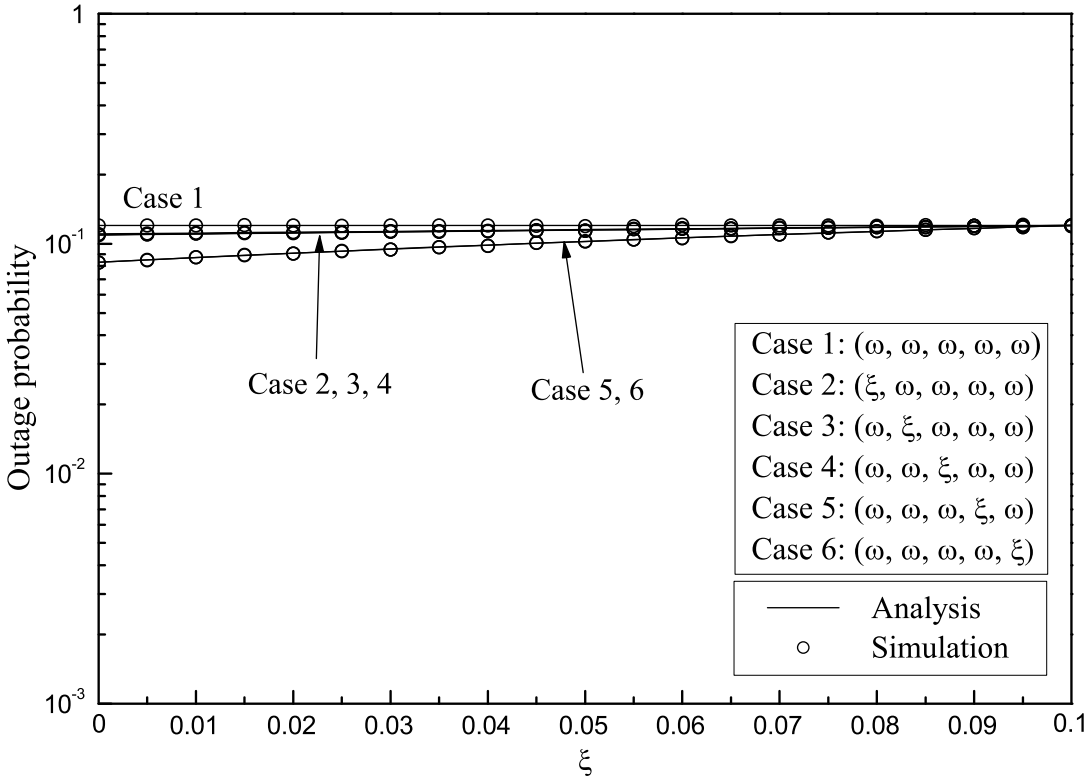

(c) $\omega = 0.1$

Figure 3.7. Outage probability of the user a versus ξ for two-way full-duplex relaying. SNR = 25 dB.

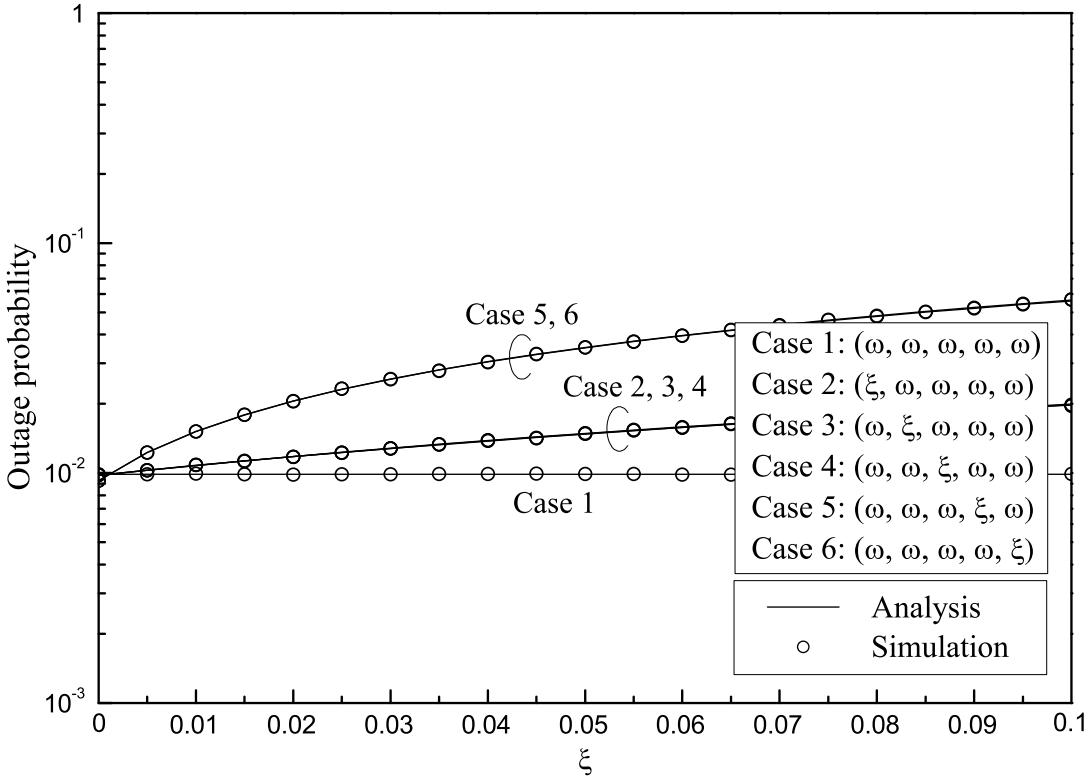
Outage probability
1
10^{-1}
10^{-2}
10^{-3}
0
0.01
0.02
0.03
0.04
0.05
0.06
0.07
0.08
0.09
0.1
ξ
Case 5, 6
Case 2, 3, 4
Case 1
Case 1: (ω, ω, ω, ω, ω)
Case 2: (ξ, ω, ω, ω, ω)
Case 3: (ω, ξ, ω, ω, ω)
Case 4: (ω, ω, ξ, ω, ω)
Case 5: (ω, ω, ω, ξ, ω)
Case 6: (ω, ω, ω, ω, ξ)
Analysis
Simulation

(a) $\omega = 0.001$

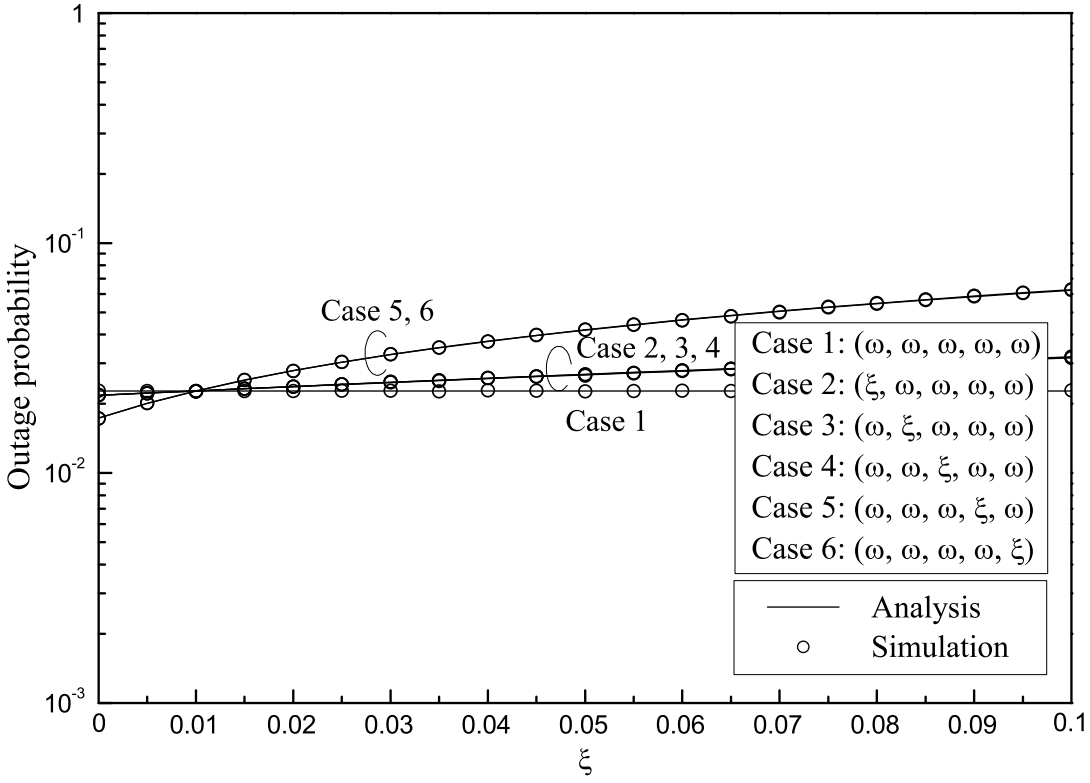
Outage probability
1
10-1
10-2
10-3
0
0.01
0.02
0.03
0.04
0.05
0.06
0.07
0.08
0.09
0.1
ξ
Case 5, 6
Case 2, 3, 4
Case 1
Case 1: (ω, ω, ω, ω, ω)
Case 2: (ξ, ω, ω, ω, ω)
Case 3: (ω, ξ, ω, ω, ω)
Case 4: (ω, ω, ξ, ω, ω)
Case 5: (ω, ω, ω, ξ, ω)
Case 6: (ω, ω, ω, ω, ξ)
Analysis
Simulation

(b) $\omega = 0.01$

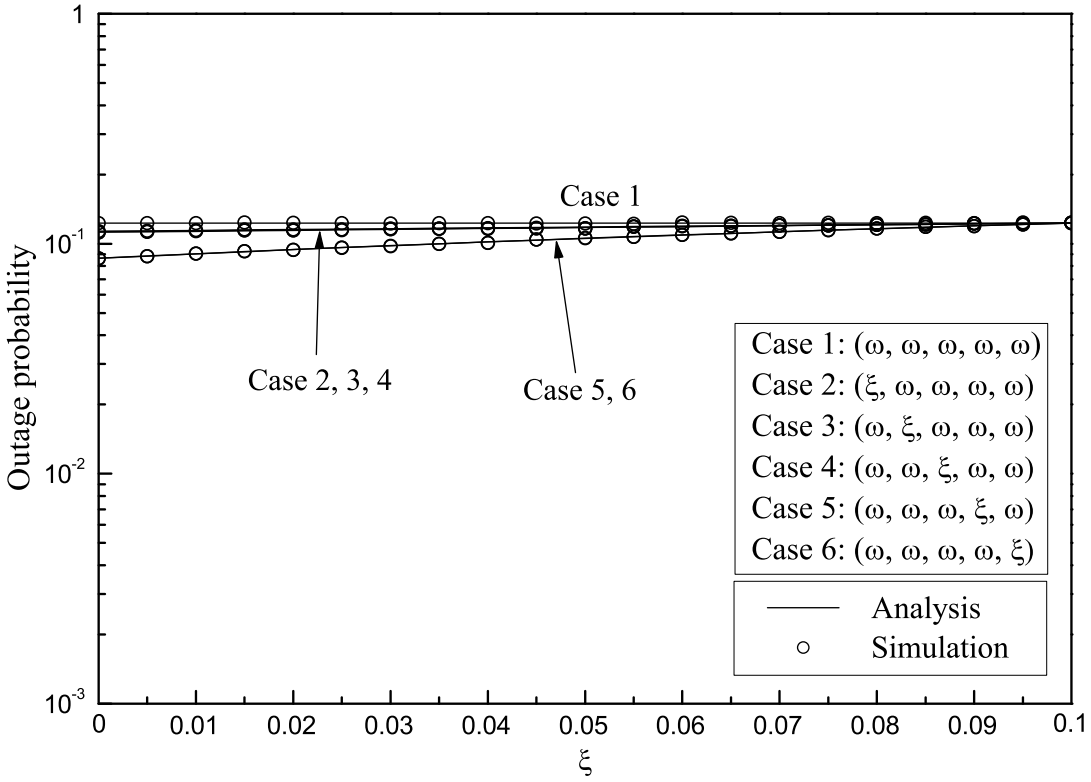

(c) $\omega = 0.1$

Figure 3.8. Outage probability of the user a versus ξ for two-way full-duplex relaying. SNR = 20 dB.

Chapter 4

Multi-hop Cognitive Radio Network with Cochannel Interference

Cognitive small cell network is an effective way to meet the demands for frequency spectrum in wireless communications [94]-[96]. If the quality of service (QoS) of licensed users in a cellular network is guaranteed, unlicensed users in the cognitive small cell network are allowed to utilize the spectrum of the cellular network [57].

Multi-hop transmission is well known as a promising technique to combat the performance degradation caused by propagation loss [1], [6]. In multi-hop transmission, when the direct path between a source and a destination is deeply faded, the source communicates with the destination via multiple intermediate relays.

The performance of multi-hop transmission for a cognitive small cell network

has been analyzed [97], [98]. In [97], the authors derive the outage probability of a cognitive small cell network over Rayleigh fading channels. In [98], the authors derive the outage probability of a cognitive small cell network over Nakagami-m fading channels. However, most of previous works have focused on the cognitive small cell networks which do not consider the effect of interference from the cellular network.

In this chapter, we investigate a cognitive small cell network which is overlaid with a cellular network. We analyze the performance of the cognitive small cell network in the presence of interference from the cellular network.

This chapter is organized as follows. In Section II, we describe the system model. In Section III, we derive the outage probability of the cognitive small cell network. Numerical results are presented in Section IV, and conclusions are drawn in Section V.

4.1 System Model

Consider an underlay cognitive small cell network which is overlaid with a cellular network as shown in Fig. 4.1, where the solid and dashed lines stand for the data and the interference, respectively. The cellular network consists of L cells each with a source and a destination, where, in the cell l, the source PS_l sends its data to the destination PD_l. The cognitive small cell network consists of a source, $K-1$ relays, and a destination. The source T_0 communicates with the destination T_K through K hop transmission using relays T_1, T_2, $\cdots$, T_{K-1}. Assume that each terminal has a single antenna and cannot transmit and receive simultaneously.

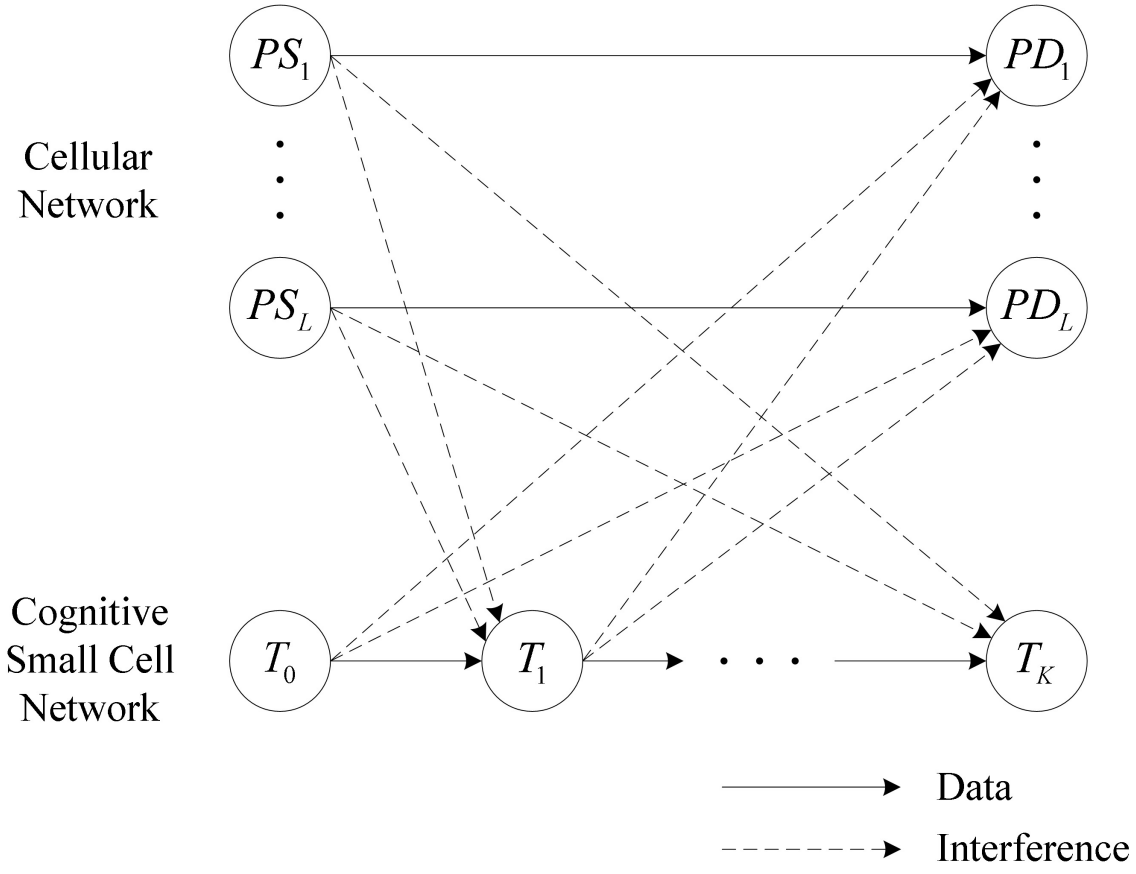

Figure 4.1. Underlay cognitive radio network which is overlaid with a cellular network.

Let $h_{i,j}$ denote the channel coefficient from the terminal i to the terminal j with $i, j \in \{PS_l, PD_l\}_{l=1}^{L} \cup \{T_k\}_{k=0}^{K}$. Assume that $h_{i,j}$ is a zero-mean circularly symmetric complex Gaussian random variable and its variance is given by [75]

$$\lambda_{i,j} = \eta d_{i,j}^{-\alpha} \tag{4.1}$$

where η is the propagation constant, α is the path-loss exponent, and $d_{i,j}$ is the distance between the terminal i and the terminal j.

Assume that the cellular network and cognitive small cell network are synchronized. In the cellular network, the sources PS_1, PS_2, $\cdots$, and PS_L transmit their own signals to the destinations PD_1, PD_2, $\cdots$, and PD_L, respectively. In the cognitive small cell network, communication from the source T_0 to the destination T_K is performed in K phases. In the phase k, $k = 1, 2, \cdots, K$, the terminal T_{k-1} transmits its signal to the terminal T_k, and then, the terminal T_k receives not only the transmitted signal from the terminal T_{k-1} but also the interference from the sources PS_1, PS_2, $\cdots$, and PS_L. The terminal T_k attempts to decode its received signal which is given by

$$y_{T_k} = h_{T_{k-1},T_k}\sqrt{P_{T_{k-1}}}x_{T_{k-1}} + \sum_{l=1}^{L} h_{PS_l,T_k}\sqrt{P_{PS_l}}x_{PS_l} + n_{T_k} \tag{4.2}$$

where P_i is the transmit power of the terminal i, x_i is the transmit signal of the terminal i, and n_i is the additive white Gaussian noise (AWGN) with zero mean and variance N_0 at the terminal i, $i \in \{PS_l\}_{l=1}^{L} \cup \{T_k\}_{k=0}^{K}$.

Assume that there are two constraints on the transmit power of the cognitive small cell network: maximum transmit power constraint and interference constraint

to guarantee the QoS of the cellular network [99]. The transmit power at the terminal T_k is given by

$$\begin{aligned} P_{T_k} &= \min\left\{P_{\max}, \frac{I}{|h_{T_k,PD_1}|^2}, \frac{I}{|h_{T_k,PD_2}|^2}, \cdots, \frac{I}{|h_{T_k,PD_L}|^2}\right\} \\ &= \min\left\{P_{\max}, \min_{l=1,\cdots,L} \frac{I}{|h_{T_k,PD_l}|^2}\right\}. \end{aligned} \tag{4.3}$$

where $P_{\max}$ is the maximum transmit power at the terminal T_k and I is the threshold of interference to the destination PD_l.

4.2 Outage Probability Derivation

4.2.1 Signal-to-Interference-plus-Noise Ratio

The signal-to-interference-plus-noise ratio (SINR) at the terminal T_k is given by

$$\gamma_{T_k} = \frac{P_{T_{k-1}}\left|h_{T_{k-1},T_k}\right|^2}{\sum_{l=1}^{L} P_{PS_l}|h_{PS_l,T_k}|^2 + N_0}. \tag{4.4}$$

4.2.2 Cumulative Density Function

The cumulative distribution function (CDF) of the SINR at the terminal T_k is given by

$$\begin{aligned} F_{\gamma_{T_k}}(\gamma) &= \Pr\left[\frac{P_{T_{k-1}}\left|h_{T_{k-1},T_k}\right|^2}{\sum_{l=1}^{L} P_{PS_l}|h_{PS_l,T_k}|^2 + N_0} < \gamma\right] \\ &= \Pr\left[\frac{X}{Y + N_0} < \gamma\right] \end{aligned} \tag{4.5}$$

where $X = P_{T_{k-1}}\left|h_{T_{k-1},T_k}\right|^2$ and $Y = \sum_{l=1}^{L} P_{PS_l}|h_{PS_l,T_k}|^2$. Then (4.5) becomes

$$F_{\gamma_{T_k}}(\gamma) = \int_0^\infty F_X(\gamma(y + N_0)) f_Y(y)\, dy. \tag{4.6}$$

The CDF of X is given by

$$\begin{aligned}
F_X(x) &= \Pr[X \le x] \\
&= \Pr\left[\min\left\{P_{\max}, \min_{l=1,\cdots,L} \frac{I}{\left|h_{T_{k-1},PD_l}\right|^2}\right\}\left|h_{T_{k-1},T_k}\right|^2 \le x\right] \\
&= \Pr\left[\min_{l=1,\cdots,L} \frac{I}{\left|h_{T_{k-1},PD_l}\right|^2} \le P_{\max}, \min_{l=1,\cdots,L} \frac{I}{\left|h_{T_{k-1},PD_l}\right|^2}\left|h_{T_{k-1},T_k}\right|^2 \le x\right] \\
&\quad + \Pr\left[\min_{l=1,\cdots,L} \frac{I}{\left|h_{T_{k-1},PD_l}\right|^2} > P_{\max}, P_{\max}\left|h_{T_{k-1},T_k}\right|^2 \le x\right] \\
&= A + B
\end{aligned} \tag{4.7}$$

where

$$A = \Pr\left[\min_{l=1,\cdots,L} \frac{I}{\left|h_{T_{k-1},PD_l}\right|^2} \le P_{\max}, \min_{l=1,\cdots,L} \frac{I}{\left|h_{T_{k-1},PD_l}\right|^2}\left|h_{T_{k-1},T_k}\right|^2 \le x\right] \tag{4.8}$$

and

$$B = \Pr\left[\min_{l=1,\cdots,L} \frac{I}{\left|h_{T_{k-1},PD_l}\right|^2} > P_{\max}, P_{\max}\left|h_{T_{k-1},T_k}\right|^2 \le x\right]. \tag{4.9}$$

After some manipulations, (4.8) is rewritten as

$$\begin{aligned}
A &= \Pr\left[\min_{l=1,\cdots,L} \frac{1}{\left|h_{T_{k-1},PD_l}\right|^2} \le \min\left\{\frac{P_{\max}}{I}, \frac{x}{I\left|h_{T_{k-1},T_k}\right|^2}\right\}\right] \\
&= \int_0^\infty \left[1 - \prod_{l=1}^{L}\left\{1 - \Pr\left[\frac{1}{\left|h_{T_{k-1},PD_l}\right|^2} < \min\left\{\frac{P_{\max}}{I}, \frac{x}{Iz}\right\}\right]\right\}\right] f_{\left|h_{T_{k-1},T_k}\right|^2}(z)dz \\
&= \int_0^{\frac{x}{P_{\max}}} \left[1 - \prod_{l=1}^{L}\left\{1 - \exp\left(-\frac{I}{\lambda_{T_{k-1},PD_l}P_{\max}}\right)\right\}\right] \frac{1}{\lambda_{T_{k-1},T_k}} \exp\left(-\frac{1}{\lambda_{T_{k-1},T_k}}z\right) dz \\
&\quad + \int_{\frac{x}{P_{\max}}}^\infty \left[1 - \prod_{l=1}^{L}\left\{1 - \exp\left(-\frac{Iz}{\lambda_{T_{k-1},PD_l}x}\right)\right\}\right] \frac{1}{\lambda_{T_{k-1},T_k}} \exp\left(-\frac{1}{\lambda_{T_{k-1},T_k}}z\right) dz.
\end{aligned} \tag{4.10}$$

By the multi-binomial theorem, (4.10) becomes

$$A = 1 - \left\{1 - \exp\left(-\frac{x}{\lambda_{T_{k-1},T_k} P_{\max}}\right)\right\} \prod_{l=1}^{L} \left\{1 - \exp\left(-\frac{I}{\lambda_{T_{k-1},PD_l} P_{\max}}\right)\right\}$$
$$- \sum_{k_1=0}^{1} \cdots \sum_{k_L=0}^{1} (-1)^{L-k_1-\cdots-k_L} \frac{\exp\left(-\frac{x}{\lambda_{T_{k-1},T_k} P_{\max}} - \sum_{l=1}^{L} \frac{(1-k_l)I}{\lambda_{T_{k-1},PD_l} P_{\max}}\right)}{1 + \sum_{l=1}^{L} \frac{\lambda_{T_{k-1},T_k}(1-k_l)I}{\lambda_{T_{k-1},PD_l} x}}. \quad (4.11)$$

Since $\left|h_{T_{k-1},PD_l}\right|^2$, $l = 1, 2, \cdots, L$, and $\left|h_{T_{k-1},T_k}\right|^2$ are independent, (4.9) is rewritten as

$$B = \Pr\left[\min_{l=1,\cdots,L} \frac{I}{\left|h_{T_{k-1},PD_l}\right|^2} > P_{\max}\right] \Pr\left[P_{\max}\left|h_{T_{k-1},T_k}\right|^2 \le x\right]$$
$$= \Pr\left[P_{\max}\left|h_{T_{k-1},T_k}\right|^2 < x\right] \prod_{l=1}^{L} \Pr\left[\frac{I}{\left|h_{T_{k-1},PD_l}\right|^2} \ge P_{\max}\right]$$
$$= \left\{1 - \exp\left(-\frac{x}{\lambda_{T_{k-1},T_k} P_{\max}}\right)\right\} \prod_{l=1}^{L} \left\{1 - \exp\left(-\frac{I}{\lambda_{T_{k-1},PD_l} P_{\max}}\right)\right\}. \quad (4.12)$$

The probability density function (PDF) of Y is given by [82]-[100]

$$f_Y(y) = \sum_{m=1}^{\rho(\mathbf{\Omega}_k)} \sum_{n=1}^{\tau_m(\mathbf{\Omega}_k)} \chi_{m,n}(\mathbf{\Omega}_k) \frac{\Omega_{[m]}^{-n}}{\Gamma(n)} y^{n-1} \exp\left(-\frac{y}{\Omega_{[m]}}\right) \quad (4.13)$$

where $\mathbf{\Omega}_k = \mathrm{diag}\left(P_{PS_1}\lambda_{PS_1,T_k}, P_{PS_2}\lambda_{PS_2,T_k}, \cdots, P_{PS_L}\lambda_{PS_L,T_k}\right)$, $\rho(\mathbf{\Omega}_k)$ is the number of distinct diagonal elements of $\mathbf{\Omega}_k$, $\Omega_{[m]}$, $m = 1, 2, \cdots, \rho(\mathbf{\Omega}_k)$, are the distinct diagonal elements of $\mathbf{\Omega}_k$ in decreasing order, i.e., $\Omega_{[1]} > \Omega_{[2]} > \cdots > \Omega_{[\rho(\mathbf{\Omega}_k)]}$, $\tau_m(\mathbf{\Omega}_k)$ is the multiplicity of $\Omega_{[m]}$, and

$$\chi_{m,n}(\mathbf{\Omega}_k) = \frac{1}{(\tau_m(\mathbf{\Omega}_k) - n)! \Omega_{[m]}^{\tau_m(\mathbf{\Omega}_k)-n}}$$
$$\times \left\{\frac{d^{\tau_m(\mathbf{\Omega}_k)-n}}{dy^{\tau_m(\mathbf{\Omega}_k)-n}} \left(1 + y\Omega_{[m]}\right)^{\tau_m(\mathbf{\Omega}_k)} \det\left(\mathbf{I}_L + y\mathbf{\Omega}_k\right)^{-1}\right\}\Bigg|_{y=-\frac{1}{\Omega_{[m]}}}. \quad (4.14)$$

From (4.6), (4.7), (4.11), (4.12), and (4.13), the CDF of the SINR at the terminal T_k is rewritten as

$$
\begin{aligned}
&F_{\gamma_{T_k}}(\gamma) \\
&= \int_0^{\infty} \sum_{m=1}^{\rho(\mathbf{\Omega}_k)} \sum_{n=1}^{\tau_m(\mathbf{\Omega}_k)} \chi_{m,n}(\mathbf{\Omega}_k) \frac{\Omega_{[m]}^{-n}}{\Gamma(n)} y^{n-1} \exp\left(-\frac{y}{\Omega_{[m]}}\right) \\
&\quad \times \left\{ 1 - \sum_{k_1=0}^{1} \cdots \sum_{k_L=0}^{1} (-1)^{L-k_1-\cdots-k_L} \frac{\exp\left(-\frac{\gamma(y+N_0)}{\lambda_{T_{k-1},T_k} P_{\max}} - \sum_{l=1}^{L} \frac{(1-k_l)I}{\lambda_{T_{k-1},PD_l} P_{\max}}\right)}{1 + \sum_{l=1}^{L} \frac{\lambda_{T_{k-1},T_k}(1-k_l)I}{\lambda_{T_{k-1},PD_l}\gamma(y+N_0)}} \right\} dy.
\end{aligned}
\tag{4.15}
$$

Using $\int_0^{\infty} x^{\nu-1} e^{-\mu x} dx = \frac{1}{\mu^{\nu}} \Gamma(\nu)$ for $\mu > 0$ and $\nu > 0$ in [101, eq. (3.381.4)], (4.15) is rewritten as

$$
\begin{aligned}
&F_{\gamma_{T_k}}(\gamma) \\
&= \sum_{m=1}^{\rho(\mathbf{\Omega}_k)} \sum_{n=1}^{\tau_m(\mathbf{\Omega}_k)} \chi_{m,n}(\mathbf{\Omega}_k) - \int_0^{\infty} \sum_{m=1}^{\rho(\mathbf{\Omega}_k)} \sum_{n=1}^{\tau_m(\mathbf{\Omega}_k)} \chi_{m,n}(\mathbf{\Omega}_k) \frac{\Omega_{[m]}^{-n}}{\Gamma(n)} y^{n-1} \exp\left(-\frac{y}{\Omega_{[m]}}\right) \\
&\quad \times \left\{ \sum_{k_1=0}^{1} \cdots \sum_{k_L=0}^{1} (-1)^{L-k_1-\cdots-k_L} \frac{(y+N_0) \exp\left(-\frac{\gamma(y+N_0)}{\lambda_{T_{k-1},T_k} P_{\max}} - \sum_{l=1}^{L} \frac{(1-k_l)I}{\lambda_{T_{k-1},PD_l} P_{\max}}\right)}{y + N_0 + \sum_{l=1}^{L} \frac{\lambda_{T_{k-1},T_k}(1-k_l)I}{\lambda_{T_{k-1},PD_l}\gamma}} \right\} dy.
\end{aligned}
\tag{4.16}
$$

From (4.16) and the fact that $\int_0^{\infty} \frac{x^{\nu-1} e^{-\mu x}}{x+\beta} dx = \beta^{\nu-1} e^{\beta\mu} \Gamma(\nu) \Gamma(1-\nu, \beta\mu)$ for $\mu > 0$

and $\nu > 0$ in [101, eq. (3.383.10)], we obtain

$$
\begin{aligned}
&F_{\gamma_{T_k}}(\gamma) \\
&= \sum_{m=1}^{\rho(\mathbf{\Omega}_k)} \sum_{n=1}^{\tau_m(\mathbf{\Omega}_k)} \chi_{m,n}(\mathbf{\Omega}_k) - \sum_{k_1=0}^{1} \cdots \sum_{k_L=0}^{1} \sum_{m=1}^{\rho(\mathbf{\Omega}_k)} \sum_{n=1}^{\tau_m(\mathbf{\Omega}_k)} \chi_{m,n}(\mathbf{\Omega}_k) \frac{\Omega_{[m]}^{-n}}{\Gamma(n)} (-1)^{L-k_1-\cdots-k_L} \\
&\quad \times \exp\left(-\frac{\gamma N_0}{\lambda_{T_{k-1},T_k} P_{\max}} - \sum_{l=1}^{L} \frac{(1-k_l) I}{\lambda_{T_{k-1},PD_l} P_{\max}} \right) \left\{ N_0 + \sum_{l=1}^{L} \frac{\lambda_{T_{k-1},T_k} (1-k_l) I}{\lambda_{T_{k-1},PD_l} \gamma} \right\}^{n-1} \\
&\quad \times \exp\left(\left\{ N_0 + \sum_{l=1}^{L} \frac{\lambda_{T_{k-1},T_k} (1-k_l) I}{\lambda_{T_{k-1},PD_l} \gamma} \right\} \left(\frac{1}{\Omega_{[m]}} + \frac{\gamma}{\lambda_{T_{k-1},T_k} P_{\max}} \right) \right) \\
&\quad \times \left[\left\{ N_0 + \sum_{l=1}^{L} \frac{\lambda_{T_{k-1},T_k} (1-k_l) I}{\lambda_{T_{k-1},PD_l} \gamma} \right\} \Gamma(n+1) \right. \\
&\quad \times \Gamma\left(-n, \left\{ N_0 + \sum_{l=1}^{L} \frac{\lambda_{T_{k-1},T_k} (1-k_l) I}{\lambda_{T_{k-1},PD_l} \gamma} \right\} \left(\frac{1}{\Omega_{[m]}} + \frac{\gamma}{\lambda_{T_{k-1},T_k} P_{\max}} \right) \right) \\
&\quad \left. + N_0 \Gamma(n) \Gamma\left(1-n, \left\{ N_0 + \sum_{l=1}^{L} \frac{\lambda_{T_{k-1},T_k} (1-k_l) I}{\lambda_{T_{k-1},PD_l} \gamma} \right\} \left(\frac{1}{\Omega_{[m]}} + \frac{\gamma}{\lambda_{T_{k-1},T_k} P_{\max}} \right) \right) \right].
\end{aligned}
\tag{4.17}
$$

4.2.3 Outage Probability

The mutual information between the terminal T_{k-1} and the terminal T_k is given by

$$
C_{T_k} = \frac{1}{K} \log_2 (1 + \gamma_{T_k}). \tag{4.18}
$$

The mutual information between the source T_0 and the destination T_K is given by

$$
C = \min \{ C_{T_1}, C_{T_2}, \cdots, C_{T_K} \}. \tag{4.19}
$$

An outage occurs when the mutual information between the source T_0 and the destination T_K falls below a target rate R. The outage probability of the cognitive small

cell network is given by

$$\begin{aligned} P_{out}(R) &= \Pr(C < R) \\ &= \Pr(\min\{C_{T_1}, C_{T_2}, \cdots, C_{T_K}\} \leq R) \\ &= 1 - \prod_{k=1}^{K} \left\{1 - F_{\gamma_{T_k}}\left(2^{KR} - 1\right)\right\}. \end{aligned} \tag{4.20}$$

4.3 Numerical Results

Consider a cognitive small cell network which is overlaid with a cellular network with L cells. Suppose that $d_{T_0T_K} = 10$, $d_{T_{k-1}T_k} = 10/K$, $\lambda_{PS_lT_k} = 0.005$, and $\lambda_{T_{k-1}PD_l} = 0.005$ for $l = 1, 2, \cdots, L$ and $k = 1, 2, \cdots, K$.

The main contribution of this chapter is the derivation of the closed-form expression for the outage probability of the cognitive small cell network which is overlaid with a cellular network. To provide insights into the impact of $P_{\max}/N_0$ and the number of hops on the outage probability, we assume that parameters except $P_{\max}/N_0$ and the number of hops have simple values such as $d_{T_0T_K} = 10$, $d_{T_{k-1}T_k} = 10/K$, $\lambda_{PS_lT_k} = 0.005$, and $\lambda_{T_{k-1}PD_l} = 0.005$. Note that although these assumptions seem not realistic, they do not affect the accuracy of the analytical results. And since the analytical results are the function of the $d_{T_0T_K}$, $d_{T_{k-1}T_k}$, $\lambda_{PS_lT_k}$, and $\lambda_{T_{k-1}PD_l}$, we can obtain more realistic results by changing the parameter values of $d_{T_0T_K}$, $d_{T_{k-1}T_k}$, $\lambda_{PS_lT_k}$, and $\lambda_{T_{k-1}PD_l}$ in (4.17) and (4.20).

Fig. 4.2 shows the outage probability of the cognitive small cell network versus $P_{\max}/N_0$ with $L = 1, 3, 5, 7$, $\alpha = 3, 4, 5$, $R = 0.1$, and $I = 0$ dB. It is shown that

the analytical results are in complete agreement with simulation results. It is shown that the outage probability decreases as $P_{\max}/N_0$ increases at the low and medium $P_{\max}/N_0$. It is shown that the outage probability exhibits error floors at high $P_{\max}/N_0$. The reason is that although $P_{\max}$ increases, the transmit power of T_k is limited as shown in (4.3) due to the interference constraint. It is shown that the outage probability increases as the number of cells increases. In addition, it is shown that the outage probability increases, as the path loss exponent increases. The reason is that the variances of the channels between two adjacent terminals decreases, as the path loss exponent increases. Fig. 4.3 shows the outage probability of the cognitive small cell network versus $P_{\max}/N_0$ with $L = 3$, $\alpha = 4$, and $R = 0.1$. It is shown that the outage probability decreases as the interference threshold increases. The reason is that the terminals in the cognitive small cell network can use more power as the interference threshold increases.

Fig. 4.4 shows the outage probability of the cognitive small cell network versus $P_{\max}/N_0$ with $L = 1, 3, 5, 7$, $\alpha = 3, 4, 5$, $R = 0.2$, and $I = 0$ dB. It is shown that the analytical results perfectly match the simulation results. It is shown that, as $P_{\max}/N_0$ increases, the outage probability decreases at the low and medium $P_{\max}/N_0$. It is shown that the outage probability exhibits error floors at high $P_{\max}/N_0$. The reason is that although $P_{\max}$ increases, the transmit power of T_k is limited as shown in (4.3) due to the interference constraint. It is shown that the outage probability increases as the number of cells increases. In addition, it is shown that the outage probability increases, as the path loss exponent increases. The reason is that the

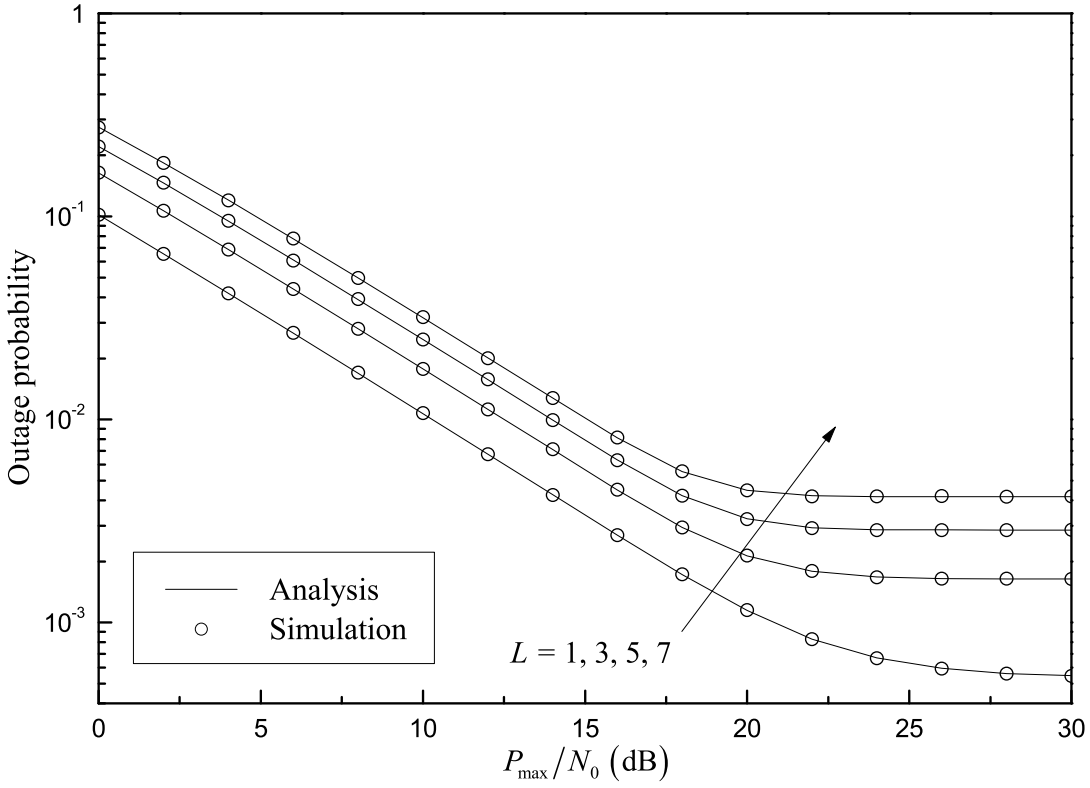
1
10^{-1}
10^{-2}
10^{-3}
Outage probability
Analysis
Simulation
L = 1, 3, 5, 7
0
5
10
15
20
25
30
$P_{\max}/N_0$ (dB)

(a) $\alpha = 3$

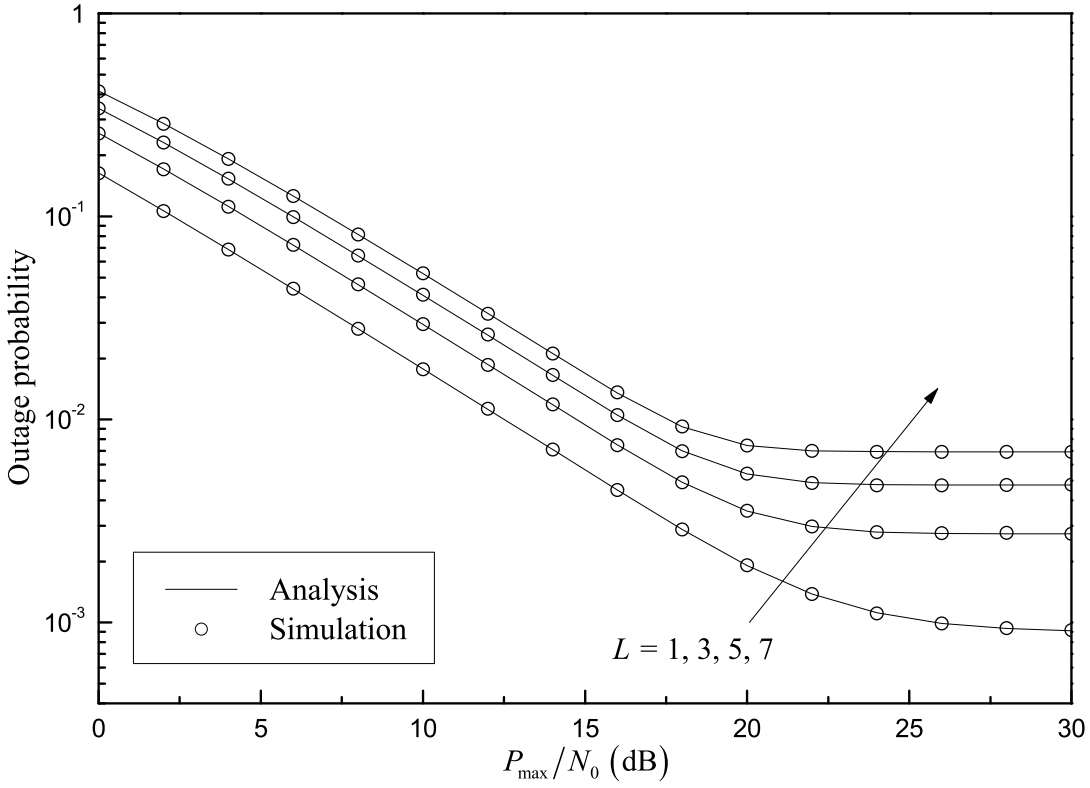
Outage probability
1
10^{-1}
10^{-2}
10^{-3}
0
5
10
15
20
25
30
$P_{\max}/N_0$ (dB)
Analysis
Simulation
L = 1, 3, 5, 7

(b) $\alpha = 4$

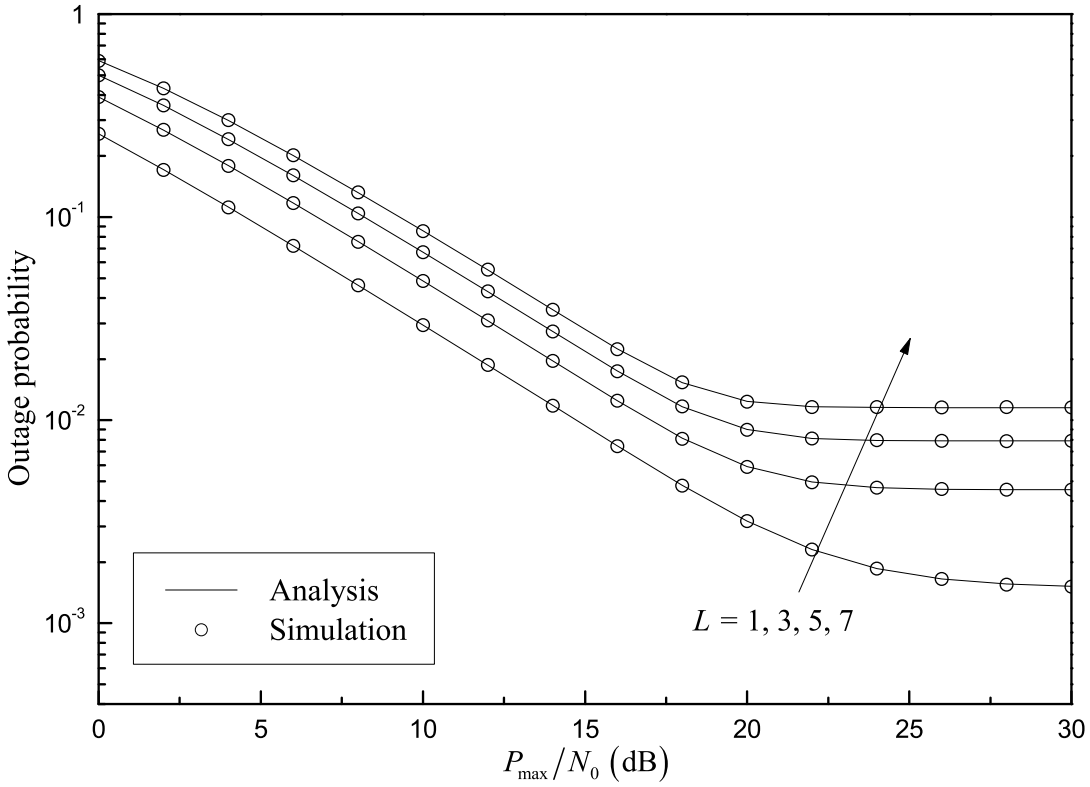

(c) $\alpha = 5$

Figure 4.2. Outage probability versus $P_{\max}/N_0$ for various number of cells. $R = 0.1$, $I = 0$ dB.

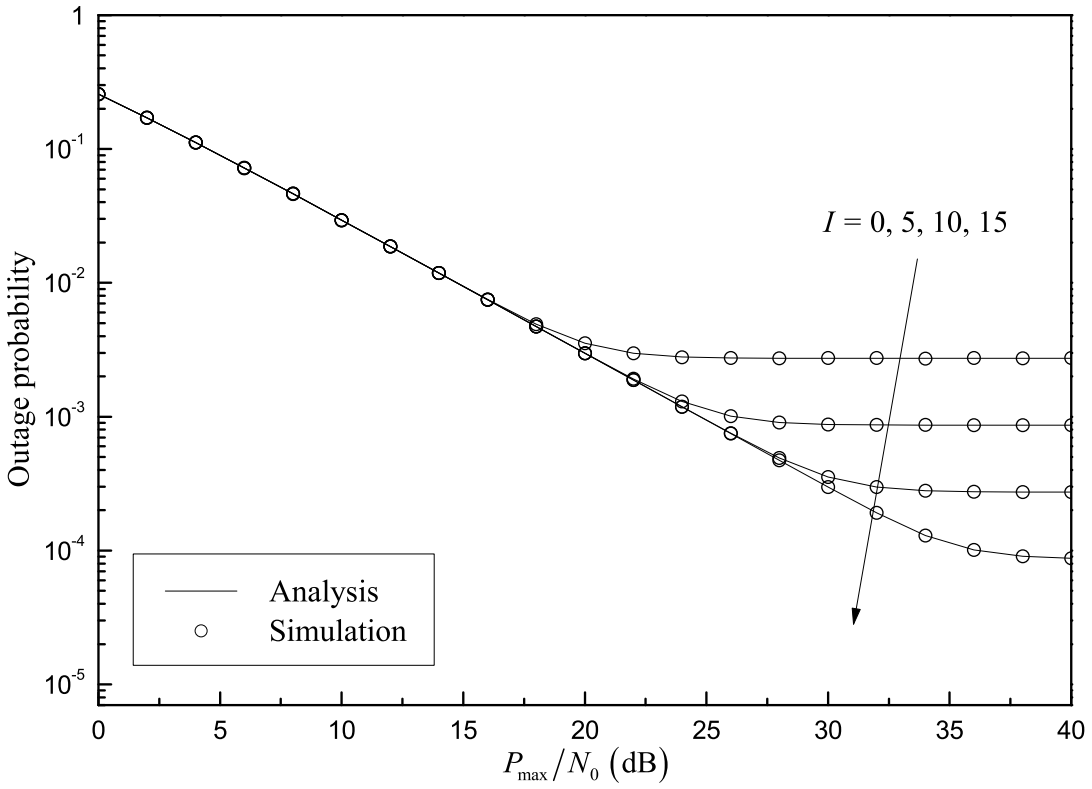

Figure 4.3. Outage probability versus $P_{\max}/N_0$ for various interference threshold. $R = 0.1$, $\alpha = 4$, $L = 3$.

variances of the channels between two adjacent terminals decreases, as the path loss exponent increases. As expected, it is shown that the outage probability of Fig. 4.2 is lower than that of Fig. 4.4 due to the target data rate. Fig. 4.5 shows the outage probability of the cognitive small cell network versus $P_{\max}/N_0$ with $L = 3$, $\alpha = 4$, and $R = 0.2$. It is shown that the outage probability decreases as the interference threshold increases. The reason is that the terminals in the cognitive small cell network can use more power as the interference threshold increases. As expected, it is shown that the outage probability of Fig. 4.3 is lower than that of Fig. 4.5 because of the target data rate.

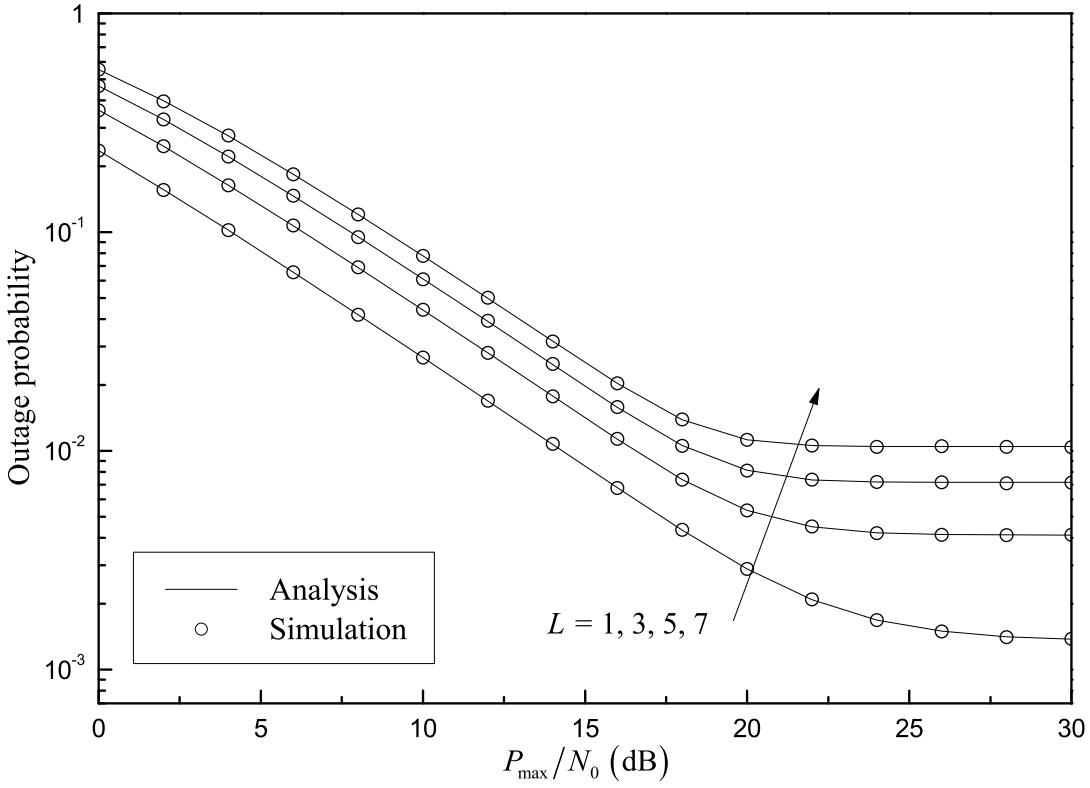
1
10^{-1}
10^{-2}
10^{-3}
Outage probability
0
5
10
15
20
25
30
$P_{\max}/N_0$ (dB)
Analysis
Simulation
L = 1, 3, 5, 7

(a) $\alpha = 3$

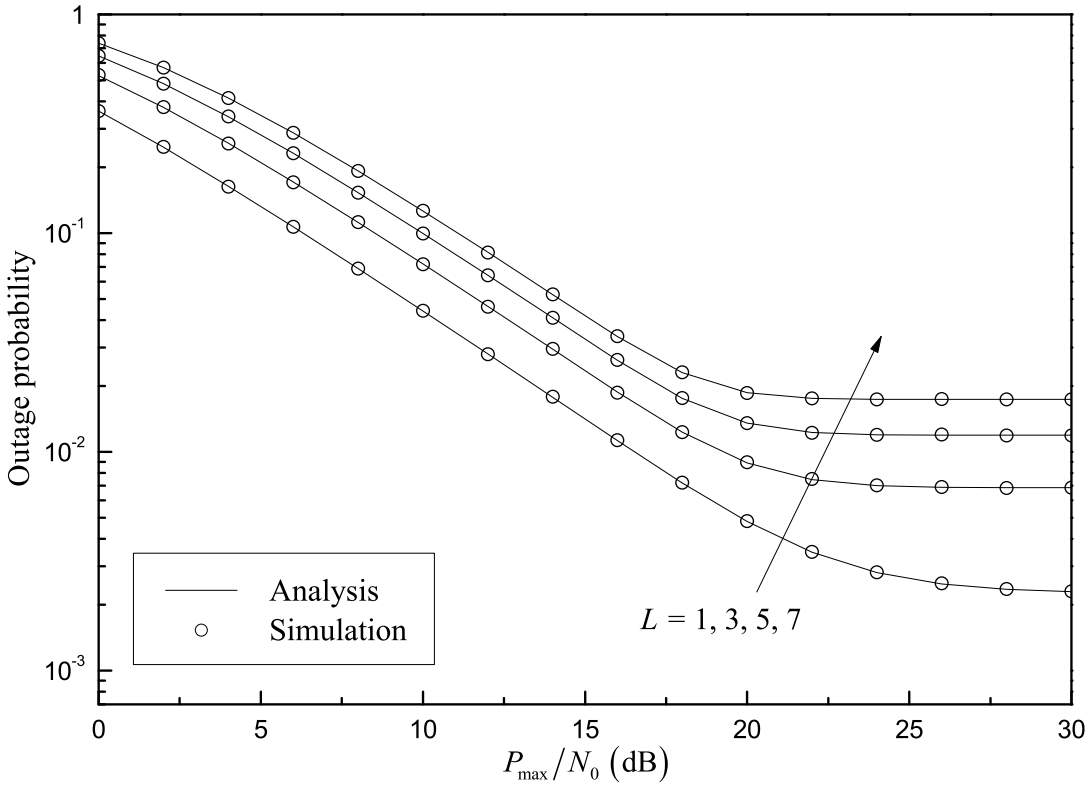
Outage probability
1
10^{-1}
10^{-2}
10^{-3}
0
5
10
15
20
25
30
$P_{\max}/N_0$ (dB)
Analysis
Simulation
L = 1, 3, 5, 7

(b) $\alpha = 4$

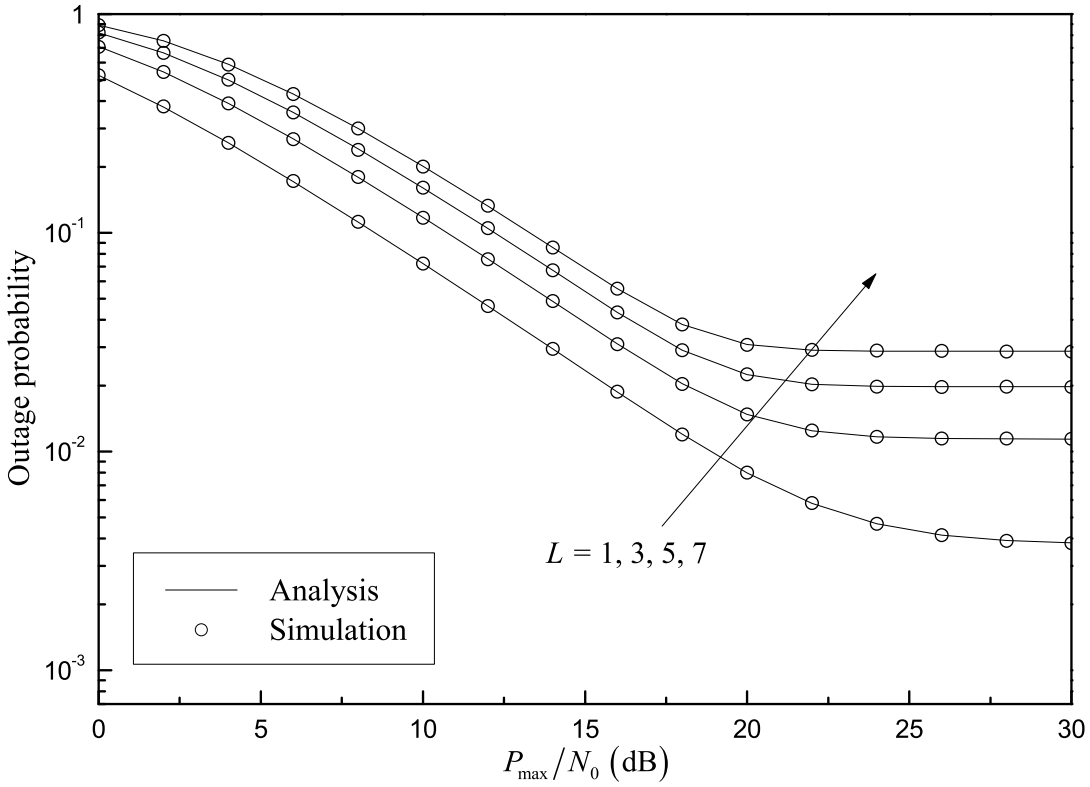

(c) $\alpha = 5$

Figure 4.4. Outage probability versus $P_{\max}/N_0$ for various number of cells. $R = 0.2$, $I = 0$ dB.

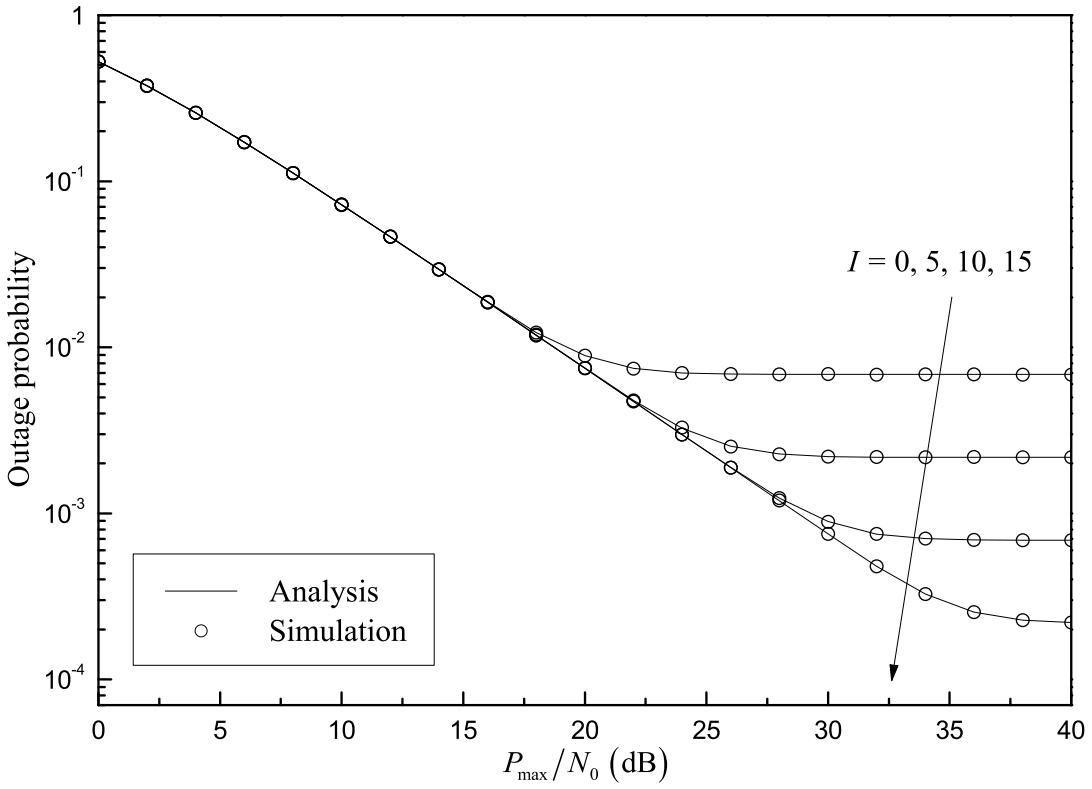

Figure 4.5. Outage probability versus $P_{\max}/N_0$ for various interference threshold. $R = 0.2$, $\alpha = 4$, $L = 3$.

Fig. 4.6 shows the outage probability of the cognitive small cell network versus the number of hops with $L = 1$, $\alpha = 3, 4, 5$, and $P_{\max}/N_0 = 20, 24, 28, 32$. It is shown that the analytical results and the simulation results are in excellent agreement. It is shown that, as $P_{\max}/N_0$ increase, the outage probability increases. It is shown that there is an optimal number of hops that minimize the outage probability of the cognitive small cell network. It is shown that the optimal number of hops is 5 and 8 at $\alpha = 3$ and 4, respectively. It is also shown that the optimal number of hops is larger than 10 at $\alpha = 5$. As α increases, the optimal number of hops increases. Fig. 4.7 shows the outage probability of the cognitive small cell network versus the number of hops with $L = 2$, $\alpha = 3, 4, 5$, and $P_{\max}/N_0 = 20, 24, 28, 32$. It is shown that the optimal number of hops is 5 and 8 at $\alpha = 3$ and 4, respectively. It is also shown that the optimal number of hops is larger than 10 at $\alpha = 5$. As α increases, the optimal number of hops increases. Fig. 4.8 shows the outage probability of the cognitive small cell network versus the number of hops with $L = 3$, $\alpha = 3, 4, 5$, and $P_{\max}/N_0 = 20, 24, 28, 32$. It is shown that the optimal number of hops is 5 and 8 at $\alpha = 3$ and 4, respectively. It is also shown that the optimal number of hops is larger than 10 at $\alpha = 5$. It is shown that the outage probability increases as the number of cells increases.

4.4 Summary

In this chapter, we examine the cognitive small cell network which is overlaid with a cellular network. We derive the closed-form expression for the outage probability

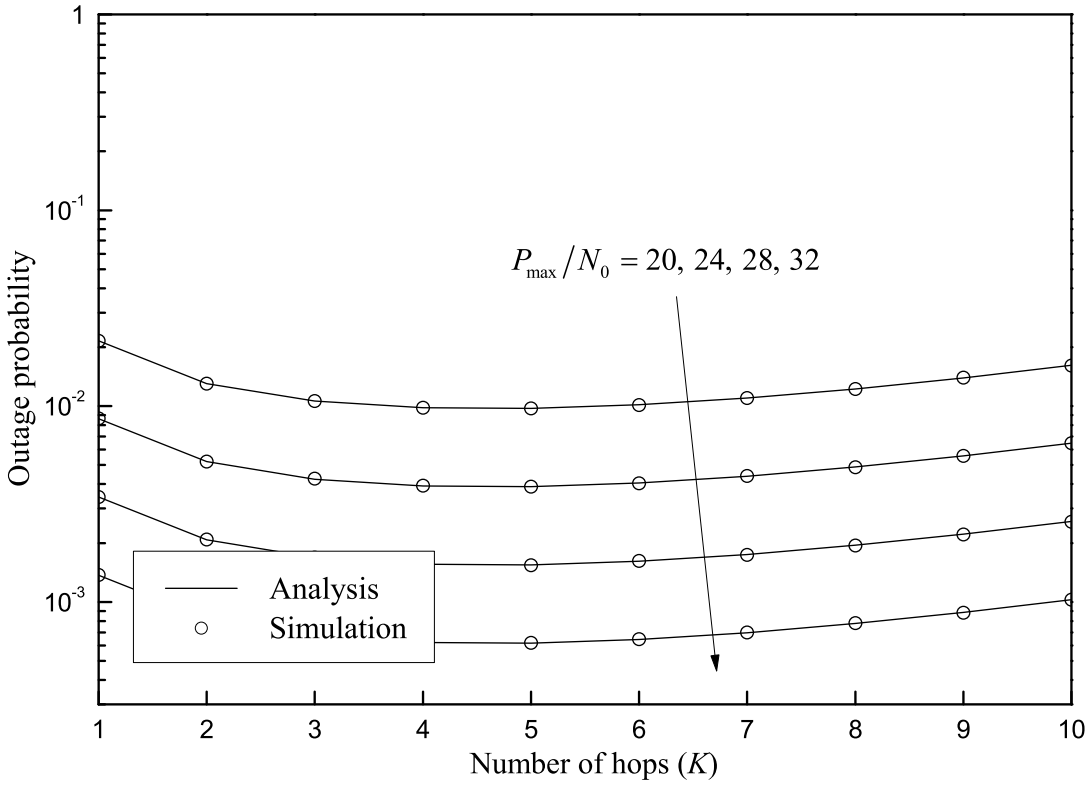
Outage probability
1
10^{-1}
10^{-2}
10^{-3}
$P_{\max}/N_0 = 20, 24, 28, 32$
Analysis
Simulation
1
2
3
4
5
6
7
8
9
10
Number of hops (K)

(a) $\alpha = 3$

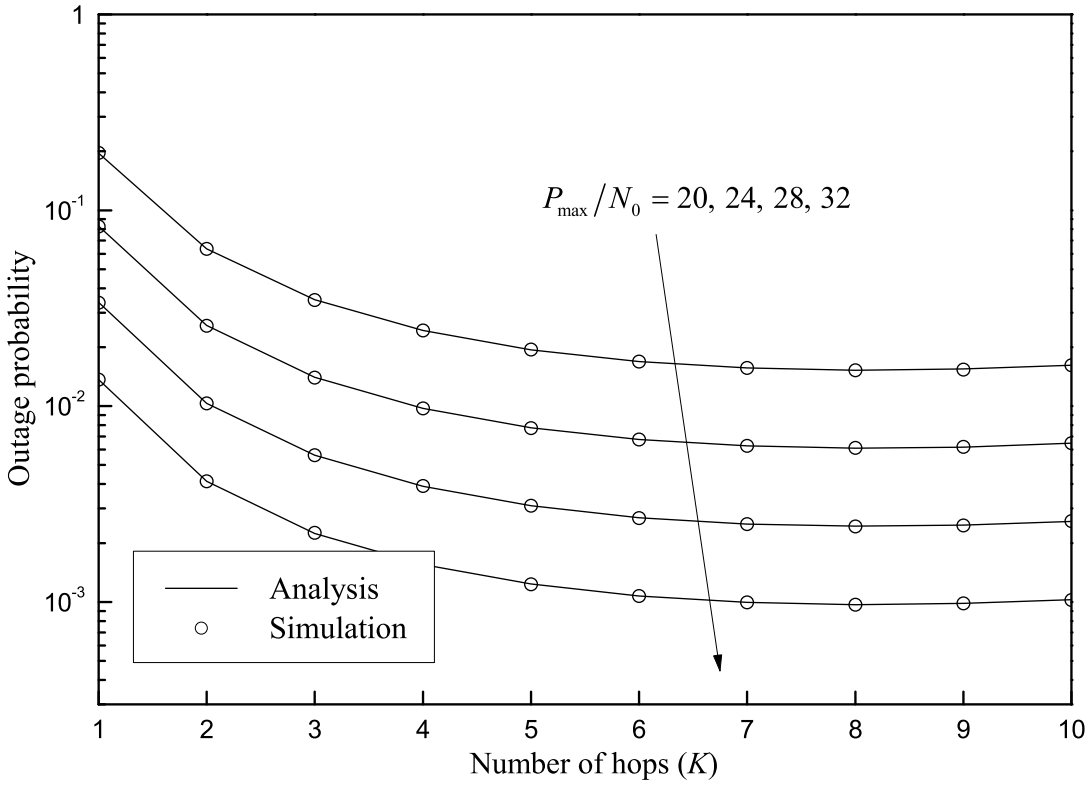
Outage probability
1
10^{-1}
10^{-2}
10^{-3}
$P_{\max}/N_0$ = 20, 24, 28, 32
Analysis
Simulation
1
2
3
4
5
6
7
8
9
10
Number of hops (K)

(b) $\alpha = 4$

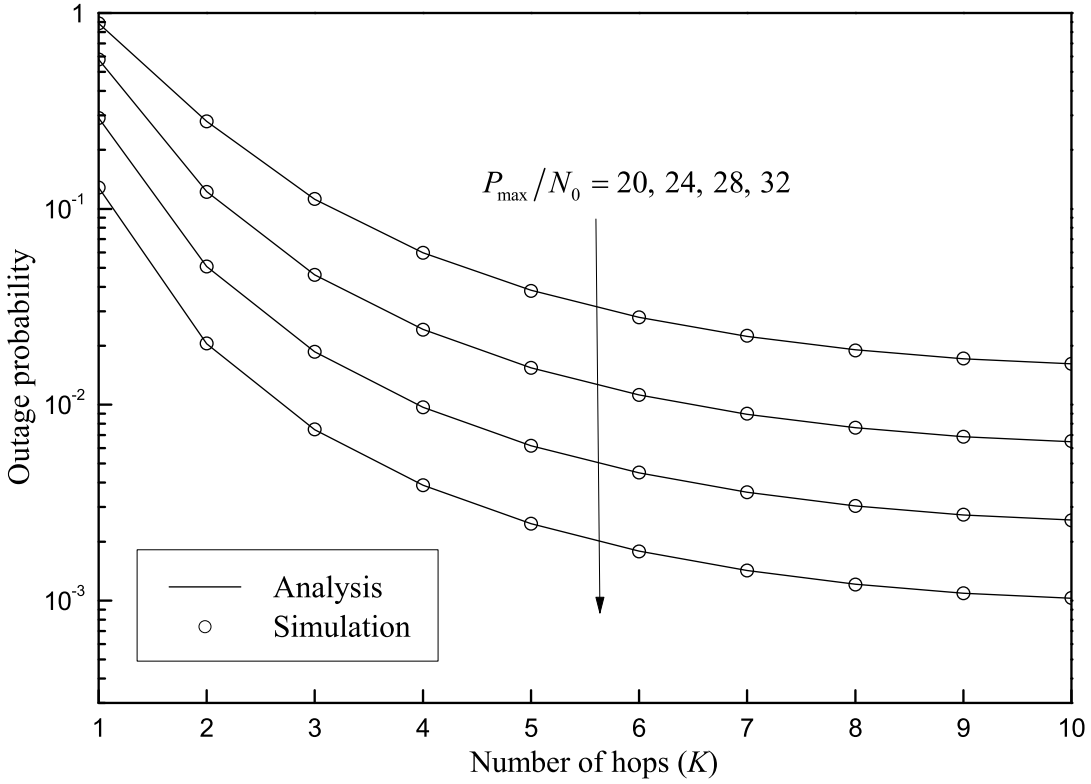

(c) $\alpha = 5$

Figure 4.6. Outage probability versus the number of hops for $P_{\max}/N_0 = 20, 24, 28, 32$. $L = 1$, $I = 20$ dB, $R = 0.5$.

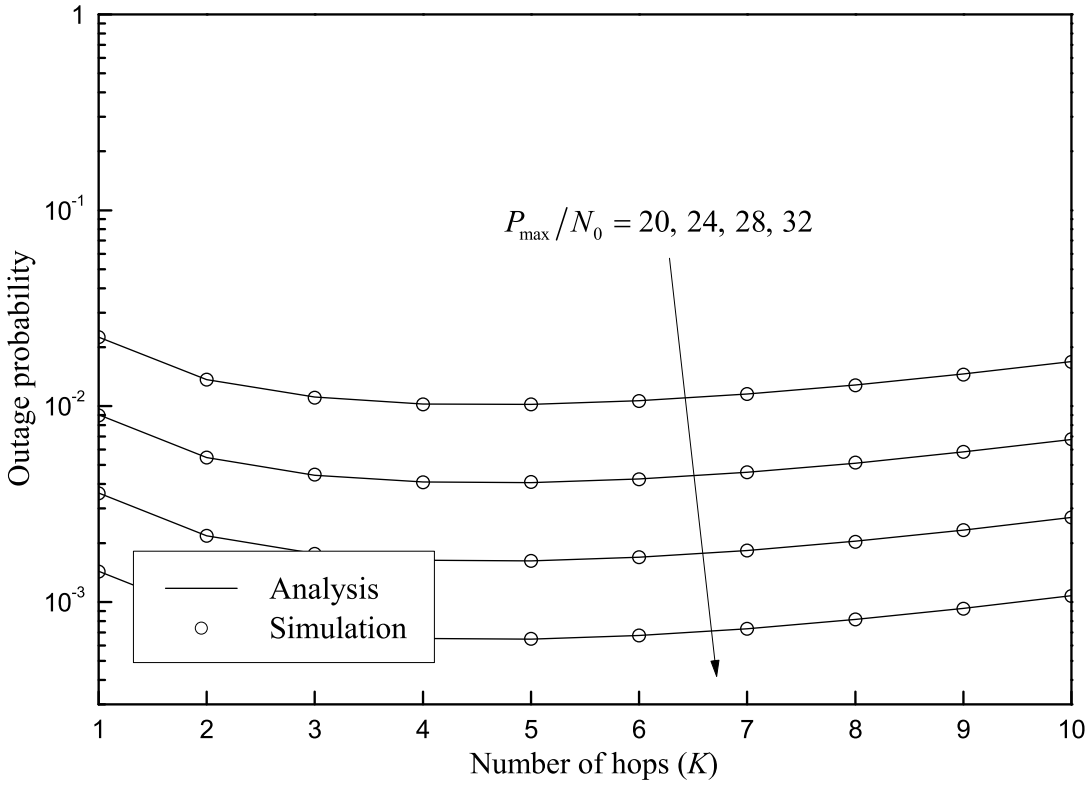
1
10^{-1}
10^{-2}
10^{-3}
Outage probability
$P_{\max}/N_0 = 20, 24, 28, 32$
Analysis
Simulation
1
2
3
4
5
6
7
8
9
10
Number of hops (K)

(a) $\alpha = 3$

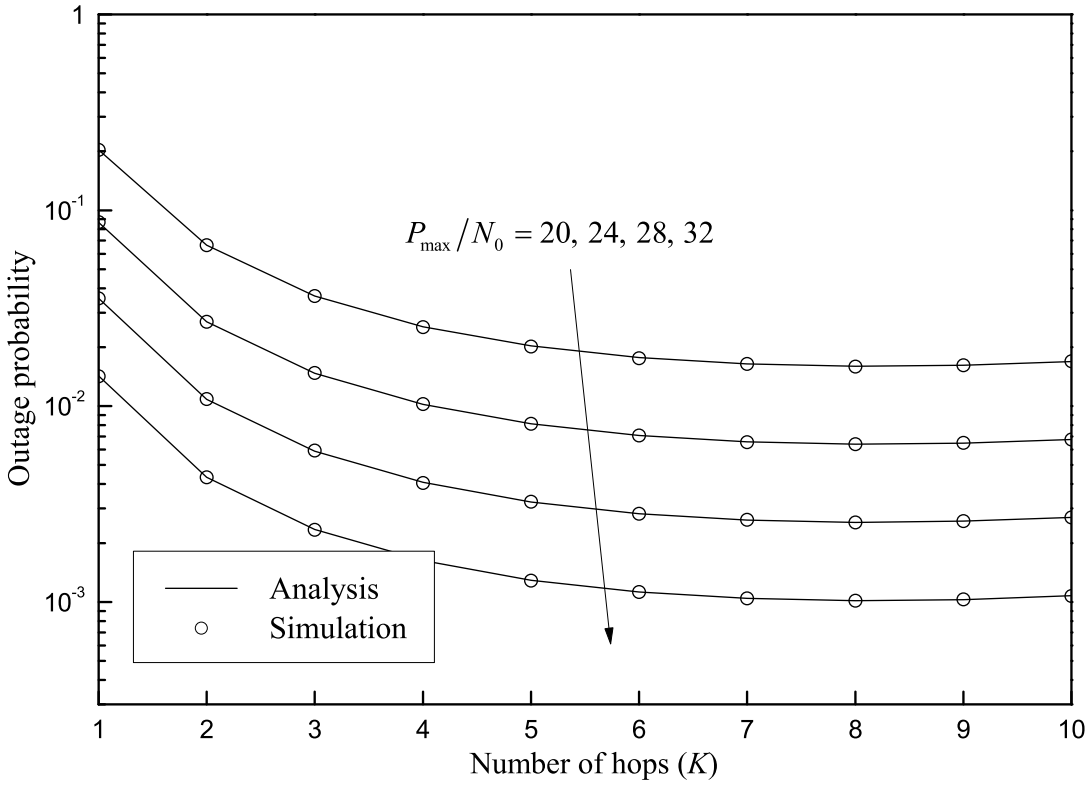
1
10^{-1}
10^{-2}
10^{-3}
Outage probability
$P_{\max}/N_0 = 20, 24, 28, 32$
Analysis
Simulation
1
2
3
4
5
6
7
8
9
10
Number of hops (K)

(b) $\alpha = 4$

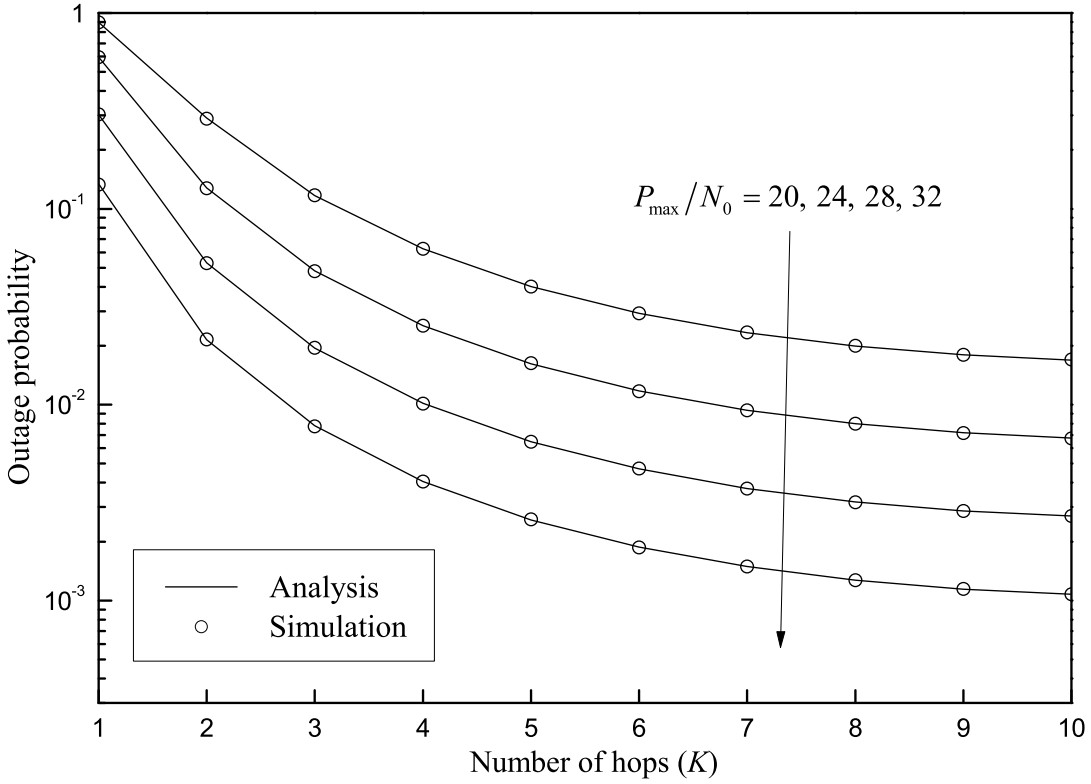

(c) $\alpha = 5$

Figure 4.7. Outage probability versus the number of hops for $P_{\max}/N_0 = 20, 24, 28, 32$. $L = 2$, $I = 20$ dB, $R = 0.5$.

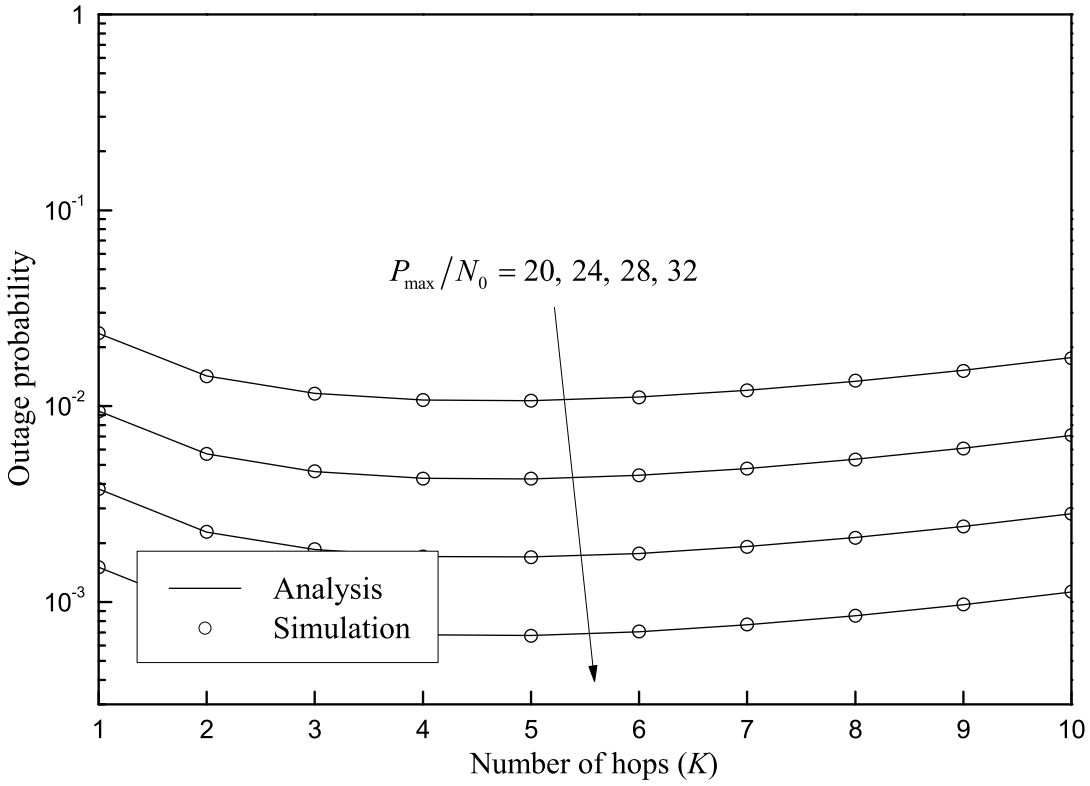
Outage probability
1
10^{-1}
10^{-2}
10^{-3}
$P_{\max}/N_0 = 20, 24, 28, 32$
Analysis
Simulation
1
2
3
4
5
6
7
8
9
10
Number of hops (K)

(a) $\alpha = 3$

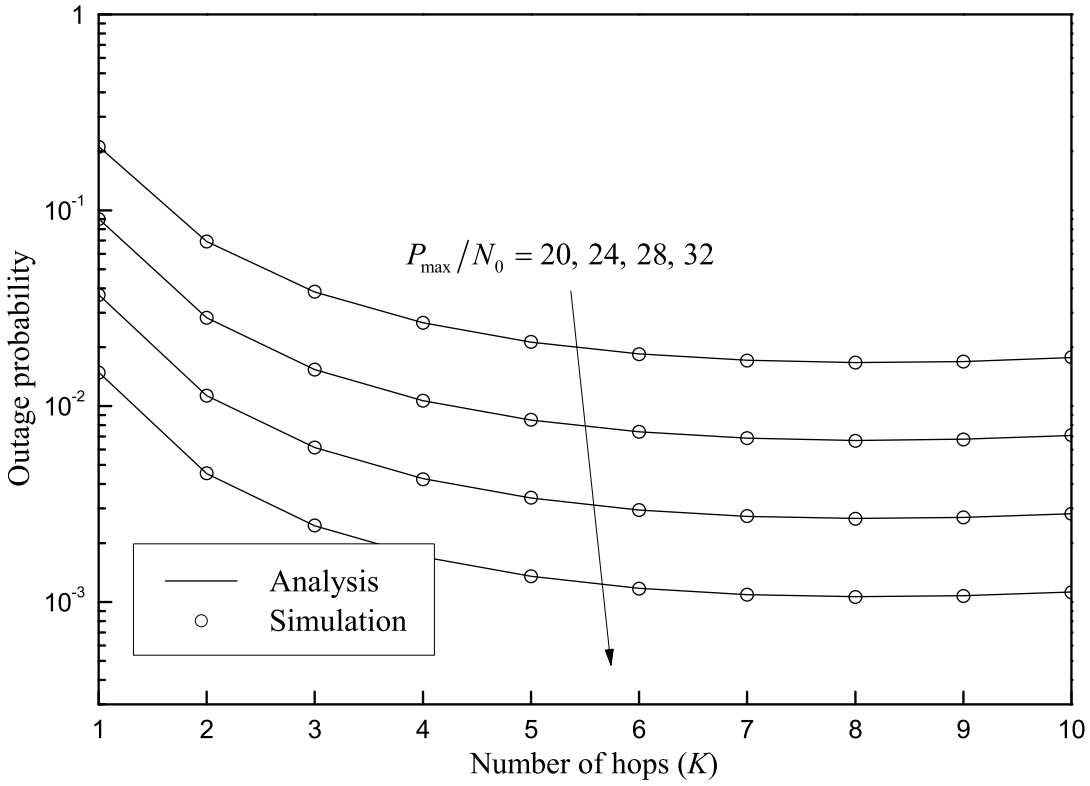
Outage probability
1
10^{-1}
10^{-2}
10^{-3}
$P_{\max}/N_0 = 20, 24, 28, 32$
Analysis
Simulation
1
2
3
4
5
6
7
8
9
10
Number of hops (K)

(b) $\alpha = 4$

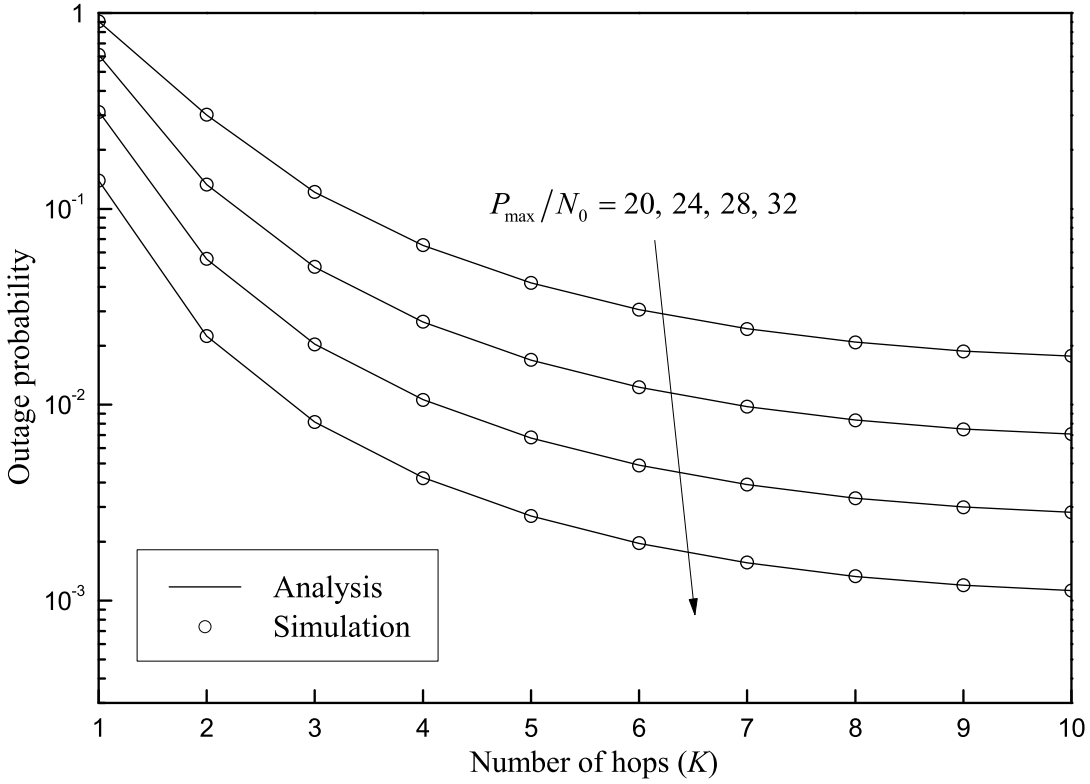

(c) $\alpha = 5$

Figure 4.8. Outage probability versus the number of hops for $P_{\max}/N_0 = 20, 24, 28, 32$. $L = 3$, $I = 20$ dB, $R = 0.5$.

of the cognitive small cell network in the presence of interference from the cellular network. Analytical results are verified by Monte Carlo simulations. It is shown that the analytical results are in complete agreement with simulation results. It is shown that the outage probability increases as the number of cells increases.

Chapter 5

Conclusions

5.1 Summary

In this dissertation, we have investigated the relay technology in the wireless networks.

In Chapter 1, we introduce the basic concept, history, and related works of the relay technology and its application to the cognitive ratio. In addition, we describe the outline of this dissertation and present the notation, abbreviations, and functions used in this dissertation.

In Chapter 2, we analyze the performance of a two-way relay network experiencing cochannel interference from multiple interferers due to aggressive frequency reuse in cellular networks. We discuss two different scenarios: Outages are declared individually for each user (individual outage) and an outage is declared simultaneously for all users (common outage). We derive the closed-form expression for the individual outage probability and the exact integral expression for the common outage

probability of the two-way relay network with multiple interferers. The validity of our analytical results is verified by a comparison with simulation results. It is shown that the analytical results perfectly match the simulation results of the individual and common outage probabilities. Also, it is shown that the individual and common outage probabilities increase as the number of interferers increases.

In Chapter 3, we examine two-way full-duplex relaying over Rayleigh fading channels. Its outage probability is derived when the perfect CSI is not available. The validity of our analysis is verified by Monte Carlo simulation. It is shown that the analysis of the outage probability well matches with simulation results. It is shown that the outage probability decreases as the variance of the channel estimation error decreases.

In Chapter 4, we investigate a cognitive small cell network which is overlaid with a cellular network. We analyze the performance of the cognitive small cell network in the presence of cochannel interference from the cellular network. Analytical results are verified by Monte Carlo simulations. It is shown that the analytical results are in complete agreement with simulation results. It is shown that the outage probability increases as the number of cells increases.

5.2 Future Works

The enormous potential of relaying for the next-generation wireless systems has been revealed in the recent literature. However, there are still a lot of challenges to be addressed on both the theoretical and practical aspects. The investigations on the

implementation of two-way half duplex/full duplex relay networks have not been yet carried out sufficiently. The future works for implementation of two-way half duplex/full duplex relay networks include: 1) optimal resource allocation (e.g., power, frequency, time, etc.) of each user, 2) optimal placement of relay, 3) efficient strategy for users to know the CSI, 4) performance analysis when a transmit antenna and a receive antenna are not isolated well, and 5) suitable strategy of synchronization between users in order to exploit the physical layer network coding. Also, the investigations on the implementation of multi-hop transmission for a cognitive small cell network have not been yet carried out sufficiently. The future works for implementation of a multi-hop cognitive small cell network include: 1) suitable strategy that each terminal of a multi-hop cognitive small cell network knows the channel from itself to the destination of the cellular network, 2) optimal resource allocation (e.g., power, frequency, time, etc.) of each terminal in a multi-hop cognitive small cell network, and 3) optimal routing for the multi-hop cognitive small cell network. Most of previous works ignores the effect of cochannel interference because of the difficulty and complexity in analysis. However, it affects the system performance (e.g., outage probability, capacity, bit/symbol error probability, etc.) of wireless relay networks. Therefore, the effect of cochannel interference should be carefully considered in the above future works.

Bibliography

[1] R. Pabst, B. H. Walke, D. C. Schultz, P. Herhold, H. Yanikomeroglu, S. Mukherjee, H. Viswanathan, M. Lott, W. Zirwas, M. Dohler, H. Aghvami, D. D. Falconer, and G. P. Fettweis, "Relay-based deployment concepts for wireless and mobile broadband radio," *IEEE Commun. Mag.*, vol. 42, no. 9, pp. 80-89, Sep. 2004.

[2] A. Sendonaris, E. Erkip, and B. Aazhang, "User cooperation diversity – Part I: System description," *IEEE Trans. Commun.*, vol. 51, no. 11, pp. 1927-1938, Nov. 2003.

[3] A. Sendonaris, E. Erkip, and B. Aazhang, "User cooperation diversity – Part II: Implemenation aspects and performance analysis," *IEEE Trans. Commun.*, vol. 51, no. 11, pp. 1939-1948, Nov. 2003.

[4] A. Nosratinia, T. E. Hunter, and A. Hedayat, "Cooperative communication in wireless networks," *IEEE Commun. Mag.*, vol. 42, no. 10, pp. 74-80, Oct. 2004.

[5] J. N. Laneman, D. N. C. Tse, and G. W. Wornell, "Cooperative diversity in wireless networks: Efficient protocols and outage behavior," *IEEE Trans. Inf. Theory*, vol. 50, no. 12, pp. 3062-3080, Dec. 2004.

[6] L. Le and E. Hossain, "Multihop cellular networks: Potential gains, research challenges, and a resource allocation framework," *IEEE Commun. Mag.*, vol. 45, no. 9, pp. 66-73, Sep. 2007.

[7] Y. Yang, H. Hu, J. Xu, and G. Mao, "Relay technologies for WiMAX and LTE-Advanced mobile systems," *IEEE Commun. Mag.*, vol. 47, no. 10, pp. 100-105, Oct. 2009.

[8] K. Loa, C.-C. Wu, S.-T. Sheu, Y. Yuan, M. Chion, D. Huo, and L. Xu, "IMT-Advanced relay standards," *IEEE Commun. Mag.*, vol. 48, no. 8, pp. 40-48, Aug. 2010.

[9] X. Tao, X. Xu, and Q. Cui, "An overview of cooperative communications," *IEEE Commun. Mag.*, vol. 50, no. 6, pp. 65-71, June 2012.

[10] E. C. V. D. Meulen, "Three-terminal communication channels," *Applied Probability Trust, Advances in Applied Probability*, vol. 3, no. 1, pp. 120-154, Spr. 1971.

[11] T. M. Cover and A. A. El Gamal, "Capacity theorems for the relay channel," *IEEE Trans. Inf. Theory*, vol. 25, pp. 572-584, Sep. 1979.

[12] D. Lee, *Performance Analysis of Multi-hop Relaying Systems in the Presence of Cochannel Interference*. Ph.D. dissertation, Seoul Nat'l Univ., Seoul, Korea, Aug. 2011.

[13] C. Jang, *Performance Analysis and Optimization for a Multi-hop and Cognitive Radio Network*. Ph.D. dissertation, Seoul Nat'l Univ., Seoul, Korea, Aug. 2013.

[14] A. Sendonaris, E. Erkip, and B. Aazhang, "Increasing uplink capacity via user cooperation diversity," in *Proc. IEEE Int. Symp. on Inf. Theory (ISIT)*, Cambridge, MA, Aug. 1998, pp. 156.

[15] B. Schein and R. G. Gallager, "The Gaussian parallel relay network," in *Proc. IEEE Int. Symp. on Inf. Theory (ISIT)*, Sorrento, Italy, June 2000, pp. 22.

[16] M. Gastpar and M. Vetterli, "On the capacity of wireless networks: The relay case," in *Proc. IEEE Int. Conf. Comput. Commun. (INFOCOM) 2002*, New York, NY, June 2002, pp. 1577-1586.

[17] J. N. Laneman and G. W. Wornell, "Distributed space-time-coded protocols for exploiting cooperative diversity in wireless networks," *IEEE Trans. Inf. Theory,* vol. 49, no. 10, pp. 2415-2425, Oct. 2003.

[18] B. Rankov and A. Wittneben, "Spectral efficient signaling for half duplex-relay channels," in *Proc. Asilomar Conf. Signals, Systems Computers*, Pacific Grove, CA, Oct. 2005, pp. 1066-1071.

[19] B. Rankov and A. Wittneben, "Achievable rate regions for the two-way relay channel," in *Proc. IEEE Int. Symp. on Inf. Theory (ISIT)*, Seattle, WA, July 2006, pp. 1668-1672.

[20] B. Rankov and A. Wittneben, "Spectral efficient protocols for half-duplex fading relay channels," *IEEE J. Sel. Areas Commun.*, vol. 25, no. 2, pp. 379-389, Nov. 2007.

[21] P. Popovski and H. Yomo, "Physical network coding in two-way wireless relay channels," in *Proc. IEEE Int. Conf. Commun. (ICC) 2007*, Glasgow, Scotland, June 2007, pp. 701–712.

[22] T. Koike-Akino, P. Popovski, and V. Tarokh, "Optimized constellations for two-way wireless relaying with physical network coding," *IEEE J. Sel. Areas Commun.*, vol. 27, no. 5, pp. 773-787, June 2009.

[23] D. Choi and J. H. Lee, "Performance analysis of a two-way relay network with multiple interferers," *IEICE Trans. Commun.*, vol. E96-B, no. 10, pp. 2668-2675, Oct. 2013.

[24] M. O. Hasna and M.-S. Alouini, "Outage probability of multihop tranmission over Nakagami fading channels," *IEEE Commun. Lett.*, vol. 7, no. 5, pp. 216-218, May 2003.

[25] J. Boyer, D. D. Falconer, and H. Yanikomeroglu, "Multihop diversity in wireless relaying channels," *IEEE Trans. Commun.*, vol. 52, no. 10, pp. 1820-1830, Oct. 2004.

[26] T. Issariyakul and E. Hossain, "Performance modeling and analysis of a class of ARQ protocols in multi-hop wireless networks," *IEEE Trans. Wireless Commun.*, vol. 5, no. 12, pp. 3460-3468, Dec. 2006.

[27] L. Le and E. Hossain, "An analytical model for ARQ cooperative diversity in multi-hop wireless networks," *IEEE Trans. Wireless Commun.*, vol. 7, no. 5, pp. 1786-1791, May 2008.

[28] B. Gui, L. Dai, and L. J. Cimini, JR., "Routing strategies in multihop cooperative network," *IEEE Trans. Wireless Commun.*, vol. 8, no. 2, pp. 843-855, Feb. 2009.

[29] Z. Yi and I.-M. Kim, "Relay ordering in a multi-hop cooperative diversity network," *IEEE Trans. Commun.*, vol. 57, no. 9, pp. 2590-2596, Sep. 2009.

[30] C. Jang and J. H. Lee, "Outage analysis and optimization of DF-based multi-hop transmission for fading channels with large path-loss exponent," *IEEE Trans. Veh. Technol.*, vol. 61, no. 9, pp. 4183-4189, Nov. 2012.

[31] Y. Liu, "A low complexity protocol for relay channels employing rateless codes and acknowledgement," in *Proc. IEEE Int. Symp. on Info. Theory (ISIT)*, Seatle, WA, July 2006, pp. 1244-1248.

[32] H. Ju, E. Oh, and D. Hong, "Catching resource-devouring worms in next-generation wireless relay systems: Two-way relay and full duplex relay," *IEEE Commun. Mag.*, vol. 47, no. 9, pp. 58-65, Sep. 2009.

[33] T. Riihonen, S. Werner, R. Wichman, and J. Hämäläinen, "Outage probabilities in infrastructure-based single-frequency relay links," in *Proc. IEEE WCNC 2009*, Budapest, Hungary, Apr. 2009, pp. 1-6.

[34] D. W. K. Ng, E. S. Lo, and R. Schober, "Dynamic resource allocation in MIMO-OFDMA systems with full-duplex and hybrid relaying," *IEEE Trans. Commun.*, vol. 60, no. 5, pp. 1291-1304, May 2012.

[35] I. Krikidis, H. A. Suraweera, P. J. Smith, and C. Yuen, "Full-duplex relay selection for amplify-and-forward cooperative networks," *IEEE Trans. Wireless Commun.*, vol. 11, no. 12, pp. 4381-4393, Dec. 2012.

[36] F. S. Tabataba, P. Sadeghi, C. Hucher, and M. R. Pakravan, "Impact of channel estimation errors and power allocation on analog network coding and routing in two-way relaying," *IEEE Trans. Veh. Technol.*, vol. 61, no. 7, pp. 3223-3239, Sep. 2012.

[37] D. Choi and J. H. Lee, "Outage probability of two-way full-duplex relaying with imperfect channel state information," *IEEE Commun. Lett.*, vol. 18, no. 6, pp. 933-936, June 2014.

[38] Y. Fan, H. V. Poor, and J. S. Thompson, "Cooperative multiplexing in full-duplex multi-antenna relay networks," in *Proc. IEEE Globecom 2008*, New Orleans, LA, Nov. 2008, pp. 1-5.

[39] T. Riihonen, S. Werner, and R. Wichman, "Mitigation of loopback self-interference in full-duplex MIMO relays," *IEEE Trans. Signal Process.*, vol. 59, no. 12, pp. 5983-5993, Dec. 2011.

[40] T. Snow, C. Fulton, and W. J. Chappell, "Transmit-receive duplexing using digital beamforming system to cancel self-interference," *IEEE Trans. Microw. Theory Tech.*, vol. 59, no. 12, pp. 3494-3503, Dec. 2011.

[41] FCC, *Spectrum Policy Task Force*. ET Docket 02-135, Nov. 2002.

[42] M. McHenry, *NSF Spectrum Occupancy Measurements Project Summary*. Shared spectrum co. report, Aug. 2005.

[43] M. McHenry, E. Livsics, T. Nguyen, and N. Majumdar, "XG dynamic spectrum access field test results," *IEEE Commun. Mag.*, vol. 45, no. 6, pp. 51-57, June 2007.

[44] S. Haykin, "Cognitive radio: Brain-empowered wireless communications," *IEEE J. Sel. Areas Commun.*, vol. 23, no. 2, pp. 201-220, Feb. 2005.

[45] I. J. Mitola, "Software radios: Survey, critical evaluation, and future directions," *IEEE Aerosp. Electron. Syst. Mag.*, vol. 8, no. 4, pp. 25-36, Apr. 1993.

[46] I. J. Mitola and G. Q. Maguire, Jr., "Cognitive radio: Making software radio more personal," *IEEE Pers. Commun.*, vol. 6, no. 4, pp. 13-18, Aug. 1999.

[47] A. Ghasemi and E. S. Sousa, "Spectrum sensing in cognitive radio networks: Requirements, challengers and design trade-offs," *IEEE Commun. Mag.*, vol. 46, no. 4, pp. 32-39, Apr. 2008.

[48] G. Ganesan and Y. G. Li, "Coopeative spectrum sensing in cognitive radio, Part I: Two user networks," *IEEE Trans. Wireless Commun.*, vol. 6, no. 6, pp. 2204-2213, June 2007.

[49] G. Ganesan and Y. G. Li, "Coopeative spectrum sensing in cognitive radio, Part II: Multiuser networks," *IEEE Trans. Wireless Commun.*, vol. 6, no. 6, pp. 2214-2222, June 2007.

[50] K. B. Letaief and W. Zhang, "Cooperative communications for cognitive radio networks," *Proc. IEEE*, vol. 97, no. 5, pp. 878-893, May 2009.

[51] J. Ma, G. Zhao, and Y. G. Li, "Soft combination for cooperative spectrum sensing in cognitive radio networks," *IEEE Trans. Wireless Commun.*, vol. 7, no. 11, pp. 4502-4507, Nov. 2008.

[52] D. Duan, L Yang, and J. C. Principe, "Coopeative diversity of spectrum sensing for cognitive radio systems," *IEEE Trans. Signal Process.*, vol. 58, no. 6, pp. 3218-3227, June 2010.

[53] C. Jang and J. H. Lee, "Sum of discrete i.i.d. random variables and its application to cooperative spectrum sensing," *IEEE Trans. Veh. Technol.*, vol. 62, no. 3, pp. 1383-1389, Mar. 2013.

[54] Y. Zou, Y.-D. Yao, and B. Zheng, "Outage probability analysis of cognitive transmission: Impact of spectrum sensing overhead," *IEEE Trans. Wireless Commun.*, vol. 9, no. 8, pp. 2676-2688, Aug. 2010.

[55] Y. Zou, Y.-D. Yao, and B. Zheng, "Cognitive transmissions with multiple relays in cognitive radio networks," *IEEE Trans. Wireless Commun.*, vol. 10, no. 2, pp. 648-659, Feb. 2011.

[56] Y. Zou, Y.-D. Yao, and B. Zheng, "A cooperative sensing based cognitive relay transmission scheme without a dedicated sensing relay channel in cognitive radio networks," *IEEE Trans. Signal Process.*, vol. 59, no. 2, pp. 854-858, Feb. 2011.

[57] J. M. Peha, "Approaches to spectrum sharing," *IEEE Commun. Mag.*, vol. 43, no. 2, pp. 10-12, Feb. 2005.

[58] Y. Zou, J. Zhu, B. Zheng, and Y.-D. Yao, "An adaptive cooperation diversity scheme with best-relay selection in cognitive radio networks," *IEEE Trans. Signal Process.*, vol. 58, no. 10, pp. 5438-5445, Oct. 2010.

[59] J. Lee, H. Wang, J. G. Andrews, and D. Hong, "Outage probability of cognitive relay networks with interference constraints," *IEEE Trans. Wireless Commun.*, vol. 10, no. 2, pp. 390-395, Feb. 2011.

[60] D. Li, "Outage probability of cognitive relay networks with relay selection," *IET Commun.*, vol. 5, no. 18, pp. 2730-2735, Dec. 2011.

[61] W. Xu, J. Zhang, P. Zhang, and C. Tellambura, "Outage probability of decode-and-forward cognitive relay in presence of primary user's interference," *IEEE Commun. Lett.*, vol. 16, no. 8, pp. 1252-1255, Aug. 2012.

[62] I. S. Gradshteyn and I. M. Ryzhik, *Table of Integrals, Series, and Products*, 6th ed. San Diego, CA: Academic Press, 2000.

[63] Y. Han, S. H. Ting, C. K. Ho, and W. H. Chin, "Performance bounds for two-way amplify-and-forward relaying," *IEEE Trans. Wireless Commun.*, vol. 8, no. 1, pp. 432-439, Jan. 2009.

[64] R. H. Y. Louie, Y. Li, and B. Vucetic, "Practical physical layer network coding for two-way relay channels: Performance analysis and comparison," *IEEE Trans. Wireless Commun.*, vol. 9, no. 2, pp. 764-777, Feb. 2010.

[65] H. Guo, J. Ge, and H. Ding, "Symbol error probability of two-way amplify-and-forward relaying," *IEEE Commun. Lett.*, vol. 15, no. 1, pp. 22-24, Jan. 2011.

[66] J. Yang, P. Fan, T. Q. Duong, and X. Lei, "Exact performance of two-way AF relaying in Nakagami-m fading environment," *IEEE Trans. Wireless Commun.*, vol. 10, no. 3, pp. 980-987, Mar. 2011.

[67] K. S. Ahn and R. W. Heath Jr., "Performance analysis of maximum ratio combining with imperfect channel estimation in the presence of cochannel interferences," *IEEE Trans. Wireless Commun.*, vol. 8, no. 3, pp. 1080-1085, Mar. 2009.

[68] I. Krikidis, J. S. Thompson, S. McLaughlin, and N. Goertz, "Max-min relay selection for legacy amplify-and-forward systems with interference," *IEEE Trans. Wireless Commun.*, vol. 8, no. 6, pp. 3016-3027, June 2009.

[69] D. Lee and J. H. Lee, "Outage probability for dual-hop relaying systems with multiple interferers over Rayleigh fading channels," *IEEE Trans. Veh. Technol.*, vol. 60, no. 1, pp. 333-338, Jan. 2011.

[70] S. S. Ikki and S. Aïssa, "Multihop wireless relaying systems in the presence of cochannel interferences: Performance analysis and design optimization," *IEEE Trans. Veh. Technol.*, vol. 61, no. 2, pp. 566-573, Feb. 2012.

[71] V. Chandrasekhar and J. G. Andrews, "Uplink capacity and interference avoidance for two-tier femtocell networks," *IEEE Trans. Wireless Commun.*, vol. 8, no. 7, pp. 3498-3509, July 2009.

[72] H.-S. Jo, C. Mun, J. Mun, and J.-G. Yook, "Interference mitigation using uplink power control for two-tier femtocell networks," *IEEE Trans. Wireless Commun.*, vol. 8, no. 10, pp. 4906-4910, Oct. 2009.

[73] X. Liang, S. Jin, W. Wang, X. Gao, and K.-K. Wong, "Outage performance for two-way relay channel with co-channel interference," in *Proc. IEEE Globecom 2011*, Houston, TX, Dec. 2011, pp. 1-5.

[74] S. S. Ikki and S. Aïssa, "Performance analysis of two-way amplify-and-forward relaying in the presence of co-channel interferences," *IEEE Trans. Commun.*, vol. 60, no. 4, pp. 933-939, April 2012.

[75] D. P. Agrawal and Q.-A. Zeng, *Introduction to Wireless and Mobile Systems.* Pacific Grove, CA: Thomson Brooks/Cole, 2003.

[76] L.-U Choi and R. D. Murch, "A transmit MIMO scheme with frequency domain pre-equalization for wireless frequency selective channels," *IEEE Trans. Wireless Commun.*, vol. 3, no. 3, pp. 929-938, May 2004.

[77] M. O. Hasna and M.-S. Alouini, "A performance study of dual-hop transmissions with fixed gain relays," *IEEE Trans. Wireless Commun.*, vol. 3, no. 6, pp. 1963-1968, Nov. 2004.

[78] M.-S. Alouini and A. J. Goldsmith, "Area spectral efficiency of cellular mobile radio systems," *IEEE Trans. Veh. Technol.*, vol. 48, no. 4, pp. 1047-1065, July 1999.

[79] S. Vakil and B. Liang, "Cooperative diversity in interference limited wireless networks," *IEEE Trans. Wireless Commun.*, vol. 7, no. 8, pp. 3185-3195, Aug. 2008.

[80] I. Trigui, A. Laourine, S. Affes, and A. Stéphenne, "Performance analysis of mobile radio systems over composite fading/shadowing channels with co-located interference," *IEEE Trans. Wireless Commun.*, vol. 8, no. 7, pp. 3448-3453, July 2009.

[81] C. Zhong, S. Jin, and K.-K. Wong, "Dual-hop systems with noisy relay and interference-limited destination," *IEEE Commun. Lett.*, vol. 58, no. 3, pp. 764-768, Mar. 2010.

[82] A. Bletsas, H. Shin, and M. Z. Win, "Cooperative communications with outage-optimal opportunistic relaying," *IEEE Trans. Wireless Commun.*, vol. 6, no. 9, pp. 3450-3460, Sep. 2007.

[83] H. Shin and M. Z. Win, "MIMO diversity in the presence of double scattering," *IEEE Trans. Inf. Theory*, vol. 54, no. 7, pp. 2976-2996, July 2008.

[84] A. Erdelyi, W. Magnus, F. Oberhettinger, and F. Tricomi, *Tables of Integral Transforms*. New York: McGraw-Hill, 1954.

[85] A. Papoulis, *Probability, Random Variables, and Stochastic Processes*, 4th ed. New York: McGraw-Hill, 2002.

[86] A. P. Prudnikov, Y. A. Brychkov, and O. I. Marichev, *Integrals and Series*. New York: Gordon and Breach, 1992.

[87] M. K. Simon and M.-S. Alouini, *Digital Communication Over Fading Channels*, 2nd ed. Hoboken, NJ: Wiley, 2005.

[88] L. Li, N. Jindal, and A. Goldsmith, "Outage capacities and optimal power allocation for fading multiple-access channels," *IEEE Trans. Inf. Theory*, vol. 51, no. 4, pp. 1326-1347, Apr. 2005.

[89] F. Xu, F. C. M. Lau, and D.-W. Yue, "Diversity order for amplify-and-forward dual-hop systems with fixed-gain relay under Nakagami fading channels," *IEEE Trans. Wireless. Commun.*, vol. 9, no. 1, pp. 92-98, Jan. 2010.

[90] T. Riihonen, S. Werner, and R. Wichman, "Optimized gain control for single-frequency relaying with loop interference," *IEEE Trans. Wireless Commun.*, vol. 8, no. 6, pp. 2801-2806, June 2009.

[91] T. M. Kim, H. J. Yang, and A. J. Paulraj, "Distributed sum-rate optimization for full-duplex MIMO system under limited dynamic range," *IEEE Commun. Lett.*, vol. 20, no. 6, pp. 555-558, June 2013.

[92] T. Riihonen, S. Werner, and R. Wichman, "Hybrid full-duplex/half-duplex relaying with transmit power adaptation," *IEEE Trans. Wireless Commun.*, vol. 10, no. 9, pp. 3074-3085, Sep. 2011.

[93] D. J. Love, R. W. Heath Jr., V. K. N. Lau, D. Gesbert, B. D. Rao, and M. Andrews, "An overview of limited feedback in wirelss communication systems," *IEEE J. Sel. Areas Commun.*, vol. 26, no. 8, pp. 1341-1365, Oct. 2008.

[94] H. ElSawy, E. Hossain, and D. I. Kim, "HetNets with cognitive small cells: User offloading and distributed channel access techniques," *IEEE Commun. Mag.*, vol. 51, no. 6, pp. 28-36, June 2013.

[95] M. Wildemeersch, T. Q. S. Quek, C. H. Slump, and A. Rabbachin, "Cognitive small cell networks: Energy efficiency and trade-offs," *IEEE Trans. Commun.*, vol. 61, no. 9, pp. 4016-4029, Sep. 2013.

[96] M. Maso, L. S. Cardoso, M. Debbah, and L. Vangelista, "Cognitive orthogonal precoder for two-tiered networks deployment," *IEEE J. Sel. Areas Commun.*, vol. 31, no. 11, pp. 2338-2348, Nov. 2013.

[97] V. N. Q. Bao, T. Q. Duong, and C. Telambura, "On the performance of cognitive underlay multihop networks with imperfect channel state information," *IEEE Trans. Commun.*, vol. 61, no. 12, pp. 4864-4873, Dec. 2013.

[98] A. Hyadi, M. Benfillali, M.-S. Alouini, and D. B. da Costa, "Performance analysis of underlay cognitive multi-hop regenerative relaying systems with multiple primary receivers," *IEEE Trans. Wireless Commun.*, vol. 12, no. 12, pp. 6418-6429, Dec. 2013.

[99] C. Zhong, T. Ratnarajah, and K.-K. Wong, "Outage probability of decode-and-forward cognitive dual-hop systems with interference constraint in Nakagami-m fading channels," *IEEE Trans. Veh. Technol.*, vol. 60, no. 6, pp. 2875-2879, July 2011.

[100] D. Lee and J. H. Lee, "Outage probability of decode-and-forward opportunistic relaying in a multicell environment," *IEEE Trans. Veh. Technol.*, vol. 60, no. 4, pp. 1925-1930, May 2011.

[101] I. S. Gradshteyn and I. M. Ryzhik, *Table of Integrals, Series, and Products*, 7th ed. San Diego, CA: Academic Press, 2007.

Korean Abstract

무선 중계 기술은 차세대 통신 시스템에서 요구되는 높은 서비스 품질/데이터 전송률 달성을 위한 가장 중요한 기술 중 하나이다. 중계 기술이 갖고 있는 다양한 장점으로 인해 중계 기술은 지금까지 IEEE 802.16j 및 3GPP LTE-Advanced 등의 무선통신 시스템 표준에 반영되기도 하였다. 그러나 실질적인 무선 중계 네트워크의 프로토콜 개발을 위해서는 여전히 해결해야하는 많은 문제들이 있다. 특히 대형셀과 소형셀이 동시에 존재하는 중첩셀 네트워크에서 이웃한 대형셀 및 소형셀로부터 받게되는 동일채널간섭은 차세대 무선통신 시스템의 성능을 저하시키는 주요 제한 요소인데 아직 연구가 미흡한 실정이다. 또한 전이중 중계 네트워크에서 단말기의 송신안테나에서 수신안테나로 들어오는 동일채널 루프간섭은 전이중 중계 네트워크의 성능을 결정하는 중요한 요소로 추가적인 연구가 필요한 실정이다.

본 논문에서는 동일채널간섭을 포함한 양방향 중계 네트워크, 동일채널 루프간섭을 포함한 양방향 전이중 중계 네트워크 및 무선 인지 다중 홉 네트워크의 성능을 분석하며, 주요한 연구결과는 다음과 같다. 첫째, 셀룰러 환경에서 높은 주파수 재사용율로 인해 발생한 동일채널간섭이 존재하는 양방향 중계 네트워크의 성능을 분석한다. 이때 임의의 한 사용자가 불능 사건이 발생하는 시나리오(개별 사용자 불능), 전체 사용자가 동시에 불능 사건이 발생한 시나리오(전체 사용자 불능)의 두 가지에 대해 성능을

분석한다. 여기에서 각 시나리오에 대하여 개별 사용자 불능 확률 및 전체 사용자 불능 확률을 폐형으로 유도한다. 모의실험을 통해 얻어진 불능 확률이 유도한 불능 확률 값과 일치함을 확인한다. 또한 동일채널간섭을 발생하는 인접 셀의 사용자가 늘어날수록 개별 사용자 불능 확률 및 전체 사용자 불능 확률이 증가함을 확인한다. 둘째, 동일채널 루프간섭이 존재하는 전이중 양방향 중계 네트워크를 연구한다. 여기에서 두 전이중 방식의 사용자들이 전이중 방식의 중계기를 이용하여 서로 신호를 교환한다. 이때 각 단말기들은 자신의 수신 신호에서 루프간섭 신호의 추정치를 제거한다. 단말기들이 채널 상태 정보를 정확하게 혹은 부정확하게 알고 있는 경우에 전이중 양방향 중계 네트워크의 불능 확률을 정확한 적분 표현 및 근사적 폐형 표현으로 유도한다. 모의실험을 통해 얻어지 결과가 유도한 수식과 일치함을 확인한다. 셋째, 대형셀과 소형셀이 동시에 존재하는 중첩셀 네트워크를 연구한다. 특히 인접 대형셀 및 소형셀에서 발생한 동일채널간섭이 존재하는 무선 인지 기반 다중 홉 소형셀 네트워크의 불능 확률을 분석한다. 모의실험을 통해 얻어진 불능 확률을 통해 유도한 불능 확률을 검증한다. 유도한 불능 확률 값과 모의실험을 통해 얻어진 불능 확률 값이 일치함을 확인한다. 대형셀의 수가 증가할수록 불능 확률이 증가함을 확인한다.

주요어: 무선 중계 기술, 동일채널간섭, 양방향 중계, 다중 홉 중계, 전이중 중계, 무선 인지, 스펙트럼 공유, 불능 확률.

학번: 2007-23057